1991

Nonphotochemical hole burning and relaxation dynamics of amorphous solids at low temperature

Luchuan Shu
Iowa State University

Order Number 9212190

Nonphotochemical hole burning and relaxation dynamics of amorphous solids at low temperature

Shu, Luchuan, Ph.D.

Iowa State University, 1991

U·M·I
300 N. Zeeb Rd.
Ann Arbor, MI 48106

Nonphotochemical hole burning and relaxation dynamics of amorphous solids at low temperature

by

Luchuan Shu

A Dissertation Submitted to the
Graduate Faculty in Partial Fulfillment of the
Requirements for the Degree of
DOCTOR OF PHILOSOPHY

Department: Chemistry
Major: Physical Chemistry

Approved:

Signature was redacted for privacy.
In Charge of Major Work

Signature was redacted for privacy.
For the Major Department

Signature was redacted for privacy.
For the Graduate College

Iowa State University
Ames, Iowa
1991

TABLE OF CONTENTS

EXPLANATION OF DISSERTATION FORMAT

This dissertation contains part of the candidate's original research work on the studies of the mechanism of nonphotochemical hole burning and relaxation dynamics of amorphous solids at low temperature. First, a "general introduction" is given, which describe the phenomenon, basic theories and scientific and technological significance of nonphotochemical hole burning. Especially, the subjects of the research and their background and current status are described in the general introduction. An "experimental methods" section follows which describes sample preparation, experimental apparatus and techniques used to study NPHB. Following these sections are the published or to-be-published papers. Parts I and II report new temperature-dependent and polarized nonphotochemical hole burning results and a new mechanism, based on an "outside-in" hierarchy of constrained configurational tunneling events, is proposed. Parts III and IV present new spontaneous hole filling and laser induced hole filling data for cresyl violet in polyvinyl alcohol films at 1.6 K, respectively.

The format used for references follows the format utilized in Chemical Physics.

GENERAL INTRODUCTION

Optical transitions in amorphous solids (e.g., glasses, polymers or proteins) are inhomogeneously broadened (~100-500 cm^{-1}), which is a consequence of the site-to-site variations of the local environments in the host material. Large inhomogeneous broadening usually limits the spectral resolution to an extent that typical features of optical lines, such as zero-phonon line structures, phonon structures and vibrational structures, are masked by the broad absorption band. Persistent spectral hole-burning (PSHB) spectroscopy is a powerful laser-based line narrowing method, which can eliminate or significantly reduce the inhomogeneous broadening contribution. Thus, PSHB can provide detailed information that often can not be obtained in any other fashion. The following is a list of several scientific applications of PSHB [1],

(1) Dephasing mechanism.

(2) Spectral diffusion.

(3) Structures and dynamics of amorphous solids.

(4) Kinetics of photoinduced processes.

(5) Electron transfer and energy transfer in photosynthetic processes [2-10].

In addition to the significance for science, PSHB also has promising technological applications [11], e.g.,

(1) Frequency-domain optical storage.

(2) Multiband transmission optical filter.

Optical spectra of amorphous solids are broadened by a variety of mechanisms which can be categorized as homogeneous or inhomogeneous. As mentioned earlier, inhomogeneous broadening is due to the site-to-site variations of the local environments in the host material. Homogeneous broadening is the broadening that is identical to every chemically identical molecule in the ensemble regardless of local environment. Homogeneous broadening limits the spectral resolution attainable by line narrowing techniques. For a matrix-isolated molecule, its excited state lifetime T_1 is characterized by various electronic relaxation processes which can be classified as radiative and radiationless decay processes. From Heisenberg's uncertainty relation, the homogeneous line width, γ_{hom}, is given as

$$\gamma_{hom} = (2\pi c T_1)^{-1} \qquad (1)$$

γ_{hom} is the full width at half-maxim (FWHM) of the spectral profile and is expressed in units of cm^{-1}, c is the speed of light in units of cm/s. For a molecule in a host material, the homogeneous linewidth, γ_{hom}, is determined by the effective dephasing time T_2 of the optical transition [12,13]:

$$1/T_2 = 1/T_1 + 2/T_2^* \qquad (2)$$

here T_1 is the life time of the excited state and T_2^* is the pure dephasing time. Dephasing processes with characteristic time T_2^* can be best described by means of the density matrix formulation of spectroscopic transitions [14-17]. Pure dephasing can be understood as being due to the interaction of the excited state with the bath phonons and other low energy excitations in glasses [18]. This interaction can be viewed as a

phonon scattering process which leads to a decay of the phase coherence of the superposition state initially created by the photon rather than electronic relaxation of the excited state. Equation (2) is not symmetrical in T_1 and T_2^* which is in contrast to similar expressions derived for NMR spectroscopy. The difference is due to the fact that for optical two-level systems the excited state cannot be populated thermally. Thus, only the excited state can decay with T_1. Pure dephasing processes can, however, occur in both ground and excited states. Considering the dephasing process, the γ_{hom} is

$$\gamma_{hom} = (2\pi c T_2)^{-1} \qquad (3)$$

here c is the speed of light in cm s^{-1}. From the above discussion, it is obvious that γ_{hom} determines the ultimate spectral resolution attainable by line narrowing techniques.

PSHB was first observed by Kharlamov et al. and Gorokhovskii et al. in 1974 [19,20]. This spectroscopic technique is a site-selective photobleaching process in which inhomogeneously broadened absorption lines in amorphous solids can be spectrally modified for long time periods (hours or days), providing the sample is maintained at or below the burn temperature and in the dark. Figure 1 is a schematic of PSHB. The broad absorption spectrum consists of an origin (0-0) band and its two vibronic bands (1_α,0) and (1_β,0). A laser light at frequency ω_B excites an isochromat in the (0,0) absorption band, the absorbers, whose transition frequencies (zero-phonon lines, ZPL) overlap the laser profile will be excited. Therefore a sharp zero-phonon hole (ZPH) is produced coincident with the laser frequency ω_B. Because the ZPL in absorption is accompanied by a phonon-side band (PSB), the ZPH is accompanied by

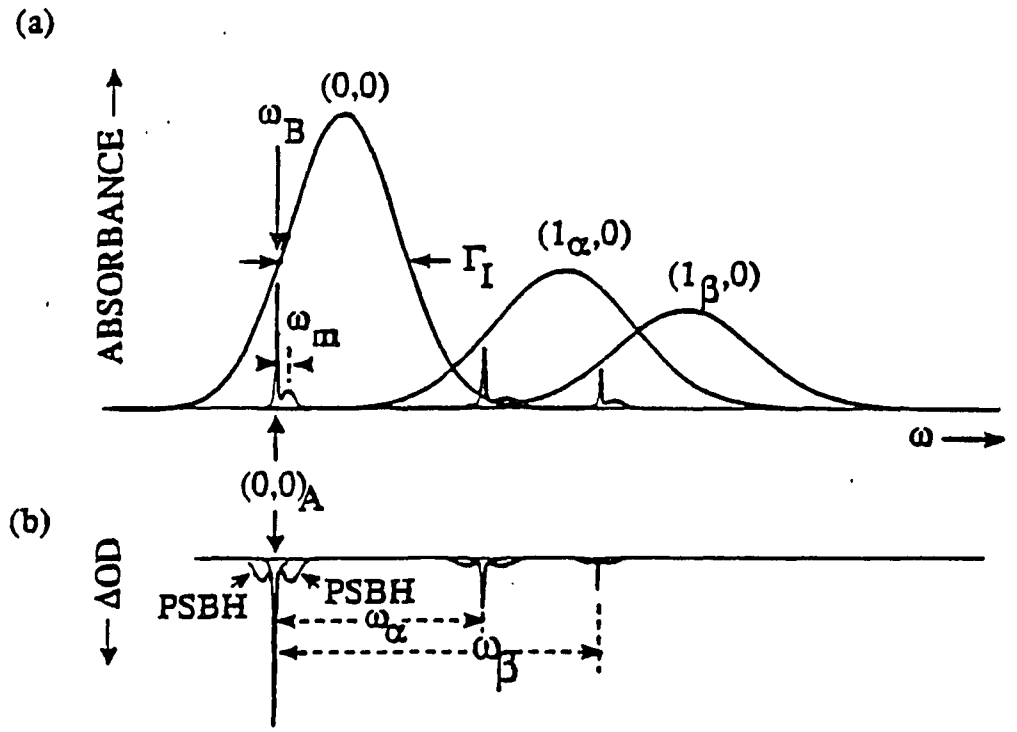

Figure 1. A schematic diagram which represents production of the ZPH and vibronic holes when laser light burns into the origin absorption band (0,0). (a) an absorption spectrum consists of one origin band (0,0) and two vibronic bands $(1_\alpha,0)$ and $(1_\beta,0)$. ω_B is the laser frequency and Γ_I is the inhomogeneous width. ω_m is the phonon mean frequency. (b) Hole spectrum consists of a ZPH, PSBH and vibronic holes. Here ω_α and ω_β are vibrational frequencies in the excited states

phonon side-band holes (PSBH). The PSBH to the higher energy side of the ZPH corresponds to the PSB in absorption and is referred to as the real-PSBH. The PSBH to the lower energy side of the ZPH results from the sites whose ZPL frequencies lie to the lower energy side of ω_B and which absorb laser light by their PSB. Thus, the lower energy side PSBH is actually composed of ZPH with their ZPL lower than the ω_B and is called pseudo-PSBH. The intensity ratio of the ZPH to the entire hole profile (ZPH+PSBH) gives the strength of the electron-phonon coupling. It should be pointed out that, for an experimental hole burning spectrum, the real-PSHB is usually interfered by the product of the hole, so called anti-hole, which is an increase in absorption. In this case, it is not easy to reveal the true structure of the real-PSBH. Figure 1 also shows that there are two vibronic satellite holes that appear in the $(1_\alpha,0)$ and $(1_\beta,0)$ bands, which are due to the sites that contribute to the original isochromat which also contribute to the $(1_\alpha,0)$ and $(1_\beta,0)$ vibronic bands. Therefore, a ZPH will always be accompanied by satellite vibronic holes. In the same manner as the pseudo-PSBH, a pseudo-vibronic satellite hole can be produced. The intensity ratio of the ZPH to the vibronic satellite holes can be used to determine their Frank-Condon factors. Figure 2 presents a hole-burning spectrum for cresyl violet in polyvinyl alcohol at 8K. A sharp ZPH is produced coincident with ω_B=15760 cm^{-1}. The real-PSBH is just to the higher energy side of ZPH at ~ ω_B+25 cm^{-1}, the pseudo-PSBH is at ω_B - 25 cm^{-1}. A weak pseudo-vibronic satellite hole is shown at ω_B-340 cm^{-1}, with 340 cm^{-1} being the frequency of a Frank-Condon active excited state vibration of cresyl violet. The

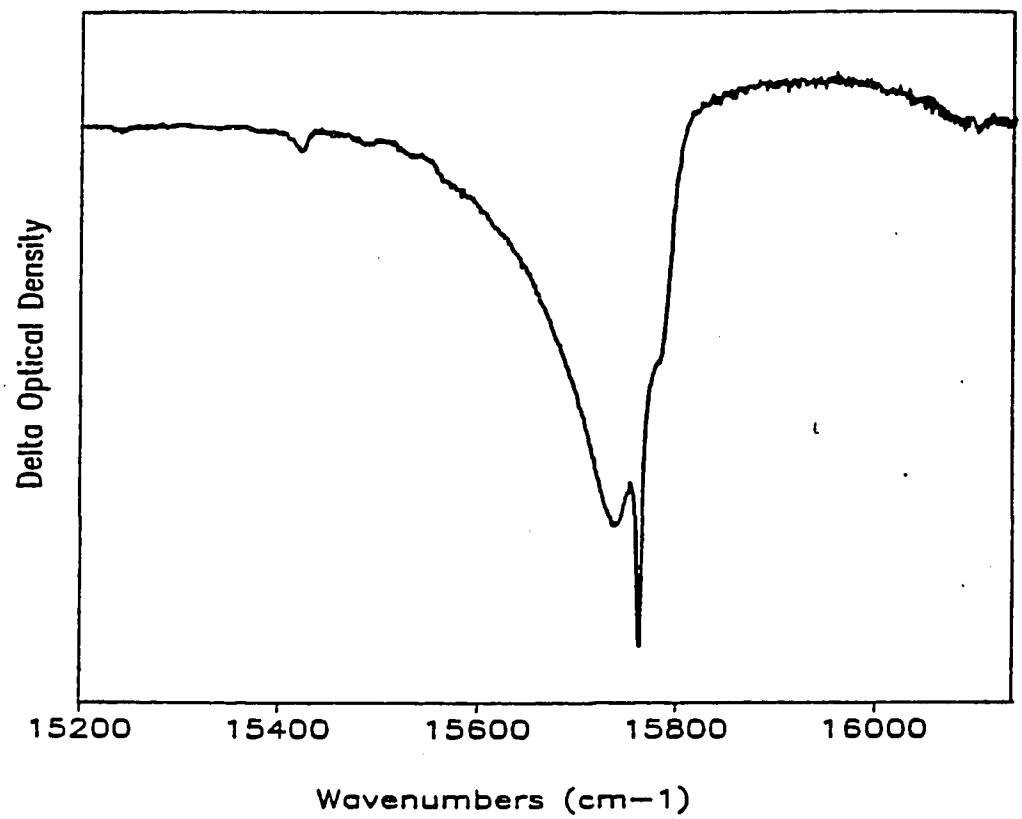

Figure 2. Hole spectrum for cresyl violet burned and read at 8 K. Burn time is 10 min. with burn intensity I_B=30 mW/cm^2. A sharp ZPH is shown at ω_B=15760 cm^{-1}. The pseudo-phonon side band hole just to the left of ZPH exhibits a maximum at ω_B-25cm^{-1}. The real-phonon side band hole just to the (higher energy side) of ZPH at ω_B+25cm^{-1} is clearly visible. The anti-hole occurs to the higher energy side of ω_B and tails for several hundred cm^{-1}

corresponding real vibronic satellite hole is at ω_B+340 cm^{-1}. The anti-hole (increase of absorption) can be seen to the higher energy side of ZPH.

There are two types of persistent hole burning: photochemical hole burning (PHB) and nonphotochemical hole burning (NPHB). PHB is due to photoactive molecules undergoing photochemical changes. The absorption of the photoproduct is, generally, spectroscopically well separated from its original absorption. The shift of the new absorption can be both blue (to higher energy side of ZPH) and red (to lower energy side of ZPH) shifted. NPHB results from the photophysical modification of molecule-matrix interactions, i.e. appropriate guest-host rearrangements. The subject of this dissertation focuses on NPHB.

Nonphotochemical hole burning of impurity optical transitions in amorphous solids has been shown to be a general phenomenon and is a versatile probe of the bistable molecular configuration of glasses [18,21]. The nature of disordered solids, e.g. glasses and polymers, is fundamental to the understanding of the nonphotochemical hole burning processes. That disordered solids are basically different from crystalline materials was first found by Zeller and Pohl [22] in 1971 in measurements of the specific heat, and thermal conductivity of glasses at very low temperatures (i.e. $\leq$ 1 K). Their results showed that the specific heat contained a linear temperature dependent term and the thermal conductivity a quadratic dependence. These results are in contrast to the cubic dependence expected for both properties as is observed in crystals. Based on these results, Anderson [23] and Phillips [24] proposed that glasses are

Table I. Comparison of glass and crystal properties

PROPERTY	CRYSTAL	GLASS	REL. MAGNITUDE[a]
Specific heat	T^3	$cT + c'T^3$	larger
Thermal conductivity	T^3	$\sim T^2$	smaller
Ultrasonic attenuation		saturates	larger
Sound velocity	T indep.	ln T	10-100
Dielectric constant	T indep.	ln T	10-100
Optical linewidth	T^7	$T\text{-}T^2$	10-100

[a]Glass value relative to crystal value.

characterized by atoms or groups of atoms which can occupy nearly isoenergetic configurations, so called two level systems (TLS).

Although the original TLS model was proposed to explain only very low temperature phenomena ($\leq$ 1 K), the model has subsequently been extended to a variety of phenomena in glasses which show anomalous behaviors in either magnitude or temperature-dependence relative to the same property in crystalline materials. Table 1 summarizes some of these anomalous glass properties which have been observed.

The exact microscopic structure of the TLS has not yet been determined either experimentally or theoretically for any glasses. However the studies of molecular dynamics computer simulations of the potential energy minima of atomic systems indicate that indeed TLS are a general attribute of amorphous media [25-27].

The mechanism for nonphotochemical hole burning was first proposed by Hayes and Small in 1978 and 1979 [18,21,28-30]. The mechanism is based on a two level system structure model for the glassy state. In this model, the glassy state is described by a distribution of asymmetric intermolecular double-well potentials (TLS). Figure 3 depicts schematically the NPHB mechanism. In the figure, TLS_α and TLS_β are the potential energy curves for a particular TLS interacting with an impurity molecule in its ground (α) and excited (β) electronic states. The coupling mechanism between the TLS and impurity molecules is electron-phonon coupling [31,32]. The potential energy is characterized by a barrier height V, a zero-point energy splitting Δ, and a well separation d, W is the tunneling rate, λ is the tunnelling parameter. For all of

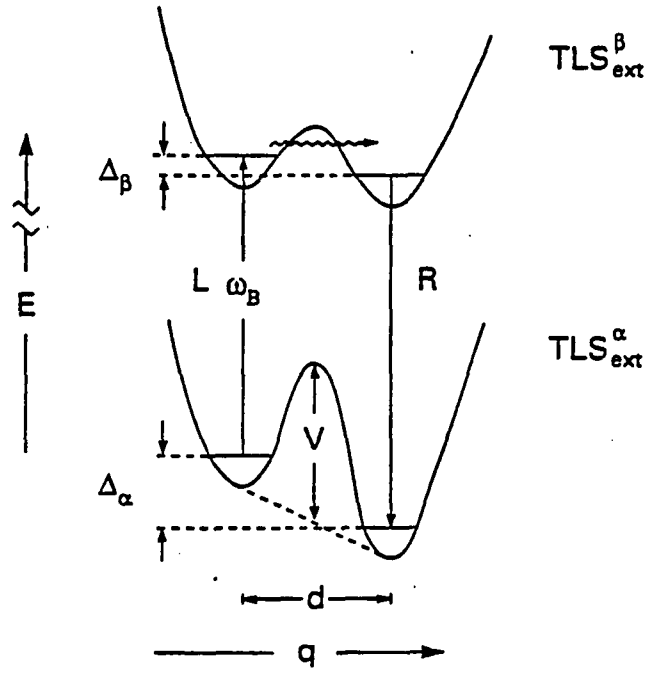

Figure 3. Potential energy curves for TLS coupled to an impurity in its ground state (α) and excited state (β). The tunneling rate between wells is given by W. ω_B is the laser frequency and d is the separation of the two wells.

these parameters there is a distribution within the glass. During the NPHB process, the impurity molecule is excited by laser light from its ground state (TLS_α) to its excited state (TLS_β), subsequently, interconversion between tunneling states occurs on a time scale that is comparable to the excited state lifetime. Therefore, the molecule which undergoes tunneling will deexcite to the other well of the TLS_α instead of going to its original well. The net result is that the absorption energy of the impurity has been shifted by an amount of Δ.

There are two types of TLS [32], extrinsic TLS (TLS_{ext}, due to impurity) and intrinsic TLS (TLS_{int}). TLS_{ext} are localized and responsible for hole formation. TLS_{int} are associated with spatially extended networks and delocalized motion and are responsible for the anomalously fast pure dephasing [33-37]. Spatially extended TLS_{int} networks have also been proposed for amorphous water [38] and vitreous silica [39]. It should be noted that TLS-model described here is based on a static distribution of asymmetric intermolecular double well potentials [40]. We will return to this point later.

Due to the inherent disorder of glasses, an observation of pure exponential decay in time which is associated with many relaxation processes is precluded and it is necessary to consider the distribution function of TLS. A large number of phenomenological functions have been developed [41-50]. Hayes et al. [18] have discussed some of these functions and indicated that the phenomenological functions pose serious difficulties for application and testing of the TLS model. Jankowiak et al.

[51] have determined that analytic forms for the TLS distribution and density of state (DOS) functions can be obtained with two reasonable assumptions. They are that a Gaussion distribution function (GDF) governs the distribution for Δ and λ and that the stochastic variables Δ and λ are independent. The analytic form for the DOS functions have been applied to optical line width and dephasing [52], thermal conductivity [53], specific heat [54], dispersive kinetics of hole growth and spontaneous hole filling [40,55,56], the experimental data for these anomalous glass properties are explainable. Based on good agreement between experimental data and theoretical calculations. Jankowiak and Small [57] argued that the two assumptions for the analytical form for the DOS are reasonable.

During the past decade persistent nonphotochemical hole burning has been shown to be a general phenomenon and has been used to study a variety of chemical and physical problems (vide supra). Despite the very considerable increase in NPHB studies during this period, however, our understanding of the NPHB mechanism has not significantly progressed beyond that provided by the simple two level system model of Hayes and Small [21,28-30] and Bogner and Schwarz [58] (vide supra). As discussed above, the simple TLS-model has proven remarkably successful in explaining the low temperature behaviors of a wide variety of properties of glasses. However, based on detailed studies of the temperature dependence of the entire hole profile of cresyl violet (CV) in polyvinyl alcohol films (PVOH), Shu and Small have argued recently that the simple TLS-model is inadequate and proposed a new mechanism [40]. By entire is

meant the ZPH plus its companion PSBH plus the anti-hole. The new experimental data show that there are different anti-hole structures for holes burnt at different temperatures (1.6 K and 8 K) and the difference is ascribed to thermally assisted photo-induced relaxation processes. The new model is based on an "outside-in" hierarchy of constrained dynamical tunneling events. The essential idea of the model involves a rapid tunneling transition of spatially extended TLS_{int} triggered by optical excitation. These "outside-shell" relaxations result in an increase in the free volume of the probe-inner shell and lead to tunneling of TLS_{ext}. The rate-determining step for NPHB is tunneling along the localized coordinates of the suitably evolved TLS_{ext}. The model is consistent with the available data. Our temperature-dependent polarized studies on cresyl violet in PVOH also suggest there is an increase for the free volumes of probe with increasing temperatures.

Although persistent holes can last for long periods of time (on the order of days), slow time-dependent hole filling (spontaneous hole filling, SPHF) is generally observed with the samples maintained at the burn temperature and in the dark [57,59]. In contrast to hole burning processes which are due to the tunneling events in excited states, SPHF results from the relaxation processes of impurities in their ground states. The average relaxation time associated with SPHF is several orders of magnitude longer than that for hole growth and seems to be affected by a saturation effect. There are two types of SPHF processes: (1) global relaxation processes associated with TLS_{int}; (2) antihole reversion that involves the TLS_{ext} directly involved in the hole formation. The

former process is called spectral diffusion which does not change the hole area but changes the hole profile. This process causes additional broadening of the homogeneous line width and may affect the measurement of the dephasing time with the hole burning technique, since the time scale of hole burning is usually longer than 1 second which is much longer than lifetime. The extent of this effect is not yet determined. The detailed studies of spectral diffusion within short time (< ms) are currently going on in several laboratories. This dissertation focuses on the second type of SPHF processes. In the following parts of this dissertation SPHF means the second type of SPHF process.

SPHF kinetics have been extensively studied for quinizarin in alcoholic glasses (photochemical hole burning) [60,61] and several nonphotochemical hole burning systems. For quinizarin in alcoholic glasses, hole width broadening was observed. No hole width broadenings were observed for nonphotochemical hole burning systems. Fearey and Small [59] have developed a model which predicts that hole filling without hole broadening may occur under certain circumstances. A dispersive kinetics approach (similar to that for hole growth) has been applied to SPHF [55]. Recently, it was discovered that the the SPHF rate depends on hole depth and shallow holes have a larger SPHF rate [56,62]. The new data raise two questions: (1) what is the physical meaning of this new finding ? (2) how to apply the dispersive kinetics theory to SPHF data ? Theoretical simulations for different hole depths will result in different sets of parameters.

The studies of relaxation dynamics of SPHF are important to completely understand the mechanism of NPHB. Although SPHF can be satisfactorily understood in terms of the standard TLS model and dispersive kinetics, the mechanism of SPHF is not well understood. Because of the lack of information on the microscopic structures of TLS, no microscopic description of the tunnelling modes has been given thus far. Studies of the effect of host deuteration on NPHB for resorufin in ethanol [63] and oxazine 720 in glycerol and PVOH [34] indicate that the TLS_{ext} coordinate, q_{ext}, is localized in the vicinity of the probe with significant amplitude of motion for the hydroxyl proton of the host. It has not been determined whether SPHF is mainly the result of reversion of the TLS^{α}_{ext} (α = ground state of the probe molecule) involved in the burn or global spectral diffusion. Polarized data for 1,4-dihydoroxyanthraquinone and tetracene in an EtOH/MeOH glass [64] indicate that no reorientation of the probe molecule occurs during the SPHF process at 4.2 K. Our temperature-dependent polarized hole burning data for CV/PVOH (see Part II.) have also shown that no significant rotation of CV molecules accompanies NPHB at 2.2 K but that a significant rotation does occur at 15 K. An understanding of the extent of correlation between the efficacies of NPHB and SPHF is important for an improved understanding of the dynamics of NPHB and SPHF and the nature of TLS_{ext}.

In addition to SPHF, the amorphous host dynamics can also be studied by means of laser induced hole filling (LIHF) [65]. By LIHF is meant the partial or complete filling or erasure of a hole burnt at ω_B which results from subsequent laser irradiation at

frequencies (ω_S) removed from ω_B. Two types of LIHF have been reported: that for which ω_B (secondary burn frequency) is located in the same electronic absorption band utilized for hole burning [28,65]; and that for which ω_S is not absorbed by the impurity and lies in the infra-red (i.e. can be absorbed by vibrational states of the host [66,67]). We refer to the two types as $LIHF_e$ and $LIHF_v$, respectively. It is the $LIHF_e$ which is studied in this work. The LIHF experiment was first performed on tetracene in an ethanol methanol glass to argue that the hole burning mechanism is non-photochemical in nature [28]. The results show that significant LIHF occurs only when the secondary irradiation frequency lies within ~ 2 cm^{-1} to the higher energy side of the primary hole at ω_{B1}. Although a mechanism for LIHF was not given in [28], it might be inferred that the LIHF results from the reversion of original burnt impurity-TLS sites back to their configurations prior to the burn, which is due to the excitation of anti-hole sites. Fearey et al [65] have intensively studied the LIHF phenomenon in systems of rhodamine 640 (R640), Nd^{3+} and D_r^{3+} in polyvinyl alcohol. Their results show that LIHF of a primary hole at ω_B occurs for both ω_S (secondary irradiation) > ω_B and < ω_B. Except for Nd^{3+}, the LIHF efficiency is significantly higher for $\omega_S > \omega_B$ than for $\omega_S < \omega_B$. For R640, the dependence of LIHF efficiency on $/\omega_S - \omega_B/$ is weak for both $\omega_S > \omega_B$ and $\omega_S < \omega_B$. The broadening of the primary hole is not observed (accuracy ≈ 6%). LIHF phenomena have also been observed for the systems of chlorophyll a and b [68,69], the chlorophyll a dimer [70], oxazine 720 [71], cresyl violet [72-74] in PVOH and resorufin and cresyl violet in alcoholic glasses [75]. Possible mechanisms involved

in LIHF were discussed by Fearey et al [65]. They argued that thermal heating, site reversion and energy transfer are not the dominant mechanism for LIHF in dye/polymer systems, and proposed a tentative model which invokes a connectivity or communication between spatially removed extrinsic (impurity) two-level systems via an ensemble of intrinsic (host) TLS.

In this dissertation the results of the detailed studies of nonphotochemical hole burning (NPHB) on cresyl violet in polyvinyl alcohol films (CV/PVOH) at low temperatures are presented. The research is directed toward the understanding of the mechanism of NPHB and the relaxation dynamics of amorphous solids at low temperatures, which involves detailed investigations on temperature-dependent NPHB, polarized NPHB, spontaneous hole filling (SPHF) and laser (light) induced hole filling (LIHF). A new mechanism for NPHB, based on an "outside-in" hierarchy of constrained configurational tunneling events, is proposed in which the time evolution of free volumes plays an important role. The model is consistent with the available data and lends itself to testing by further experiments. A high degree of positive correlation between the rates of burning and filling has been observed. It is determined that the dominant mechanism for filling is not global spectra diffusion but rather anti-hole reversion. The results of LIHF on cresyl violet in PVOH films establish that the primary mechanism of laser-induced hole filling ($LIHF_e$) is electronic excitation of the anti-hole sites produced by the primary burn at ω_B for $\omega_S > \omega_B$, which can account for the principal features of LIHF.

EXPERIMENTAL METHODS

Sample Preparation

For most studies, the samples used were cresyl violet (CV) doped in polyvinyl alcohol (PVOH) films. There are several reasons for choosing this system: (1) previous work has shown that CV undergoes nonphotochemical hole burning efficiently [64]; (2) the range of the absorption spectrum of CV covers the frequencies of available dye lasers and the He-Ne laser in this lab; (3) the polymer films do not crack even at extremely low temperature (~1.6 K), which is required for most of the experiments of this work; (4) the utilization of polymer films minimizes the scattered light and makes it easier to overlap the two light beams at sample.

The absorption maximum of CV is at 601 nm with an extinction coefficient of $\varepsilon \sim 8.3 \times 10^4$ ($Lmole^{-1}cm^{-1}$) [76]. The fluorescence maximum is at 630 nm. The absorption maximum for the sample films (CV in PVOH) utilized for experiments is at 610 nm. It should be noted that different concentration ratios of CV to PVOH result in different shifts of the absorption maximum for the sample. The smaller the CV to PVOH ratio, the more the absorption maximum shifts toward lower frequencies. Cresyl violet perchlorate (molecular weight=362) was purchased from Exciton. The polyvinyl alcohol, from Aldrich Chemicals, was 100% hydrolyzed and possessed an average molecular weight of 14000. Both chemicals were utilized as purchased, without further

purification.

The polymer film samples were prepared as follows. PVOH was dissolved into distilled and deionized hot water until a syrupy solution was attained. Then, CV was added into the polymer solution (~100 ml), in very small increments until the proper concentration was attained (~10^{-4}-10^{-5} M). Subsequently, the sample solution was poured onto the surface of a 15" x 15" glass plate and a liquid layer of ~2-3 mm was formed. The samples were allowed to air dry for 3 days. The glass plate should be placed in a proper place, such that wind, heat and any draft (under a fume hood) will not affect the sample film. The reason for choosing a relatively large glass plate is to make sure that a homogenous film can be obtained. The determination of the exact concentration is not practical, since the extinction coefficient for CV is very large (ε ~ 8.3 x 10^4 $Lmole^{-1}cm^{-1}$). Therefore, the concentration was estimated by measuring the optical density of the sample. The thickness of the prepared film was ~ 100-200 microns and was cut into sample sized pieces (4 mm x 4 mm). The samples were selected for optical clarity and uniformity. For optical uniformity, the samples were cut from the same area of the prepared film, thus separate samples can be viewed as identical. The optical densities of samples were measured with a Fourier-transform spectrometer. The samples can be repeatedly used until the optical quality becomes poor.

The sample films were mounted on a brass plate (~0.8" x 2") with five holes (d = 2mm-3mm for each hole) on it. The hole functions as window frames for burning

and probing light. Each hole was covered by a sample film.

Cryogenic Equipment

The samples were cooled to 4.2 K in a Janis Model 8-DT Super Vari-Temp liquid helium cryostat. The temperature of 1.6 K was achieved by further pumping on the helium with an auxiliary vacuum pump. The sample temperature was monitored with a silicon diode thermometer (Lake Shore Cryogenic, Inc. Model DK-500 k) calibrated over the range from 1.4 K to 300 K. The thermometer was mounted into the brass sample holder to assure good thermal contact. For temperature-dependent experiments, the temperature was changed by controlling the helium flow by slight adjustment of the throttle valve on the cryostat.

Experimental Techniques

The nonphotochemical hole burning experiments were performed with monitoring the change of absorption of the samples. For different types of experiments, different experimental setups have been utilized. Figure 4 presents a basic configuration of the apparatus employed for hole burning and hole probing. A single frequency stabilized CW ring dye laser (Coherent 699-21) which is pumped by a 5 W argon ion laser (Coherent Innova 90-5), was utilized to perform hole burning. Narrow

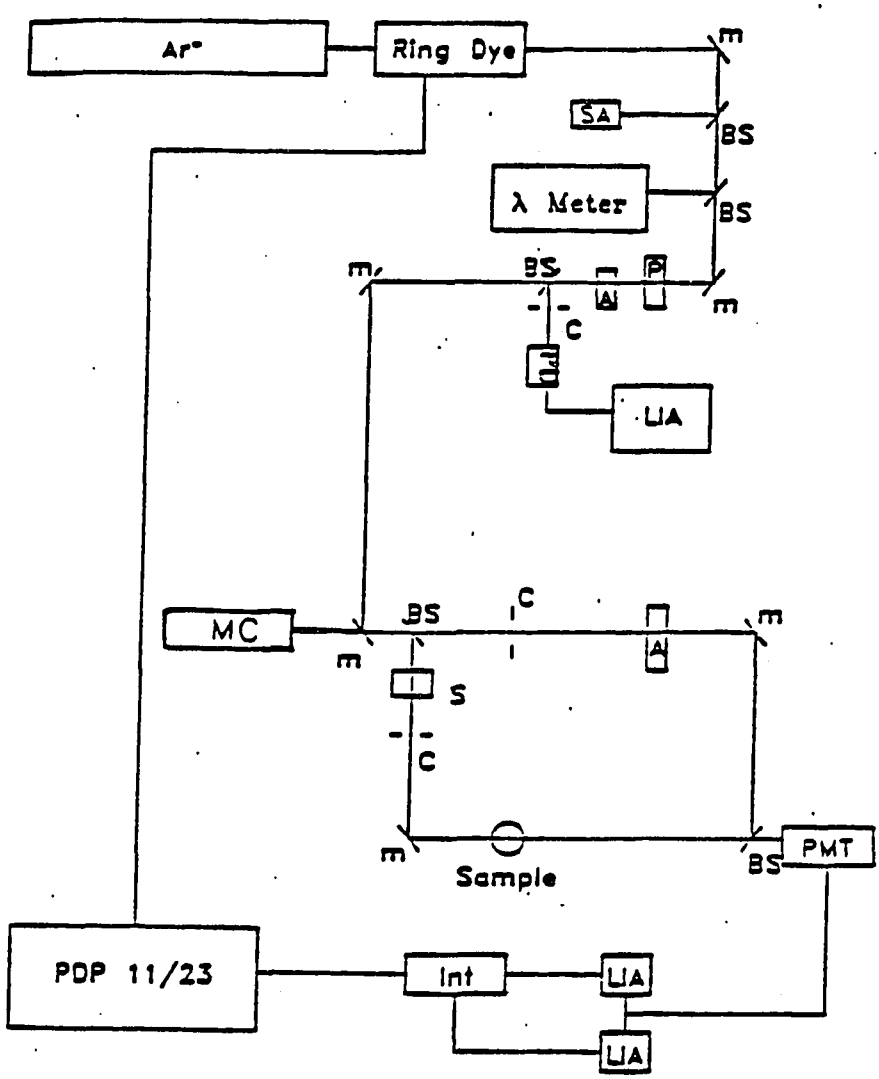

Figure 4. Experimental absorbtion/hole burning apparatus. Ar^+--argon laser; M--mirrors; SA--spectrum analyzer; λ Meter--wavemeter; P--polarizer; A--attenuator; C--chopper; PD--photodiode; LIA--lock-in amplifier; S--shutter; PMT--photomultiplier tube; INT--integrator; MC--monochromater; BS--beam splitter

laser linewidths of ~0.001 cm^{-1} are obtainable through the use of two low finesse intra-cavity etalons with free spectral ranges of 10 GHz and 100 GHz, respectively, and a three plate birefringent filter (~380 MHz). In most experiments, the laser dye used was DCM. A double beam configuration [77] was utilized for detecting the signals. The advantages of a double beam configuration are that the nonlinear frequency response of the photo-multiplier tube and intensity fluctuations can be essentially eliminated.

The output beam of the ring dye laser was split into two portions, the main portion and the small portion (~4%), with a beamsplitter. The small portion of the beam was directed into a confocal spectrum analyzer (Spectra-Physics model 470-40, FSR= 8GHz) to monitor the stability (mode hops) of the beam. The output of the spectrum analyzer was displayed on an oscilloscope. A 1/3 meter monochromator (McPherson model 218) was used to measure the wavelength of the laser beam. The power of laser beams was measured by a detecting system which consists of neutral density filters, a mechanical chopper (PAR model 125), a photodiode detector (Molectron 4P-141) and lock-in amplifier (PAR model 124 with a model 118 preamplifier). The laser beam power was adjusted with neutral density filters and a variable attenuator (NRC model 935-3). It should be noted that any tiny rotation of the chopper will cause a phase shift leading to inaccurate measurements.

The laser beam is then directed to the double beam spectrometer and split equally into a sample beam and a reference beam, with a 50% beam splitter. The intensity of the reference beam can be attenuated with a variable attenuator (NRC 925B)

to match the sample beam which experiences optical losses due to scattering by the cryostat windows and sample. The two beams are mechanically chopped with different frequencies and recombined and focused into a cooled photomultiplier tube (PMT-C 31034). The output of the PMT is then sent to two lock-in amplifiers (Ithaco model 397EO) and integrated (at multiples of 1/60 second) with an integrator (Ithaco model 385EO-2). The digitized signals are sent respectively to a ratio meter (Evans Associates card No. 4122) and a computer (Digital Equipment Corporation Micro PDP-11/23+with PT11 operating system), which convert the signals into absorbance. A chart recorder is connected to the ratio meter, for monitoring during data acquisition. The data are stored in the computer. Utilizing the technique described above, we can either monitor the optical density change (hole depth) for hole growth kinetics while the hole is burning or scan the hole profile. For the latter case, the ring dye laser can be scanned through 30 GHz ($1cm^{-1}$) by tuning an intra-cavity brewster plate. The intensities of the laser beams should be attenuated properly, so that no further hole burning occurs. It should be noted here that the burn and probe beams have exactly the same polarization. A 500W short-arc Xenon lamp (Canrad-Hanovia model 959c 1980) and a 1.5M monochromator (Jobin-Yvon HR1500) are also available for scanning the hole. The monochromator has a linear dispersion of 0.19nm/mm (2400 grooves/mm grating). It can scan a much larger frequency range than the laser, but possesses a lower resolution (~$0.2cm^{-1}$). Considerable care should be taken to overlap the probe beam path with the laser beam path. The size of the probing beam should be smaller than that of the burning beam to

ensure the obtained signals come from the burned area of the sample.

A Fourier-transform spectrometer (FTS) (Bruker IFS 120 HR) was also utilized as a detecting system. There are several advantages for using the FTS. (1) It can read spectra over a broad spectral range with high resolution (<0.002 cm^{-1}) in a short period of time. This is essential for attaining the entire hole profile. By entire is meant the zero-phonon hole plus phonon-side band hole plus antihole (~1000 cm^{-1}); (2) A good signal to noise ratio can be obtained. The FTS can take an average of 1000 scans within 8 min. operating with a 2 cm^{-1} resolution; (3) The FTS is very convenient to operate. All data acquisition and data processing are controlled by computer (ASPECT-3000/AOAKOS). There is one major disadvantage of using FTS for hole burning experiments. For certain types of samples, the white light from FTS can cause photochemical reactions of samples or disfigure the hole profiles. In such cases, great care should be taken in terms of attenuating the white light intensity, reducing the scan time or using band pass filters. In addition, reflections from the two surfaces of the film can generate interference patterns (so called 'fringes')and disfigure the entire hole profile. This effect can be completely eliminated by turning the surface of the film ~30° relative to the probe beam, provided the probe beam is not too tightly focused.

There are several important techniques that deserve a detailed discussion. Laser induced hole filling (LIHF) experiments were for the first time performed simultaneously with two separate lasers, a ring dye laser (vide supra) and a frequency and power stabilized He-Ne laser, (Spectra-Physics, model 117A). The simultaneous

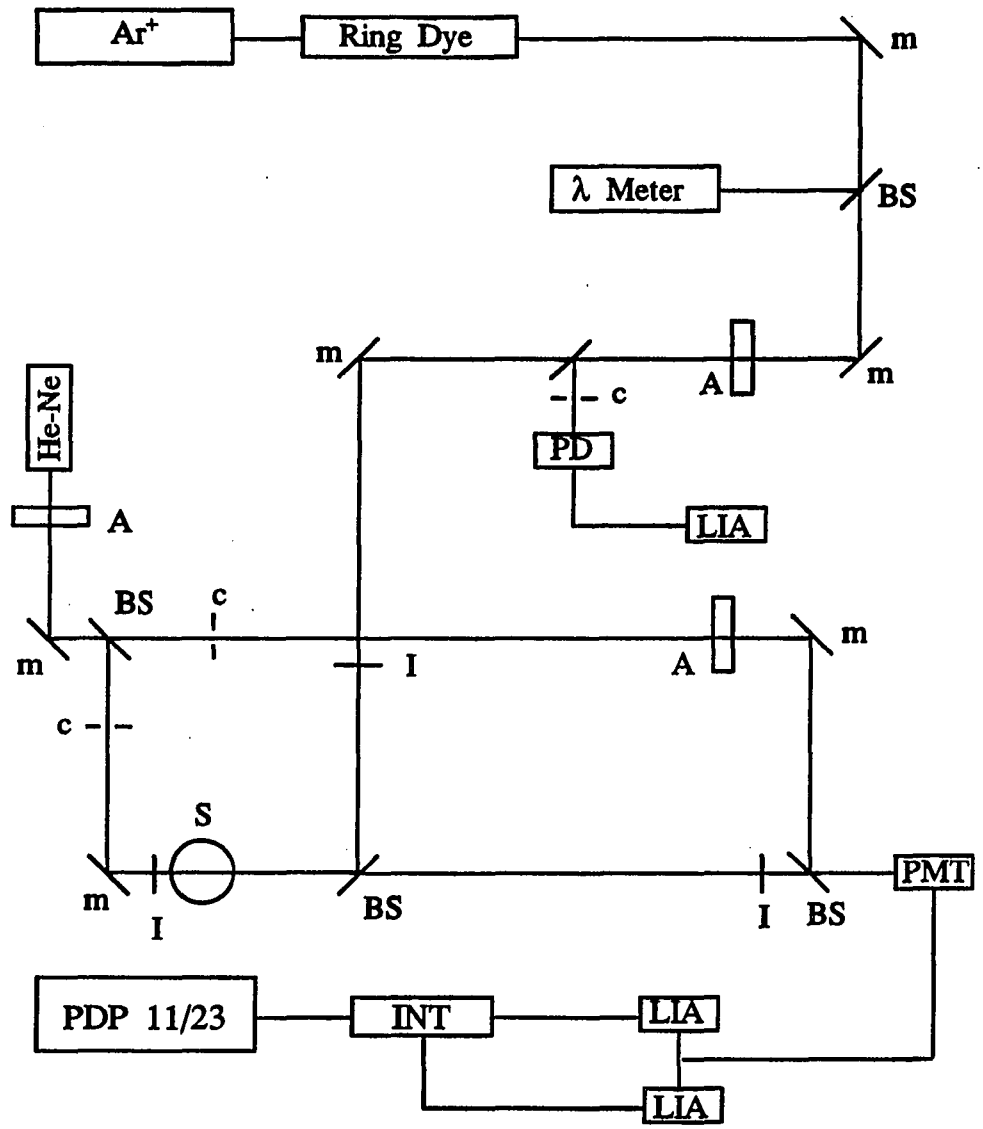

Figure 5. Experimental setup for laser induceded hole filling. Ar^+--argon laser; M--mirrors; I-- iris; λ Meter--wavemeter; A--attenuator; C--chopper; PD--photodiode; He-Ne--helium-neon laser; LIA--lock-in amplifier; sh--shutter; PMT--photomultiplier tube; INT--integrator; BS--beam splitter; S--sample

employment of two lasers allows continuous monitoring of the hole refilling while burning the secondary hole. By this manner, one can obtain a continuous LIHF kinetics curve so that the data obtained are more reliable. This is very important for determining small optical density changes, which occur for the LIHF experiment. The key requirements for the experiment are to overlap well the two laser beams on the sample and to prevent the secondary burning beam from entering the detection system. This can be achieved with two methods. In the first method, the secondary burning beam is directed through the sample in the opposite direction to that of the primary burning beam. This can be accomplished by setting a 50% beamsplitter right behind the sample. The advantage of this method is that it is easier to overlap the primary burning beam with the secondary burning beam. The disadvantage is the loss of half the signal. Reflected light from the cryostat window can be minimized by turning the cryostat slightly. In the second method, the secondary burning beam is sent in the same direction as that of the primary burning beam with a slight angle. It is difficult to ensure a good overlap of the two beams by using this method. Both methods were tested and the former one was adopted. For both methods, an iris should be placed before the detection system to block the secondary burning beam. For a good signal/noise ratio, it was found that using a larger beam size (~2 mm) was beneficial.

For the polarized hole burning experiment, two polarizers (Glan-Taylor) were used to control the polarizations of the burn and probe beams, respectively. The polarizers should be placed as close to the samples as possible, because of

depolarization caused by the steering mirrors. The cryostat window can also depolarize the light beams.

PART I. ON THE MECHANISM OF NONPHOTOCHEMICAL HOLE BURNING OF OPTICAL TRANSITIONS IN AMORPHOUS SOLIDS

30

ON THE MECHANISM OF NONPHOTOCHEMICAL HOLE BURNING OF OPTICAL TRANSITIONS IN AMORPHOUS SOLIDS

Luchuan SHU and Gerald J. Small

Chemical Physics 1990, 141, 447

ABSTRACT

New temperature-dependent nonphotochemical hole burning results are reported for cresyl violet perchlorate in polyvinyl alcohol which indicate that the simple model for spectral hole production based on a static distribution of two-level systems (TLS) provides an inadequate description. One of the key observations reported is noted to have been made for a variety of other systems. A new mechanism, based on an "outside-in" hierarchy of constrained configurational tunneling events, is proposed in which the time evolution of free volumes plays an important role. The model is consistent with the available data and lends itself to testing by further experiments.

INTRODUCTION

During the past decade persistent nonphotochemical hole burning (NPHB) of electronic transitions of molecules imbedded in amorphous (glassy) solids has been shown to be a general phenomenon and has ben used to study a variety of chemical and physical problems [1,2], the latter associated with configurational tunneling dynamics in glasses at low temperatures. Most recently NPHB has been successfully applied to photosynthetic pigments in protein complexes [3-11] and pure vibrational transitions [12-14]. Despite the very considerable increase in NPHB studies during this period, however, our understanding of the NPHB mechanism has not significantly progressed beyond that provided by the simple two-level system (TLS) model of Hayes and Small [15] and Bogner and Schwarz [16].

In this model the bistable probe-glass configurations whose phonon-assisted tunneling gives rise to hole formation are approximated by a static distribution of extrinsic asymmetric double well potentials (TLS_{ext}). The distribution is mandated by the inherent disorder of the glass and at the very least, distribution functions for the tunneling frequency and asymmetry parameter must be introduced. Given that the TLS_{ext} depend on the electronic state of the probe the model can be used to rationalize the formation of a post-burn TLS_{ext} ground state configuration that is different from and thermally inaccessible (at the burn temperature T_b) to the pre-burn configuration [17]. The tunneling which ultimately leads to hole formation is restricted to the TLS_{ext} of the

excited electronic state. In 1981 it was proposed [18] that two types of TLS play an important role in the photophysics of the optical transition, the above TLS_{ext} for hole formation and a faster relaxing type (referred to now as intrinsic TLS, TLS_{int}) responsible for the anomalously fast pure dephasing. Since then deuteration studies with hydroxylated glasses and polymers have shown that while the NPHB quantum yield is markedly reduced by deuteration of the hydroxyl proton, the pure dephasing and zero-phonon hole width are not [19-23]. Thus for molecular systems the picture which has emerged is that the TLS_{int} are associated with spatially extended networks and delocalized motion and that the TLS_{ext} coordinates are of a significantly more localized (probe-inner shell) type. Spatially extended TLS_{int} networks have also been proposed for amorphous water [24] and vitreous silica [25].

Considerable progress has been made in the development of new TLS distribution functions [26,27] which have proven successful for the interpretation of dispersive nonphotochemical hole growth [27-30,17] and spontaneous hole filling kinetics [17,13,14,30]. In these studies a Gaussian distribution function for the tunneling parameter was used to derive the distribution function for the tunneling or relaxation frequency. The superiority of the latter over earlier phenomenological functions was recently rediscovered in a study of spectral diffusion [31]. With this function and a Gaussian for the TLS asymmetry parameter, Jankowiak and Small have demonstrated that the anomalous low-temperature behaviors of the specific heat and thermal conductivity and pure dephasing of optical transitions for vitreous silica can be

understood in a consistent manner [32-34]. The internally consistent distribution function parameter values obtained for the TLS_{int} were used to calculate the TLS_{int} density of states [32], which exhibited a gap at very low energy in reasonable agreement with the specific heat data [35,36]. However, the above studies and those that have focused on the pure dephasing and spectral diffusion optical transitions have shed no light on the actual NPHB mechanism.

In one sense the TLS model introduced originally by Anderson et al. [37] and Phillips [38] in 1972 to explain the anomalous low-temperature specific heat behavior of glasses has proven frustrating since, despite its simplicity, it has proven capable of explaining the low-temperature behavior of a vide variety of physical properties [1,17]. Experiments which provide convincing evidence of TLS-TLS connectivity, i.e.take us beyond the simple model, have proven to be elusive.

In this paper we present results from a new type of NPHB experiment which we believe provides compelling evidence for the inadequacy of the TLS_{ext} model for spectral hole production. The experiment involves careful measurement of the burn temperature dependence of the entire spectrum. By entire is meant the zero-phonon hole plus its companion phonon-side band holes plus the anti-hole. A new model based on a hierarchy of constrained tunneling events is proposed which is consistent with the data. In the language of TLS, the model invokes a coupling between the TLS_{ext} and TLS_{int} and introduces the notion of an increase in the free volume of the "probe-inner shell" triggered by a reduction of the excess free volume in the "outer shell", the latter

induced by rapid TLS_{int} tunneling. The rate determining step is the tunneling of the TLS_{ext} of the inner shell following its expansion. Thus, the hierarchy of dynamical events is more or less viewed as occurring from the outside-in.

EXPERIMENTAL

Hole burning was performed with a Coherent 699-21 ring dye laser possessing a line width of ≤ 0.001 cm^{-1}. Burn intensities were measured with a Coherent model 210 power meter. Hole spectra were read with a Bruker IFS 120 HR Fourier-transform spectrometer operated at 2 cm^{-1} resolution. Spectra over the desired broad spectral range (25 scan average) could be recorded in 2 min. The same burn-read protocol was used for all burn temperatures and it was determined that spontaneous hole filling between termination of the burn and termination of the read was insignificant. The hole spectra reported here were read with unpolarized probe light of the spectrometer (burn laser polarized)). However, polarized hole spectra have been obtained [39] which show that the features of the spectra discussed, e.g., burn temperature dependence of the anti-bole profile, are independent of read polarization.

Cresyl violet perchlorate was purchased from Exciton. The polyvinyl alcohol, Aldrich Chemicals, was 100% hydrolyzed and possessed an average molecular weight of 14000. Doped polymer films (thickness~0.1mm) were prepared in a manner similar to that described in ref. [40]. The films were allowed to dry at ambient conditions for several weeks prior to use.

All burn conditions are given in the captions to the figures. The absorption spectrum of cresyl violet in PVOH at helium temperatures (not shown) exhibits an origin band at ~16400 cm^{-1} and a weaker vibronic shoulder ~ 1000 cm^{-1} to the blue.

To minimize vibronic excitation during hole burning, the burn frequencies utilized were located far to the red of the origin band maximum, at ~ 15760 cm^{-1}.

RESULTS

Spectra for burn and read temperatures (T_B, T_R) equal to 1.6 K are shown in figure 1 for burn times τ_B = 10 s, 1, 3.5 and 23.5 min. Horizontal lines to the zero-phonon hole (ZPH) labeled as a, b and c indicate the ZPH peak intensity for the three shorter burn times. The widths of the ZPH are determined by the read resolution of 2 cm^{-1}. The pseudo-PSBH (phonon-sideband hole) is asymmetric, tailing on the low energy side, and exhibits a single maximum at ω_B-25 cm^{-1} (mean phonon frequency ω_M=25 cm^{-1}). The pseudo-PSBH is due to sites that absorb ω_B via phonon sideband transitions which build on and to higher energy of their ZPL [1,2,21]. The pseudo-PSBH can be seen to tail into a weak pseudo-vibronic satellite hole at ω_B-340 cm^{-1} (at 15416 cm^{-1}), with 340 cm^{-1} being the frequency of a Franck-Condon active excited state vibration of cresyl violet [40]. The corresponding real-vibronic satellite hole is at ω_B+340 cm_{-1} near 16100 cm^{-1} and as expected, exhibits an overall profile which is similar to that at ω_B (ZPH plus pseudo-PSBH), since it builds on the latter. Although not evident in figure 1, the τ_B=23.5 min. spectrum (curved) exhibits a weak ZPH at precisely ω_B+340 cm^{-1}.

Of particular interest in figure 1 is the increase of absorption (anti-hole) associated with NPHB which appears predominantly to higher energy of ω_B. The anti-hole is very broad and would visibly extend further to the blue of $\approx\omega_B$+340cm^{-1} were it not for interference from the 340 cm^{-1} real-vibronic satellite hole. Furthermore,

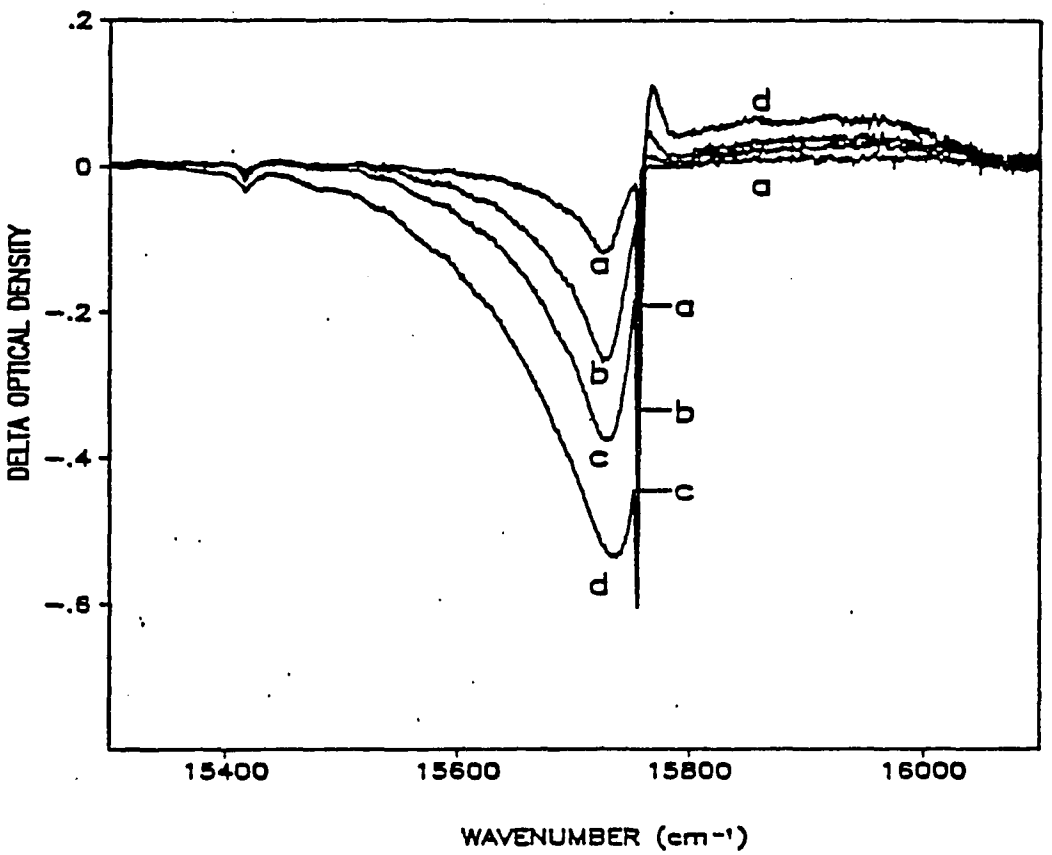

Figure 1. Hole spectra for cresyl violet burned and read at 1.6 K. Curves a-d correspond to burn times of 10 s 1, 3.5 and 23.5 min with I_B=30 mW/cm^2 (ω_B=15760 cm$_{-1}$). for the vertical scale a value, for example, of -0.6 corresponds to a 60% optical density change. Horizontal lines to zero-phonon hole (coincident with ω_B) labeled a-c indicate ZPH depth. The pseudo-phonon side hole just to the left of the ZPH exhibits a maximum at ω_B-25 cm^{-1}. The anti-hole occurs to the blue of ω_B and tails several hundred cm^{-1}, see text for further discussion

at 1.6 K the "apparent" anti-hole exhibits a sharp peak only a couple of cm^{-1} to the blue of ω_B followed by a relatively broad minimum at $\approx\omega_B$+25cm^{-1}. It will become clear that these two features are due to an interesting interplay between the anti-hole and real PSBH. It should be noted that the anti-hole is derived primarily from the pseudo-PSBH since the latter is considerably more intense than the ZPH at ω_B for the burn fluences employed. For these fluences the relative intensities of the ZPH and pseudo-PSBH cannot be directly employed to determine the linear electron-phonon coupling strength since the short burn time limit is not satisfied [41]. An important observation is that the principal features of the apparent anti-hole, i.e. the sharp maximum near ω_B, the minimum at $\approx\omega_B$+25cm^{-1}, broad maximum near 15950 cm^{-1} and isoabsorptive point at 16057 cm^{-1}, do not exhibit a strong dependence on the burn time (fluence). At 1.6 K no isoabsorptive point is observed in close proximity to ω_B.

Figure 2 presents hole burned spectra for T_B=T_R=8 K, I_B= 30 mW/cm^2 (same as fig.1) and τ_B = 30 s, 1.5, 10 and 23.5 min. From a comparison of figs.1 and 2 it is apparent that the anti-hole has undergone pronounced changes at 8 K. These include a blue shift and significant loss of amplitude just to the blue of ω_B. As a result, the real-PSBH at ω_B+25cm^{-1} is now clearly discernible in the spectra of fig. 2 along with an isoabsorptive point which appears at ω_B+50cm^{-1}. These anti-hole changes cannot be described to optical transitions from hot phonon levels since at 8 K kT≈5 cm^{-1} ≤25 cm^{-1}, the mean frequency of the optically active polymer phonons. As was the case for figure 1, the shape of the anti-hole for T_B=T_R=8 K does not exhibit a strong

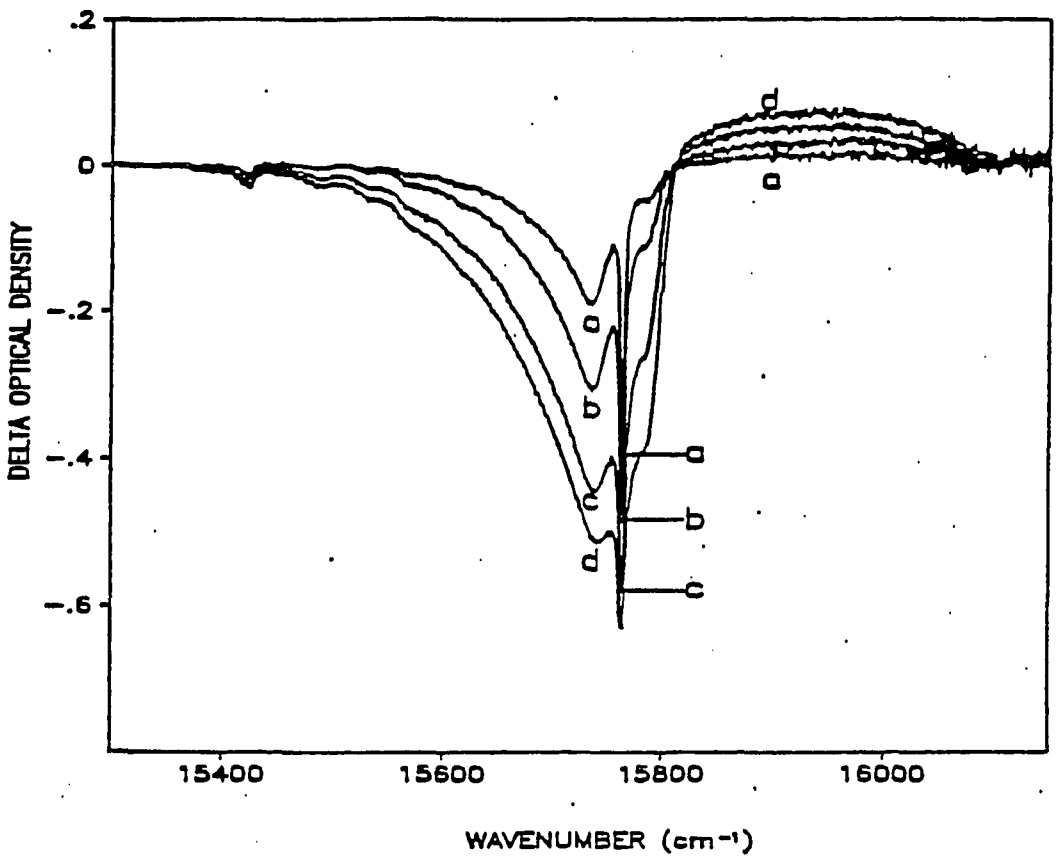

Figure 2. Hole spectra for cresyl violet burned and read at 8 k. Curves a-d correspond to burn times of 30 s 1.5, 10 and 23.5 min with I_B=30 mW/cm^2. See caption to figure 1. In contrast with figure 1 (T_B=T_R=1.6 k) the real phonon sideband hole just to the blue of the ZPH at $\approx\omega_B$+25cm^{-1} is clearly visible. See text for discussion

dependence on burn fluence.

The question arises as to whether the T_B dependence of the anti-hole is due to thermally assisted photo-induced relaxation processes or dark ground state processes that occur following electronic deexcitation of the probe. Figure 3 gives the results of a thermal cycle experiment in which burning was performed at T_B=1.6 K and read at T_R=1.6 K (spectrum a), subsequently at T_R=8 K (spectrum b) and finally again at 1.6 K (spectrum c) following completion of the temperature cycle. The loss of hole intensity produced by raising the temperature to 8 K is due primarily to "dark" thermally induced polymer-probe molecule configuration changes which serve to fill the gradient in frequency space produced by the critical burn at 1.6 K [42-44]. Nevertheless, figure 3 demonstrates that the interesting anti-hole-real PSBH interference observed in fig. 1 for T_B=1.6 K persists throughout the above temperature cycle. Therefore, the difference between the anti-holes for T_B=1.6 and 8 K, figures 1 and 2, must be ascribed to thermally assisted photo-induced relaxation processes.

Finally the results of figures 1 and 2 and those obtained at higher burn temperatures (up to T_B=15K, data not shown) can be used to show that the dispersive NPHB kinetics, as measured from the pseudo-PSBH$^{\#1}$, are independent of burn temperature, despite the dependence of the anti-hole on this temperature. A detailed discussion of the kinetics will appear elsewhere[39].

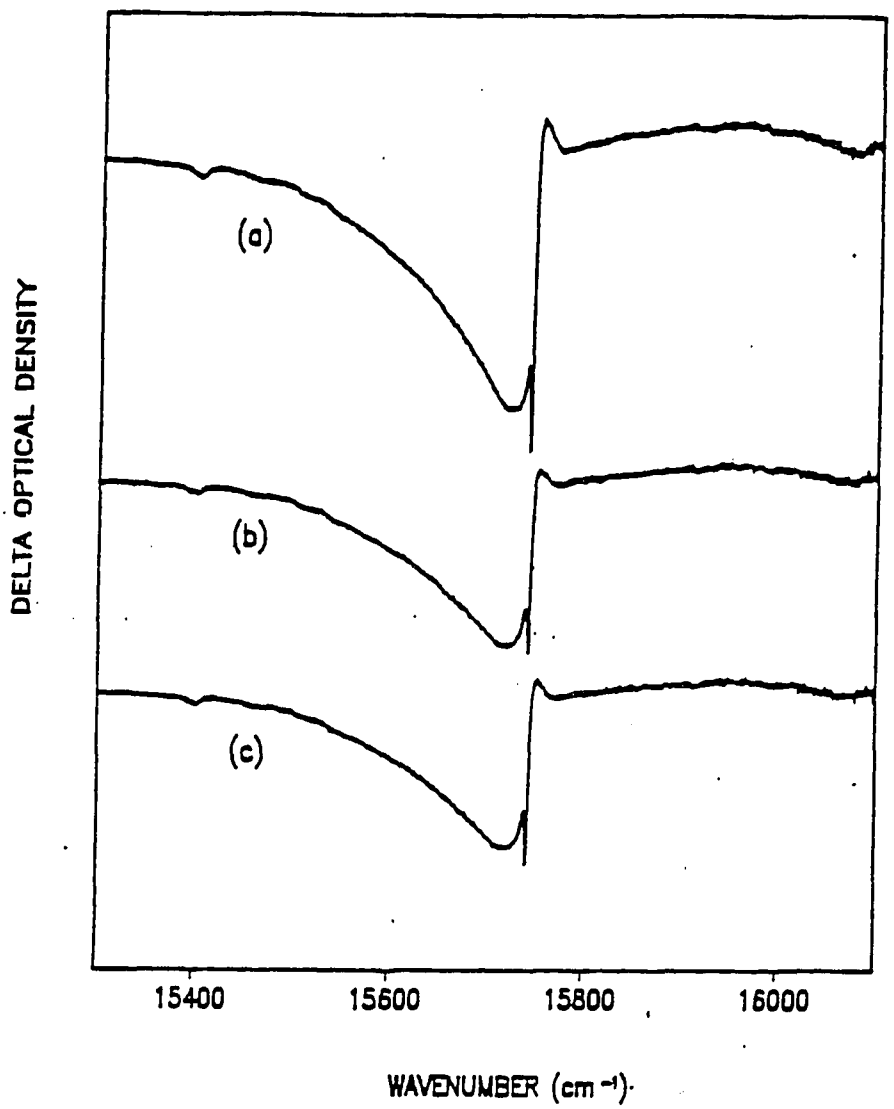

Figure 3. Thermal cycle hole spectra for cresyl violet, burn temperature of 1.6 K. Burn time=13 min, I_B=30 mW/cm^2. Spectra a-c correspond to reads at 1.6, 8 and 1.6 K, see text. Optical density changes for these spectra can be directly compared

DISCUSSIONS

A. General

The above results for cresyl violet on PVOH show that the anti-hole from NPHB occurs at energies which are higher than those of the ZPLs which undergo burning and that the shape and location of the anti-hole exhibit a very significant dependence on T_B. That the anti-hole is predominantly blue-shifted appears to be the rule rather than an exception. Such behavior has been observed for a wide variety of systems including other laser dyes (e.g., oxazine 720) in PVOH and glycerol [20], resorufin in polymethylmethacrylate [45], perylene in polyvinylbutyral, polymethane and polyvinyl chloride [16], tetracene in 2-methyl-tetrahydrofuran [46], and chlorophylls in photosynthetic antenna complexes [6-8]. We are not aware of any systems involving amorphous hosts in which electronic hole burning (NPHB) of a molecular impurity transition results in significant red shifted anti-hole intensity. The phenomenon of the blue-shifted anti-hole in NPHB would appear to be linked to the structural disorder and tunneling dynamics of the glass.

Although data are presented here for only two burn temperatures, 1.6 and 8 K, we have obtained results for other temperatures including T_B = 15 K. At 15 K, for example, the anti-hole is shifted further to the blue than the anti-hole for T_B = 8 K, figure 2. As emphasized by Bogner and Schwarz [16] and Childs and Francis [45], the

observation that the anti-hole encompasses a frequency region that is comparable in width to the inhomogeneous line broadening (several hundred cm^{-1}) is noteworthy. Our studies of cresyl violet in PVOH appear to be the first that deal with the T_B dependence of the anti-hole and its interplay with the real PSBH. However, we have recently observed similar behavior for chlorophyll a of the core antenna complex of photosystem I of green plants [47]. Thus, we believe that the marked T_B dependence of the anti-hole for cresyl violet in PVOH may be a general phenomenon which, along with the blue shift, is linked to structural disorder. These two phenomena together with other observations, vide infra, are important for improving our understanding of the NPHB mechanism for glasses.

Before considering this mechanism we briefly discuss the results in figure 4. As mentioned in the RESULTS section, the real PSBH interferes with the anti-hole. To obtain the true anti-hole profile the real-PSBH must be deconvolved from the apparent anti-hole. An approximate procedure for doing so has recently been reported by Lee et al. [41] and applied to chlorophyll a of the aforementioned antenna complex. It is based on the theory of Hayes et al. [48,49] for the hole profile which is valid for arbitrarily strong linear electron-phonon coupling. The their employs a realistic single site absorption profile in which the two-and higher-phonon sideband profiles are obtained analytically by proper folding of the one-phonon profile. In ref. [41] and for cresyl violet in PVOH the mean phonon frequency approximation is reasonable (see spectrum a of fig. 1). For the present calculations an asymmetric one-phonon profile

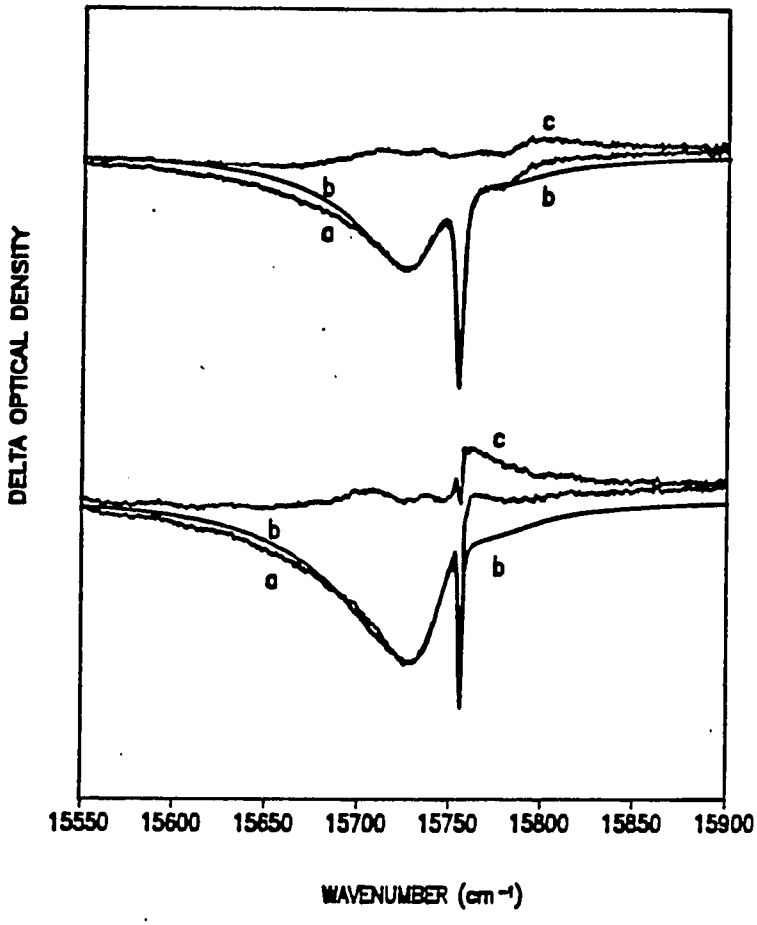

Figure 4. Theoretical fits to cresyl violet hole spectra. Upper and lower sets are for $T_B = T_R = 8$ K ($\omega_B = 15763$ cm^{-1}) and $T_B = T_R = 1.6$ K, respectively. Spectra labeled a,b and c are experimental (I_B=30 mW/cm^2), calculated (ZPH plus phonon sideband holes) and deconvolved (a-c) anti-hole spectra, respectively, see text for discussion. Note that the 8 K anti-hole maximum at is blue shifted by ≈ 30 cm^{-1} relative to its value at 1.6 K and that both anti-holes continue to tail further to the blur of 15900 cm^{-1}, see figs, 1 and 2. For both calculated (b) spectra: S=0.4; Γ_{inh}=1200 cm^{-1} with center of inhomogeneous distribution at 16430 cm^{-1}; ;ow and high energy one-phonon profile half-widths (Gaussian and Lorentzian, respectively)=14 and 27 cm^{-1}. 1.6 K calculated spectrum: γ=0.015 cm^{-1} and $\sigma I_B \phi \tau_B$=403.4 cm^{-1}; $\sigma\phi$was treated as a variable whose value, determined by the fit to the 8 K spectrum, was also used for the 1.6 K calculation (see ref. [41] for detailed discussion of method)

is employed, see figure 4, caption. The procedure of Lee et al. [41] involves characterization of the linear electron-phonon coupling by fitting the burn time dependence of the ZPH plus pseudo-PSBH (neither of which are significantly interfered with by the blue-shifted anti-hole). The parameter values determined in this way are then used to calculate the entire hole spectrum which is then subtracted from the observed spectrum to yield the anti-hole profile. Figure 4 shows the results for T_B=1.6 and 8 K for a calculative resolution equal to the experimental read resolution of 2 cm^{-1}. For both temperatures the linear electron-phonon coupling parameters used were the same, cf. caption to figure 4, and the effective NPHB quantum yield was taken to be T_B independent, as indicated by the data, cf. section RESULTS. The former parameter values were obtained by fitting the 8 K spectrum. The fit yielded a ZPL linewidth of 0.2 cm^{-1} (presumably due to both pure dephasing and spectral diffusion) at 8 K. For the 1.6 K fit the ZPL linewidth was reduced to 0.015 cm^{-1}, which is slightly smaller than the value predicted by scaling the 8 K value by the $T^{1.3-1.5}$ power law observed for the ZPH width in many organic systems [23]. For both burn temperatures the fit to the ZPH and pseudo-PSBH is quite good especially near the peak of the pseudo-PSBH and to higher energy. The deviation on the low energy tail of the pseudo-PSBH may be due to an inadequate description of the multi-phonon transition profiles and the neglect of dispersive kinetics. Because the coupling is weak, S=0.4, and the fits to the ZPH and one-phonon part of the pseudo-PSBH are good, we believe that the anti-hole profiles in figure 4 are reasonable approximations to the actual profiles since the one-phonon

sideband hole that builds on and to the blue of the ZPH is the major source of interference for the anti-hole. One observes that at 8 K the peak of the anti-hole is shifted by ≈ 30 cm^{-1} to higher energy relative to its location at 1.6 K. It must be emphasized again that at both temperatures the anti-hole extends several hundred cm^{-1} to the blue of ω_B.

This extensive tailing plus interferences due to the real vibronic satellite holes makes it impossible to determine the integrated intensity of the anti-hole (for comparison with the loss of absorption intensity due to the hole). For the NPHB of Chla in the antenna complex of photosystem I the tailing of the blue-shifted anti-hole is less severe and conservation of absorption intensity is observed [8]. Our polarized hole and anti-hole spectra for cresyl violet in PVOH (not shown) indicate that the apparent lack of conservation of absorption intensity in figures 1 and 2 cannot be attributed to rotation of cresyl violet. Although the apparent lack of conservation could be due to photochemistry, it might also be due to exceptionally large tailing of the anti-hole which may extend from ω_B further than the inhomogeneous linewidth. Support for the latter possibility comes form recent hole burning experiments on becteriochlorophyll a in the antenna complex of Prosthecochloris aestuarii [50]. The linear electron-vibration and phonon coupling is very weak for this system and simple visual inspection of the pre-burn and hole burned spectra shows that the entire absorption spectrum comprised of several exciton components is blue-shifted due to NPHB, i.e. the center of the distribution for the ZPL is blue-shifted.

We consider next the implications of our results for the NPHB mechanism. The mechanism of Hayes and Small [15], which is very similar to that of Bogner and Schwarz [16], has often been employed for qualitative discussions although it has been noted that [17] it is most likely an oversimplification. In this model the relevant parts of the probe-glass potential energy surface are approximated by a static distribution of extrinsic intermolecular asymmetric double-well potentials (extrinsic two-level systems, TLS_{ext}). For a given tunneling coordinate, q_{ext}, distribution functions are introduced for the asymmetry and barrier height parameters. We define $TLS_j^{u,l}$ as the upper and lower oscillator states for the ground ($j = \alpha$) and excited ($j = \beta$) states of the probe molecule. To explain the hole persistence at a given burn temperature, TLS_α^u and TLS_α^l must be genetically inaccessible to each other while interconversion between TLS_β^u and TLS_β^l, either by phonon assisted tunneling or barrier hopping, is competitive with $\beta \rightarrow \alpha$ relaxation. The difficulties encountered in applying the simple TLS model to the data are now considered.

When excitation (ω_B) from both TLS_α^u and TLS_α^l is considered, eight burn schemes result. Of these, four yield a blue-shifted anti-hole, the remaining four yield a red-shifted anti-hole. Equal statistical weighing for the energy level orderings associated with these schemes leads to the prediction that in the low-temperature limit the maximum depth for the ZPH or pseudo-PSBH should be 50% (less when S>0), a prediction at odds with the cresyl violet/PVOH results which show that when the Huang-Rhys factor S is taken into account it is possible to burn essentially all ZPLs (for

S=0.4, the ZPL Franck-Condon factor exp(-S)=0.65). This has been observed for other systems as well including oxazine 720 in glycerol and PVOH for which the ZPH hole growth kinetics (dispersive) has been studied as a function of T_B [20]. The T_B dependence between 1.6 and 7 K (range studied) could be explained by the T dependence of the induced absorption rate for the ZPL, i.e. the rate determining step for hole formation following excitation is T independent. The same result is obtained in the present work since the induced absorption rate for the multi-phonon transitions, which lead to the pseudo-PSBH, is T independent (due to the large width (40 cm^{-1}) of the one-phonon profile, cf. figure 4 caption). With this result and the one related to hole depth one is forced to eliminate the four burn schemes that involve "up-hill" TLS_β relaxation (tunneling by phonon absorption). However, of the four remaining burn schemes, which involve tunneling assisted by phonon emission, three result in a red-shifted anti-hole, a prediction at odds with the data for cresyl violet/PVOH and many different systems, vide supra. This together with the strong T_B dependence of the anti-hole profile and T_B independence of the hole growth kinetics and saturated hole depth for the pseudo-PSBH lead us to the conclusion that the simple TLS model with its static distribution is untenable (even when more than one type of q_{ext} is considered).

Nevertheless, in consideration of other models it is useful to define the one burn level scheme that is most consistent with the data. It involves optical excitation from TLS_α^u to TLS_β^u with $0<E(TLS_\beta^u)-E(TLS_\beta^l)<E(TLS_\alpha^u)-E(TLS_\alpha^l)$. The question is how does the probe-glass system manage to impose this inequality?

B. A new mechanism for nonphotochemical hole burning

We propose a model for NPHB that is based on the notion that hole formation and persistence ate the result of a hierarchy of constrained configurational tunneling events. In developing this model we had in mind the nature of the glassy state, i.e. its exceedingly complex potential energy surface [51], excess free volume relative to the crystalline state [52] and that at a given temperature relaxation from a particular configuration to other which are degenerate to within kT will often be kinetically frustrated [51]. Furthermore, and as already discussed, the tunneling of the spatially extended intrinsic bistable configurations of the host responsible for pure dephasing of the probe optical transition occurs on a time scale that is fast relative to the tunneling of the considerably more localized extrinsic bistable configuration that leads to hole formation. For convenience we will continue at times to use the terminology of TLS_{int} and TLS_{ext} while recognizing that a multiple minima description is more appropriate. The coordinates of the TLS_{int} and TLS_{ext} may be roughly viewed as being of the "outer shell" and "probe-inner shell" type, respectively. However, the principal difference between the TLS_{int} and TLS_{ext} is that the rapid tunneling motions of the former are considerable more delocalized than those for the latter. In fact there is no physical reason to exclude the inner shell host molecules (or even the probe) from participation in the TLS_{int} coordinates.

The essential ideas of the model are: (1) electronic excitation from the pre-burn

probe-glass configuration first triggers rapid tunneling along delocalized TLS_{int} coordinates; (2) the rapid tunneling produces an annealing effect which leads to a reduction of the excess free volume for the host molecules which interact which the probe; (3) concomitantly, the free volume for the probe undergoes an increase (since the inner shell will tend to expand due to the above free volume reduction); (4) as the free volume of the probe (and nearest neighbor inner shell atoms) increases, the TLS_{ext} potential becomes more symmetric with, for example, a lowering of the barrier height; and (5) the rate determining step for NPHB is tunneling along the localized q_{ext} of the suitably evolved (cf. fig. 4) TLS_{ext}. With our such evolution the large amplitude tunneling motion along q_{ext} would be kinetically thwarted.

Consider now the application of the above model to $\pi\pi^*$ transitions of large delocalized π-electron molecules such as cresyl violet. Firstly, the energy stabilization of the ground and $\pi\pi^*$ state due to the reduction of intermolecular atom-atom repulsions, which accompany the probe free volume increase, should be nearly identical. Secondly, it is well known that the concomitant loss of stabilization energy for the $\pi\pi^*$ state associated with attractive interactions (van der Waals, point charge-dipole, etc., which carry a significantly weaker R^{-n} dependence than that of the repulsive interactions) would be greater than that for the ground state. With these considerations it follows immediately that the model predicts a blue shifted anti-hole.

However, to explain the T_B independence of the hole growth kinetics and the saturated pseudo-PSBH depth it is necessary to propose that there is a net energy

stabilization for both the ground and excited states due to the probe free volume increase, i.e. unless the rate determining tunneling step along q_{ext} of the evolved TLS_{ext} is quasi-elastic (within kT), it must involve phonon emission. Given the considerable strain energy (due to repulsions) associated with the trapped and kinetically frustrated probe-glass pre-burn configurations, we believe that net stabilization is a physically reasonable conjecture.

The proposed NPHB model appears to be capable to explaining the T_B dependence of the anti-hole profile in terms of thermally assisted photo-induced tunneling,cf. section RESULTS. Given earlier reports on the strong effects of "dark" thermal cycling on spectral holes [21,42-44], it is reasonable to suggest that by complementing electronic excitation with small amounts of the thermal energy (e.g., T_B = 8 K $\approx$ 5 cm^{-1}) one can affect the extent of the free volume increase in the "outer-shell" region and, as a consequence, the free volume increase of the probe region.

As already discussed, the NPHB hole growth kinetics for probe molecules in hydroxylated polymers and glasses are significantly slowed upon deuteration of the hydroxyl protons, whereas pure dephasing is not. In the proposed model the rate determining step involves tunneling of TlS_{ext} which have undergone appropriate evolution in time due to the probe free volume increase. The corresponding TLS_{ext} coordinate must therefore be pseudo-localized and, for the case of hydroxylated hosts, must involve considerable amplitudes for the hydroxyl protons. But given the immense disorder for amorphous solids a distribution of TLS_{ext} tunneling frequencies would be

anticipated and, in any event, is required to account for dispersive hole kinetics. The T dependence of a broad distribution could be sufficiently weak to escape detection even when there is an observable dependence of the anti-hole profile on temperature.

CONCLUSIONS

In summary, the hierarchy of constrained events model presents an "outside-in" mechanism for NPHB in which time-dependent free volume changes play an important role. The separation of tunneling entities into fast relaxing TLS_{int} and slow relaxing TLS_{ext} was introduced about then years ago [18] in connection whit NPHB but we believe that a role for the former in hole formation has not been previously proposed. It is interesting to note that Onsager's controversial "outside-in" conjecture [53] for liquid solvent relaxation dynamics around a point charge or dipole shares certain features with the proposed model for NPHB. We note also that Cohen and Grest have argued, on theoretical grounds, that excess free volumes (voids) in glasses are intimately associated with the tunneling bistable configurations of glasses [52].

There are number of experiments that can be performed to further test the NPHB model including polarized hole burning and hole burning of molecular electronic transitions of a type other than $\pi\pi^*$. Our preliminary T_B-dependent polarized studies on cresyl violet in PVOH indicate that while reorientation of cresyl violet during NPHB is not significant for NPHB at 1.6 K, it becomes so at higher temperatures. This is consistent with an increase in the probe free volume with increasing temperatures. Further experiments are in progress and will be reported on in the near future.

ACKNOWLEDGEMENTS

The research was supported by the Division of Materials Research of the National Science Foundation under Grant No. DMR-8612270. We thank Arieh Warshel for a stimulating discussion on the chemical aspects of the proposed hole burning mechanism.

REFERENCES

1. J. M. Hayes, R. Jankowiak and G. J. Small, In: Topics in Current Physics, Persistent Spectral Hole Burning: Science and Applications, ed. E. W. Moerner (Springer, Berlin, 1988) p. 153.

2. G. J. Small, In: spectroscopy and Excitation Dynamics of Condensed Molicular systems, eds. V. M. Agranovich and R. M. Hochstrasser (North-Holland, Amsterdam, 1983) P. 555.

3. J. K. Gillie, J. M. Hayes, G. J. Small and J. H. Golbeck, J. Phys. Chem. 91 (1987) 5524.

4. K. Measuring, I. Renge and R. Avarmaa, FEBS Letters 223 (1987) 165.

5. I. Renge, K. Mauring and R. Vladkova, Biochim. Biophys. Acta 935 (1988) 333.

6. W. Köhler, J. Friedrich, R. Fischer and H. Scheer, J. Chem. Phys. 89 (1988) 871.

7. S. G. Johnson and G. J. Small, Chem. Phys. Letters 155 (1989) 371.

8. J. K. Gillie, G. J. Small and J. H. Golbeck, J. Phys. Chem. 93 (1989) 1620.

9. R. Jankowiak, D. Tang, G. J. Small and M. J. Seibert, Phys. Chem. 93 (1989) 1649.

10. I. Renge, K. Mauring and R. Avaarma, Biochim. Biophys. Acta 766 (1984) 766.

11. W. Köhler, J. Friedrich, R. Fischer and H. Scherr, Chem. Phys. Lett. 43 (1988) 169.

12. J. S. Shirk, R. Pong and A. W. Snow, Chem. Phys. 90 (1989) 3380.

13. S. P. Love and A. J. Sievers, Chem. Phys. Lett. 153 (1988) 379.

14. S. P. Love and A. J. Sievers, In: Advances in Disordered Semiconductors, ed. Fritzsche, H. (World Scientific, Singapore, 1989)

15. J. M. Hayes and G. J. Small, Chem. Phys. 27 (1987) 151; Chem. Phys. Lett. 54 (1987) 435.

16. V. Bogner and R. Schwarz, Phys. Rev. B 24 (1981) 2846.

17. R. Jankowiak and G. J. Small, Science, 237 (1987) 618.

18. J. M. Hayes, R. P. Stout and G. J. Small, J. Chem. Phys. 74 (1981) 4266.

19. H. Hardle, G. Weiss, S. Hunklinger and F. Baumann, Z. Phsik B 65 (1987) 291.

20. M. J. Kenney, R. Jankowiak and G. J. Small, to be submitted.

21. J. Friedrich and D. Haarer, In: Optical Spectroscopy of Glasses, ed. I. Zschokke, (Reidel, Dordrecht, 1986) P. 149.

22. M. Berg, C. A. Walsh, L. R. Narasimhan, K. A. Littau and M. D. Fayer, J. Chem. Phys. 88 (1988) 1564.

23. S. Völker, In: Relaxation Processes in Molicular Excited States, ed. J. Fünfschilling, (Kluwer, Deventer, 1989) P. 113.

24. L. Guttman and S. M. Rahman, Phys. Rev. B 33 (1986) 5665.

25. B. L. Fearey, R. P. Stout, J. M. Hayes and G. J. Small, J. Chem. Phys. 1983, 78 (1983) 7013.

26. R. Jankowiak and G. J. Small, J. Phys. Chem. 90 (1986) 3896; Chem. Phys. Lett. 128 (1987) 377; J. Phys. Chem. 90 (1986) 5612.

27. R. Jankowiak, R. Richert and H. Bässler, J. Phys. Chem. 89 (1985) 4569.

28. A. Elschner, R. Richert and H. Bässler, Chem. Phys. Lett. 127 (1986) 105.

29. A. Elschner and H Bässler, Chem. Phys. 123 (1988) 305.

30. R. Jankowiak, L. Shu, M. J. Kenney and G. J. Small, J. Luminescence, 36 (1987) 293.

31. K. A. Littau, Y. S. Bai and M. D. Fayer, Chem. Phys. Lett. 159 (1989) 1.

32. R. Jankowiak and G. J. Small, Phys. Rev. B 37 (1988) 8407.

33. R. Jankowiak, J. M. Hayes and Small, Phys. Rev. B 38 (1988) 2084.

34. R. Jankowiak, G. J. Small and B. Ries, Chem. Phys. 118 (1987) 223.

35. J. C. Lasjaunias, R. Maynard and M.J. Vandorpe, J. Phys. (Paris) 39 (1978) C6-973.

36. J. C. Lasjaunias, R. Maynard and D. Thoulouze, Solid State Commun. 10 (1972) 215

37. P. W. Anderson, B. I. Halperin and C. M. Varma, Phil. Mag. 25 (1972) 1.

38. W. A. Phillips, J. Low Temp. Phys. 7 (1972) 351.

39. L. Shu and G. J. Small, to be published.

40. B. L. Feaney, T. P. Carter and G. J. Small, J. Phys. Chem. 87 (1983) 3590.

41. I.-J. Lee, J. M. Hayes and G. J. Small, J. Chem, Phys. 91 (1989) 3413.

42. A. Guiterrez, G. Castro, G. Shulte and D. Haarer, In: Organic Molecular Aggregates, eds. P. Reineke, H. Haken and H. C. Wolf (Springer, Berlin, 1983) p.

43. J. Friedrich and D. Haarer, Angew. Chem. 23 (1984) 113.

44. G. Schulte, W. Grond, D. Haarer and R. Silbey, J. Chem. Phys. 88 (1988) 679.

45. A. F. Childs and A. H. Francis, J. Phys. Chem. 89 (1985) 466.

46. R. Jankowiak and H. Bässler, J. Mol. Electron. 1 (1985) 73.

47. I.-J. Lee, P. Lyle and G. J. Small, to be published.

48. J. M. Hayes and G. J. Small, J. Phys. Chem. 90 (1986) 4928.

49. J. M. Hayes, J. K. Gillie, D. Tang and G. J. Small, Biochim. Biophys. Acta 1988,932, 305.

50. S. G. Johnson and G. J. Small, to be published.

51. F. H. Stillinger and T. A. Weber, Science 225 (1984) 983.

52. M. H. Cohen and G. S. Grest, Phys. Rev. Lett. 45 (1980) 1271.

53. M. Maroncelli, J. MacImmis and G. R. Fleming, Science 243 (1989) 1674, and references therein.

PART II. ON THE MECHANISM OF NONPHOTOCHEMICAL HOLE BURNING: CRESYL VIOLET IN POLYVINYL ALCOHOL FILMS

ON THE MECHANISM OF NONPHOTOCHEMICAL HOLE BURNING: CRESYL VIOLET IN POLYVINYL ALCOHOL FILMS

Luchuan Shu and Gerald J. Small

Submitted to the Journal of Optical Society of America
November, 1991

ABSTRACT

Polarized non-photochemical hole burned spectra of cresyl violet in polyvinyl alcohol films are presented for different burn temperatures (T_B). For T_B = 15 K, but not 2.2 K, a significant rotation of cresyl violet is indicated. The broad and tailing anti-hole is observed to depend on T_B. The quantum efficiencies (distributions thereof) for the zero-phonon hole and pseudo-phonon sideband are very similar, proving that the phonons created via excitation of the phonon sideband are not important for hole burning. The quantum efficiency is independent of T_B over the range studied, 1.6-15 K. Over this range, essentially 100% of the zero-phonon lines can be burned. The results show that the standard two-level system (extrinsic) model for non-photochemical hole burning is inadequate. They are discussed in terms of an "outside-in" hierarchy of configurational relaxation events model [Shu and Small, Chem. Phys. *141*, 447 (1990)] as well as others.

INTRODUCTION

Persistent non-photochemical hole burning (NPHB) of electronic transitions of molecules imbedded in amorphous solids has proven useful for the study of configurational relaxation processes of glasses at low temperatures ($\lesssim$10 K) [1] and high resolution vibronic spectroscopy (e.g. of chlorophylls in protein complexes [2,3]). The efficacy of NPHB in glasses stems from their intrinsic structural disorder which allows for the production of a probe-glass configuration, following completion of the ground to excited state and back to ground state cycle, which is different from and more or less kinetically inaccessible to the pre-excitation (pre-burn) configuration quantum. Yields for NPHB are generally low with the highest average value observed being 5×10^{-3} for oxazine 720 in polyvinyl alcohol [4] (structural disorder leads to dispersive kinetics [5-11]). When measured against the S_1-state lifetime of oxazine 720, the average value of the NPHB rate constant is 1.9×10^6 s^{-1}. In sharp contrast, pure dephasing occurs with a rate that is about 10^{10} s^{-1} at ~4 K [1,11-14]. This indicates that the configurational relaxation processes leading to dephasing and hole burning are distinct [13,15]. It is generally held that the "bistable" configurations responsible for NPHB are introduced by the probe, i.e. are extrinsic (ext), while those largely responsible for dephasing at sufficiently low temperatures are intrinsic (int) to the glass.

The standard two-level system (TLS) tunnel model has been extensively used for the interpretation of the anomalous thermal and acoustic properties of glasses at very

low temperatures ($\lesssim$1 K) [16-18], the pure dephasing and spectral diffusion of optical transitions [1,19-24], and the dispersive kinetics of NPHB [1,4,7,11,25-27] and spontaneous hole filling (SPHF) [7]. In this model the tunnelling configurations are approximated by a distribution of asymmetric intermolecular double well potentials (TLS_{int} or TLS_{ext} depending on the problem at hand) with varying barrier height and asymmetry. The distribution is assumed to be temperature independent (static) and connectivity between TLS is neglected. Furthermore, it is assumed that both TLS_{ext} and TLS_{int} can be characterized by a single coordinate, q_{ext} and q_{int}. When used with sufficiently accurate distribution functions, the standard model can account for the temperature dependences of thermal properties and pure dephasing and the dispersive kinetics of NPHB and SPHF. Thus, certain types of measurements appear to be incapable of taking us beyond the standard model, which is an obvious over simplification.

The standard TLS_{ext} model for NPHB proposed by Hayes and Small [28,29] is illustrated in Figure 1. The superscripts α and β label the TLS_{ext} for the ground and excited electronic state of the probe. In the figure, excitation of the zero-phonon transition is pictured as occurring on the left (L) with the critical L $\rightarrow$ R relaxation taking place in the excited electronic state (β). Note that the transition frequency of the absorber in the post-burn configuration is higher than for the pre-burn configuration. The distribution of probe sites conforming to the energy-excitation scheme of Figure 1 would lead to a blue-shifted anti-hole. If instead, excitation corresponded to the R-side,

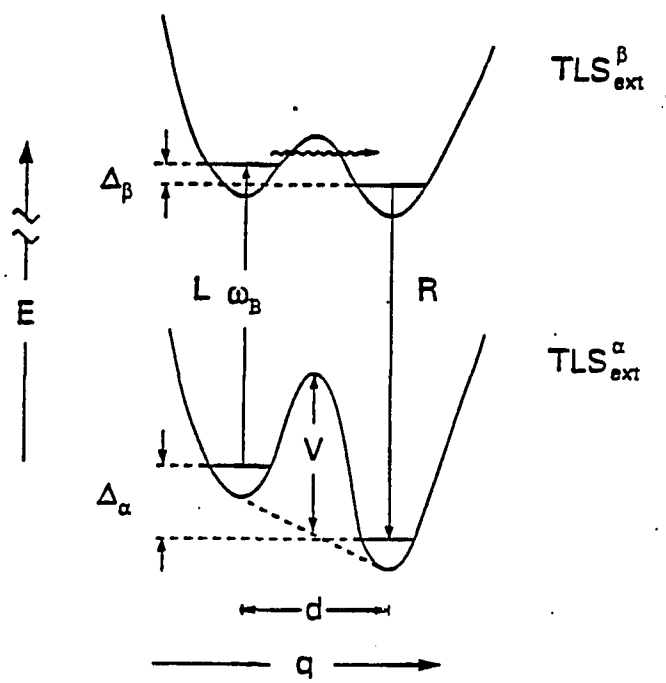

Figure 1. Potential energy diagrams for a two level system coupled to an impurity in its ground state (α) and excited electronic state (β). Δ is the asymmetry parameter, V the barrier height and q the intermolecular coordinate. ω_B is the laser frequency

the anti-hole would be red-shifted. There are six more energy-excitation schemes including two that obtain from Figure 1 with $\Delta_\alpha < \Delta_\beta$ and the relative energies of the R and L minima of α and β still correlated. The remaining four correspond to the uncorrelated case. Of the eight schemes, four yield a blue-shifted anti-hole and four yield a red-shifted anti-hole. According to the mechanism of Hayes and Small, hole burning occurs at very low temperatures by phonon-assisted tunnelling in state β (the persistence of the hole being a consequence, for example, of a higher TLS_{ext} barrier for state α). In the $T_B \rightarrow 0$ K limit, hole burning must occur by phonon emission. Of the four schemes that conform to this scenario, only one corresponds to a blue-shifted anti-hole (cf. Figure 1). That is, the anti-hole should be predominantly red-shifted in the low temperature limit provided the four schemes are equally probable. One further point is that one would expect to be able to burn only 50% of the ZPL (zero-phonon lines) at ω_B in the low temperature limit provided all eight schemes are equally probably. In fact, a lesser degree of burning might be anticipated since equilibration between the tunnel states of TLS^{α}_{ext}, which is rapid relative to the time scale of the experiments (seconds), could exist for a subset of the TLS_{ext} at the burn temperature T_B [30].

It was recently demonstrated for oxazine 720 in polyvinyl alcohol films and glycerol glasses, however, that essentially 100% of the ZPL [31] could be burned for $1.6 \leq T_B \leq 7.0$ K (the range studied) and, furthermore, that the anti-hole of NPHB lies predominantly to the blue [4]. The same observations have been made for chlorophyll

a in the light harvesting complex of photosystem I [32]. The S_1 states of these probes are $\pi\pi^*$ and it has been noted that [33] the anti-hole from NPHB lies predominantly to the blue for all other $S_1(\pi\pi^*)$ states which have been studied, including those of tetracene in 2-methyl-tetrahydrofuran [34], resorufin in polymethylmethacrylate [35], and perylene in polyvinylbutyral, polymethane and polyvinyl chloride [36]. (To the best of our knowledge, NPHB has not been reported for an $^1n\pi^*$ state of any molecule.) The above two observations cannot be reconciled in terms of the standard TLS_{ext} model of Hayes and Small or that of Bogner and Schwarz who proposed that [36] NPHB is the result of barrier hopping in TLS^{α}_{ext} triggered by a non-equilibrium distribution of phonons localized at the probe following $S_1 \rightarrow S_0$ electronic relaxation (see section IV for further discussion). In light of these results, the early thermal annealing and burn temperature dependent data for tetracene in an ethanol/methanol glass [30] can be taken as evidence that the standard TLS_{ext} model for NPHB is too simplistic.

The same results together with new burn temperature dependent hole spectra (encompassing the zero-phonon hole (ZPH), phonon sideband holes (PSBH) and anti-hole) for cresyl violet (CV) in PVOH led us to recently propose a new NPHB mechanism [33]. Like the aforementioned systems, CV/PVOH exhibits a broad and tailing blue-shifted anti-hole and, furthermore, one that shifted further to the blue as T_B was increased from 1.6 to 15 K. The change in shape of the anti-hole with T_B showed that a substantial subset of the sites which yield stable (persistent) anti-hole sites when burned at 1.6 K do not yield the same stable anti-hole sites at higher burn temperatures.

The data available on the linear electron-phonon coupling indicated that close to 100% of the ZPL could be burned at temperatures between 1.6 and 15 K (one expects that at a sufficiently high burn temperature this would not be possible due to rapid spontaneous hole filling in the ground state). The above mechanism retains the notion that at a given temperature there is a more or less well-defined TLS_{ext} coordinate, q_{ext}. (From deuteration studies of resorufin in ethanol [13,37] and oxazine 720 in glycerol and PVOH [4] it is known that, at $T_B \sim 1.5$ K, q_{ext} involves a large amplitude of motion of the hydroxyl proton of the host). It was proposed that persistent NPHB occurs as a result of an outside-in hierarchy of dynamical events, which are triggered by electronic excitation, and result in an increase in the free volume of the probe for the post-burn configuration. The free volume increase would explain the blue-shifted anti-hole since $^1\pi\pi^*$ states typically undergo a red shift in going from the gas to the condensed phase. The free volume increase for the probe in its inner shell of host molecules was proposed to occur following relatively fast configurational relaxation processes in the outer shell which lead to a reduction in the excess free volume of the outer shell. With reference to Figure 1, the TLS^{β}_{ext} shown, which leads to $L \rightarrow R$ relaxation by phonon emission (operative at 0 K), is viewed in the model as having evolved on a relatively long time scale (if it is not preformed).

The above mechanism stimulated the experiments whose results are reported here. Of particular importance are the results of the burn temperature dependence of the linearly polarized hole spectra. The spectra show that the TLS_{ext} coordinate(s) itself is

dependent on T_B and that, at higher temperatures, it involves a substantial rotation of CV in its inner shell. Nevertheless, the quantum yield of NPHB does not depend strongly on T_B between 1.6 and 15 K (range studied). The extent to which these results support the above mechanism of NPHB is discussed. Alternative mechanisms are also considered. Finally, the extended scans of the hole spectra demonstrate that integration of the spectra out to several thousand cm^{-1} to the blue of the burn frequency is required in order to determine whether or not absorption intensity is conserved during hole burning.

EXPERIMENTAL

Hole burning was performed with a Coherent 699-21 ring dye laser possessing a linewidth of < 0.001 cm^{-1}. Burn intensities were measured with a Coherent model 210 power meter. Hole spectra were recorded with a Bruker IFS 120 HR Fourier-transform spectrometer possessing a resolving power of 10^6. However, because the spectra presented correspond to quite hard burns (zero-phonon hole saturated), the spectrometer was operated at a resolution of 2 cm^{-1}. This is more than adequate to resolve the phonon-sideband hole and anti-hole profiles. The poorer signal/noise ratio in the spectra near 500 nm is due to the weak intensity of probe light from FT light source. For the polarization studies one Glan-Taylor polarizer was inserted in the laser beam and another between the FT spectrometer white light (source) and sample. The polarization extinction ratio was > 500. The scans were initiated 20 s after termination of the burn. In order to avoid deleterious effects of white light filling on the polarization ratios, the probe light was reduced in intensity to 2.5 mW/cm^2 and spectra over the desired broad range recorded in 70 s (15 scan average). Under these conditions no difference in the polarization ratios for read parallel (to laser polarization) first, perpendicular second and vice-versa was observed. Details concerning the liquid helium cryostat and sample preparation are given elsewhere [33].

RESULTS

A. General features of the hole spectra for cresyl violet in PVOH

A persistent hole spectrum of CV in PVOH, which extends from 14,000 to 20,000 cm^{-1}, is shown in Figure 2, $T_B = T_R$ (read temperature) = 1.6 K. The burn frequency (ω_B) used was 15837 cm^{-1} and is coincident with the ZPH which can be seen as a spike riding on the high energy side of the pseudo-phonon sideband hole (PSBH) at $\omega_B - 25$ cm^{-1} [33]. This is more evident in Figures 3-5. Under the burning conditions used, cf. Figure caption, the fractional optical density (OD) change at the peak of the pseudo-PSBH is 0.43. The spectrum corresponds to a hard burn (close to saturated) so that the entire hole profile centered at ~ $\omega_B - 25$ cm^{-1} is due predominantly to the broad (relative to the ZPH) pseudo-PSBH even though the Huang-Rhys factor S is < 1, see the following paper. It is only in the short burn time limit that the intensity of the pseudo-PSBH relative to that of the ZPH can be used to determine S [32]. Noting that the horizontal line corresponds to $\Delta OD = 0$, it follows that the broad anti-hole from NPHB, which onsets just to the blue of the ZPH with an apparent maximum at $\omega_B + 230$ cm^{-1} stems predominantly from the pseudo-PSBH. We say apparent because the relatively sharp dip at $\omega_B + 25$ cm^{-1} to the left of the maximum of the anti-hole is due, to a considerable extent, to an interference between the real-PSBH, which builds in a Franck-Condon sense on the ZPH, and the anti-hole [33]. The theoretical simulations

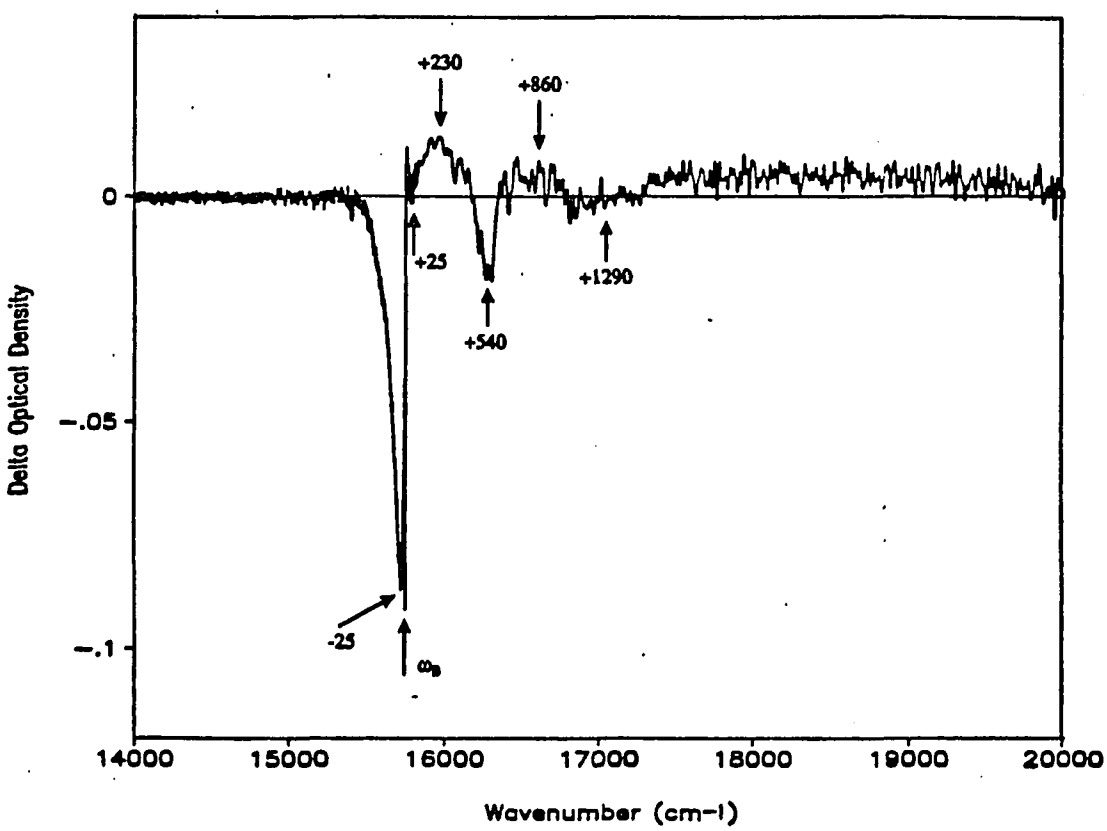

Figure 2. Hole burned spectrum for cresyl violet in PVOH burned and read at 1.6 K. Burn time (t_B) is 4 minutes and I_B = 30 mW/cm^2. Pre-burn OD is ~0.2 at 15837 cm^{-1} (ω_B). The vertical scale gives the optical density change and the horizontal line indicates ΔOD = 0. The anti-hole lies predominantly to the blue of ω_B, cf. text

presented in this reference indicate that the true maximum of the anti-hole at T = 1.6 K is at ~ ω_B + 10 cm^{-1} (35 cm^{-1} to the blue of the pseudo-PSBH maximum). This anti-hole would extend further to the blue were it not for the interference from a real vibronic hole at ω_B + 540 cm^{-1} (solid arrow), whose own anti-hole contributes to the positive ΔOD at ω_B + 860 cm^{-1}. The right-most arrow indicates a broad vibronic hole which is contributed to by several fundamental vibrations. We return to a discussion of the vibronic hole structure shortly. From the spectrum in Figure 2 and those from other extended scans (not shown) it is apparent that the vibronic hole (right-most arrow) is followed to higher energy by an exceedingly broad region of positive absorption (ΔOD). To determine whether or not the total absorption is conserved we find that it is necessary to integrate out to ~4000 cm^{-1} to higher energy of ω_B. Integration of the spectrum in Figure 2 out to 20,000 cm^{-1} showed that the regions of negative ΔOD are compensated by regions of positive ΔOD to within 10%. We conclude, therefore, that the mechanism of hole burning is nonphotochemical.

Figure 3 shows a NPHB spectrum of CV/PVOH obtained at a higher signal to noise ratio than in Figure 2. The real vibronic holes labeled a-i correspond to excited state CV modes with frequencies of 345, 540, 580, 670, 820, 925, 1160, 1365, and 1515 cm^{-1}. Feature g is likely due to two or more weak and unresolvable holes. The vibronic hole frequencies are measured relative to the peak of the "origin" pseudo-PSBH at ω_B – 25 cm^{-1} [38]. These frequencies are in reasonable agreement with those determined on the basis of pseudo-vibronic hole structure [39]. Figure 3 reveals that

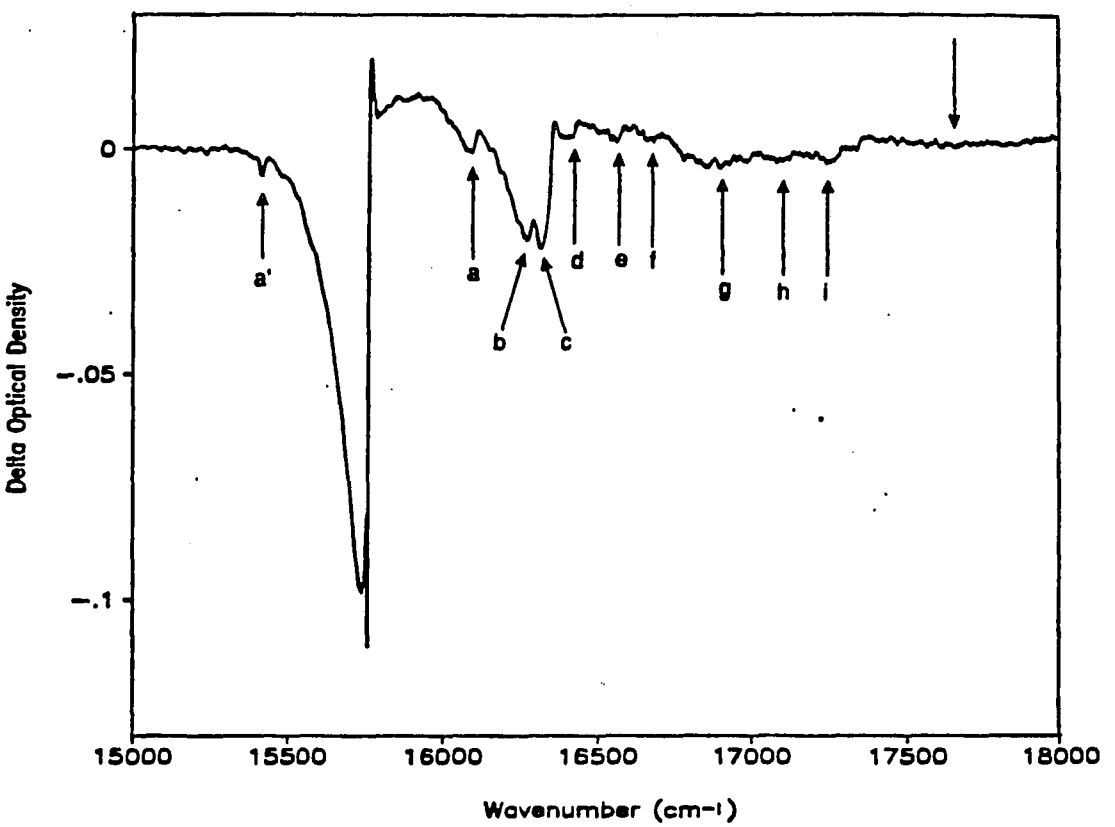

Figure 3. Hole spectrum for cresyl violet in PVOH burned and read at 1.6 K. I_B = 30 mW/cm^2 and t_B = 20 minutes. The higher signal to noise ratio allows for clearer identification of the real vibronic satellite holes (a-i). A weak pseudo-vibronic satellite hole (a′) can be seen at ω_B − 340 cm^{-1}

the dominant vibronic hole seen in Figure 2 is a doublet (b,c). The polarized hole spectra shown later reveal that the 540 and 580 cm^{-1} modes carry the same polarization as the origin hole. This, together with the fact that the S_1 state of CV is strongly electric-dipole allowed, indicates that the two modes derive their intensity by the Condon mechanism. Under the assumption that the ground electronic state mode frequencies do not differ from the above by more than ~20%, the intensities of the 540 and 580 cm^{-1} real-vibronic holes relative to that of the origin hole yield a Franck-Condon factor of about 0.1 for both modes. The FC factors for the other modes labeled in Figure 3 are considerably smaller (estimatable from their vibronic hole intensities relative to those of the 540 and 580 cm^{-1} vibronic holes). The very weak and broad vibronic hole indicated by the downward solid arrow is due mainly to combination of the 540/580 hole with the g-i vibronic holes. The relatively sharp feature labeled as a′ is the pseudo-vibronic satellite hole [40] that corresponds to the 345 cm^{-1} real vibronic satellite hole (feature a). The former is actually a ZPH whose frequency should, therefore, be measured relative to ω_B and is 340 cm^{-1}. It is observed as a ZPH because it is being read in the short burn time limit, i.e. its pseudo-PSBH has not yet evolved (the Franck-Condon factor for the 345 cm^{-1} mode is ~0.03).

B. Polarized hole spectra

We have obtained linearly polarized hole spectra of CV/PVOH for burn and read

temperatures of 2.2, 8.0 and 15 K. We give here only the results for 2.2 and 15 K obtained with a burn intensity of 30 mW/cm^2 for burn times of 2, 4, 8 and 12 minutes; Table I.

The polarized spectra for $T_B = T_R = 2.2$ K are shown in Figures 4 and 5 for burn times of 4 and 12 minutes, respectively. The read resolution used to record these spectra and those that follow was 2.0 cm^{-1}. No base-line correction has been made for the spectra shown. The solid and dashed line spectra correspond to a read polarization that is parallel and perpendicular to the burn polarization respectively. The OD of the absorption spectrum at $\omega_B - 25$ cm^{-1} (peak of the pseudo-PSBH) is 0.16. The values of the polarization factor, $\rho = (I_{\parallel} - I_{\perp})/(I_{\parallel} + I_{\perp})$, given in Table I for the anti-hole of the origin hole were measured at the apparent maximum of the anti-hole (solid arrows in Figures 4 and 5). The ρ-value for the pseudo-PSBH was measured at its peak position, Table I. From this table it is apparent that the ρ-value for the anti-hole is greater than that for the pseudo-PSBH for all burn fluences. This observation is discussed in section IV. Pertinent to the discussion is Figure 6 in which polarized spectra are shown for a much lower burn fluence ($I_B = 4$ mW/cm^2, $t_B = 1$ min). The ρ-value for the pseudo-PSBH, measured at its peak position, is 0.40 (considerably higher than the corresponding values in Table I) while the ρ-value for the ZPH at ω_B is 0.26.

Polarized spectra for $T_B = T_R = 15$ K are shown in Figures 7 and 8 for burn times of 4 and 12 minutes. Comparison of these spectra with those of Figures 4 and 5 (see also Table I) clearly reveals that at 15 K the ρ-values for the anti-hole (measured at the

Table I.

Time (min)	2	4	8	12	
ρ_p	0.20	0.12	0.14	0.08	T = 2.2 K
	0.21	0.16	0.16	0.10	T = 15 K
ρ_a	0.46	0.43	0.40	0.33	T = 2.2 K
	0.25	0.11	0.15	0.10	T = 15 K
ΔOD(PSBH)	0.34	0.40	0.46	0.48	T = 2.2 K
	0.32	0.38	0.44	0.46	T = 15 K

ρ_p: degree of polarization for PSBH (at peak of PSBH)
ρ_a: degree of polarization for anti-hole
ΔOD(PSBH): fractional OD change for PSBH (at its maximum)

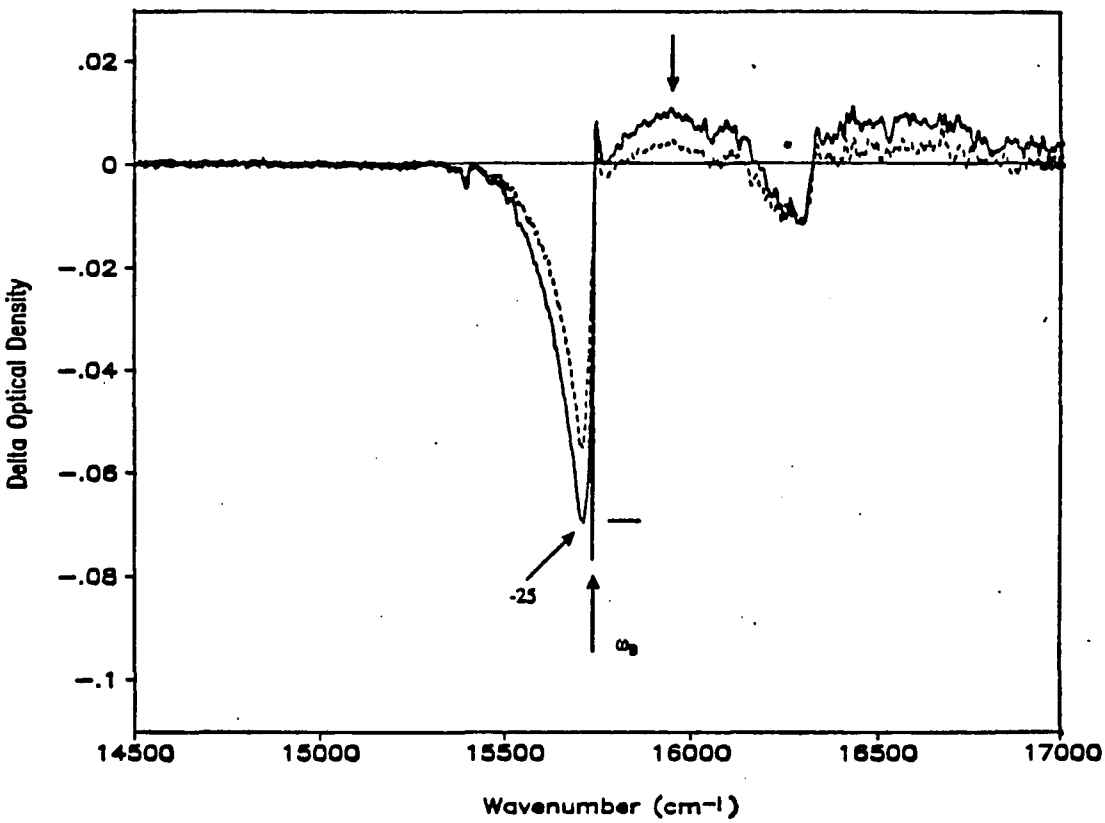

Figure 4. Polarized hole spectra for cresyl violet in PVOH burned and read at 2.2 K. The solid line and dashed line spectra correspond to a read polarization that is parallel and perpendicular to the burn polarization respectively. I_B = 30 mW/cm^2 and t_B = 4 minutes. ω_B = 15735 cm^{-1} (pre-burn OD ~ 0.18). The horizontal bar of the zero-phonon hole indicates ZPH depth for the dashed spectrum

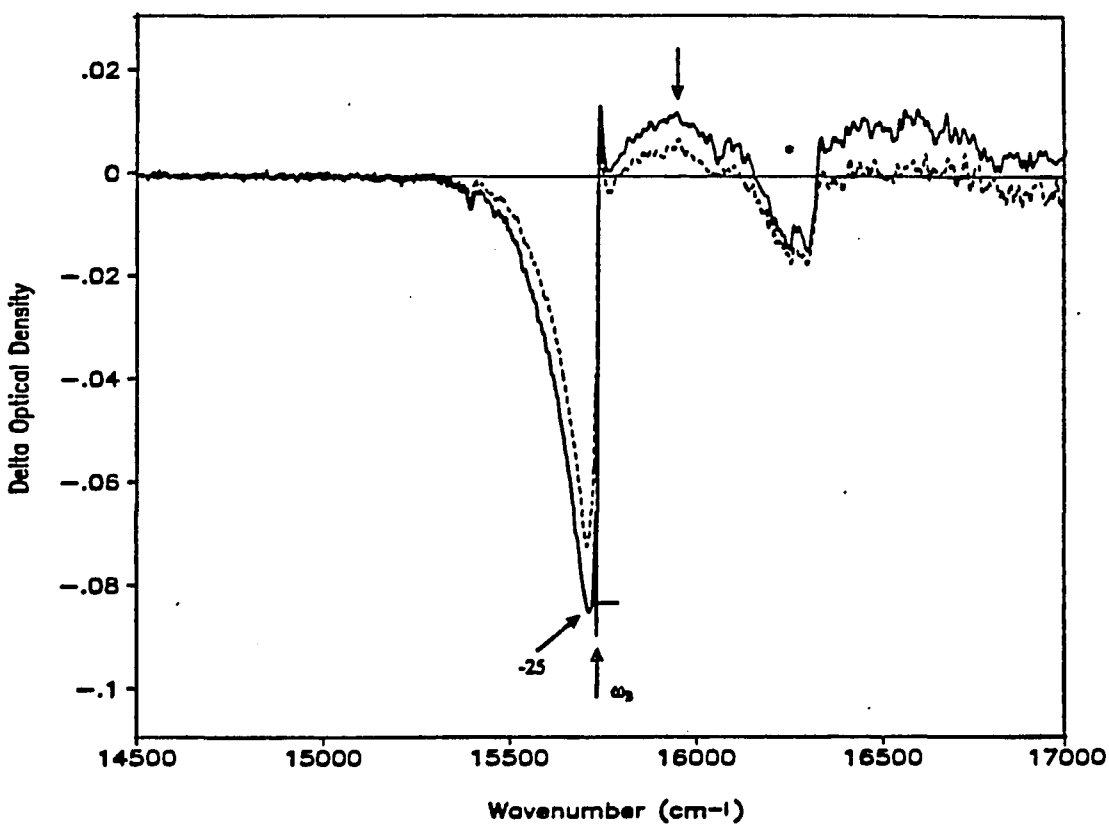

Figure 5. Polarized hole spectra for cresyl violet in PVOH for a burn time of 12 minutes. The other conditions are the same as those for Figure 4

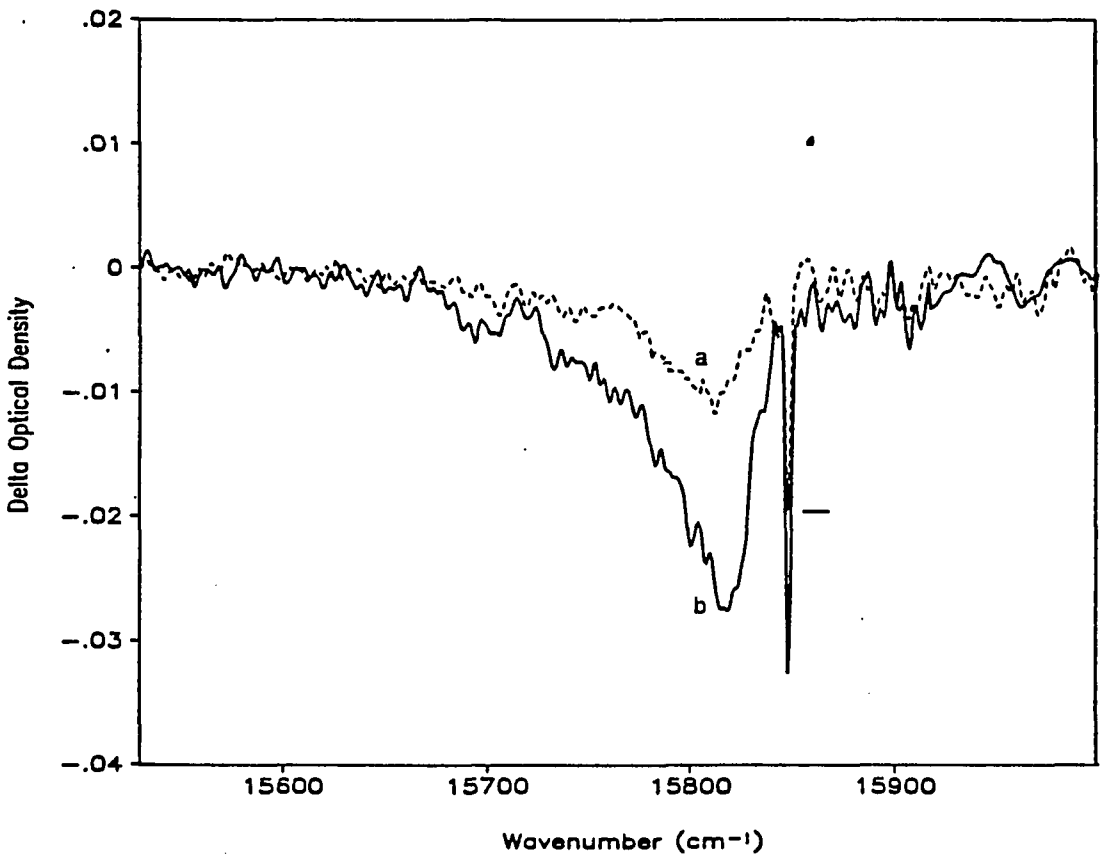

Figure 6. Polarized hole spectra burned for cresyl violet in PVOH and read at 1.6 K for a lower burn fluence (I_B = 4 mW/cm^2, t_B = 1 min.). The horizontal bar indicates the ZPH depth for the dashed spectrum

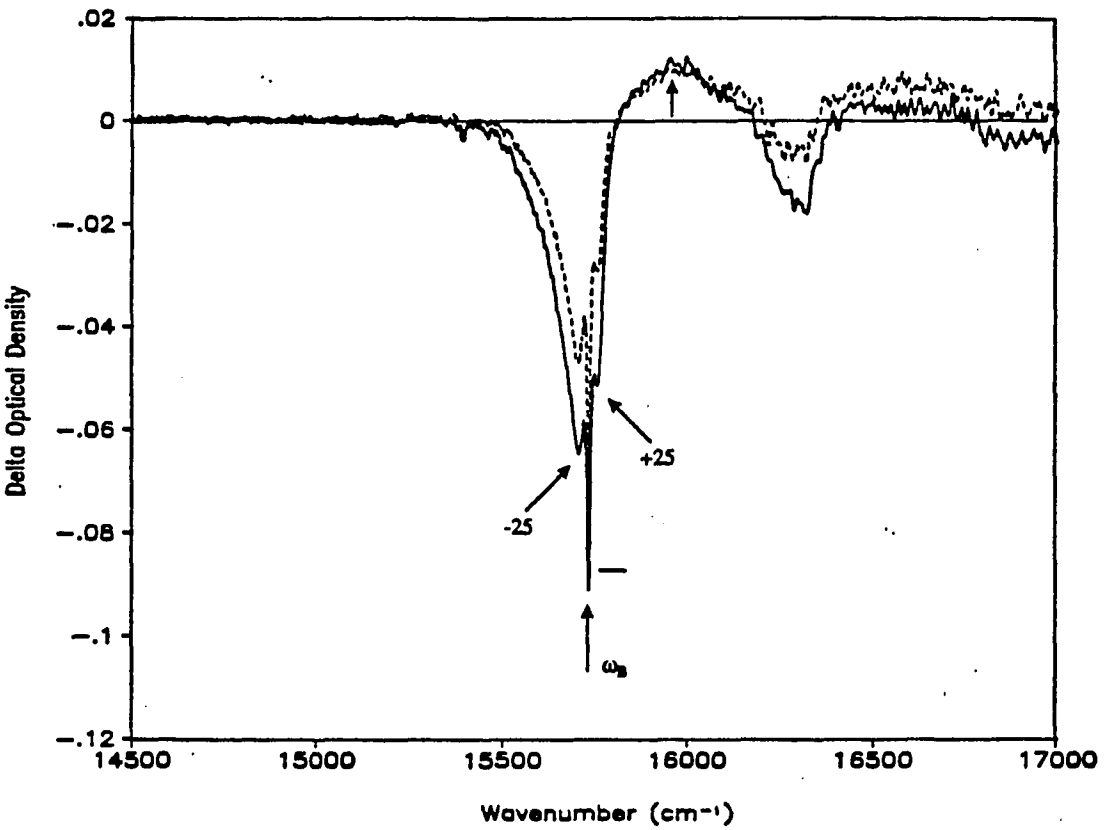

Figure 7. Polarized hole spectra of cresyl violet in PVOH burned and read at 15 K. t_B = 4 minutes with other burn conditions the same as those given in the caption to Figure 4

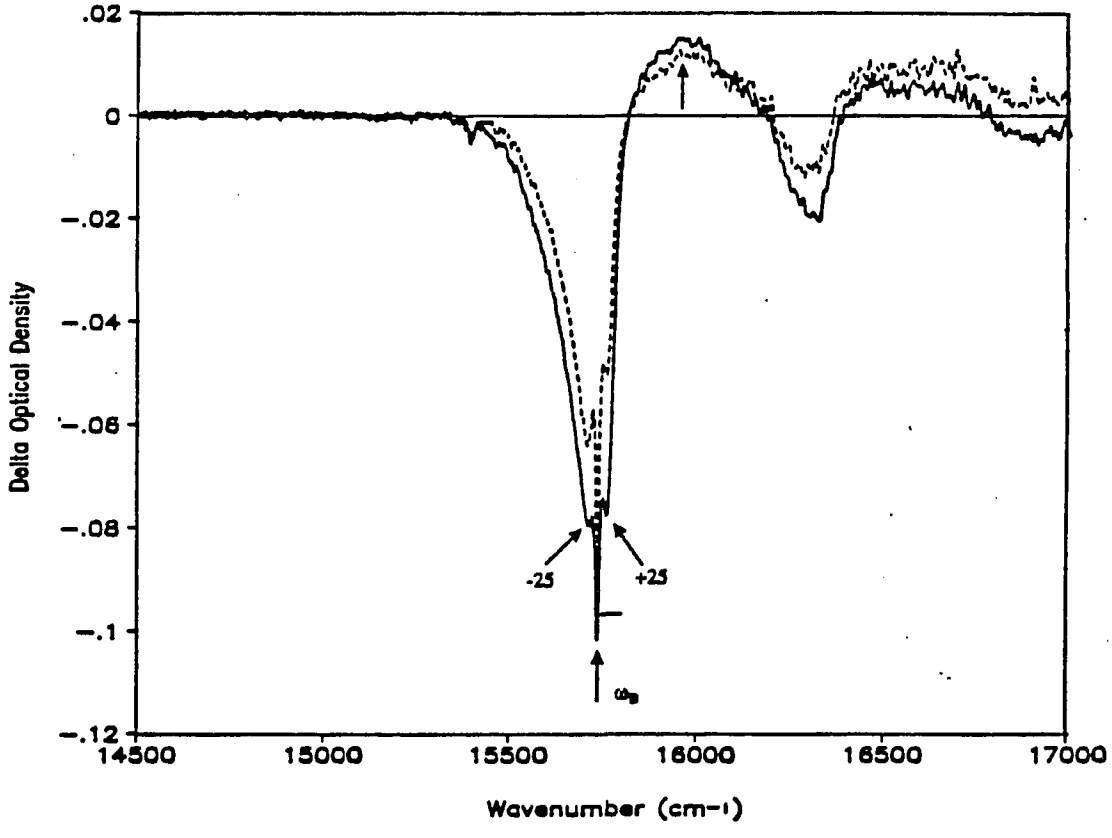

Figure 8. Polarized hole spectra of cresyl violet in PVOH burned and read at 15 K. t_B = 12 minutes with other burn conditions the same as those given in the caption to Figure 4

solid arrow) have undergone a substantial decrease while the ρ-values for the pseudo-PSBH at the two temperatures are not significantly different. Since the vibronic bands (holes) carry the polarization of the origin band hole, the decrease in the ρ-value of the anti-hole at 15 K results in the ΔOD of the parallel polarization being lower than that of the perpendicular polarization over a frequency range extending from the low energy tail of the 540/580 cm^{-1} real vibronic hole to over 2000 cm^{-1} to higher energy of ω_B. This interesting result was confirmed by a second set of experiments. Although the uncertainty for the ρ-values in Table I is ~ ± 20% (estimated from a comparison of the results from two sets of experiments) the spectra show that NPHB at 15 K involves a substantial rotation of CV in its inner shell.

DISCUSSIONS

A. Hole, anti-hole profiles and polarization

The hole spectra of Figures. 4, 5, 7 and 8 and the results of Table I were obtained with burn fluences (I_b = 30 mW/cm^2, t_B = 2, 4, 8, 12 min) sufficiently high to provide easily measurable anti-hole profiles. The ρ-values for the ZPH coincident with ω_B are not included in Table I because the ZPH is saturated (attains maximum depth) at a burn fluence several orders of magnitude lower than those used in the present paper (see following paper, referred to hereafter as II). Thus, low ρ-values (≈ 0) for the ZPH would be expected [41]. Additionally, theoretical simulations are required for a determination of the ∥ and ⊥ ZPH intensities when the burns are sufficiently hard to produce a ZPH as a spike on intense PSBHs, as is the case here. We note also that the ZPH at ω_B in the spectra are broadened by saturation and the read resolution of 2.0 cm^{-1}. Utilization of the pseudo-PSBH (which corresponds to the burning of a broader distribution of ZPL following excitation of the corresponding sites via their PSB) avoids saturation and read resolution broadening. Nevertheless, the burn fluences used are too high to satisfy the short burn time limit at which ρ = 0.5 [41]. Table I also gives the fractional OD changes of the pseudo-PSBH for T_B = 2.2 and 15 K and the four burn times. However, the actual changes associated with the ZPL contribution to the absorption are considerably larger since the Huang-Rhys factor S ~ 0.7 (see Part III).

Exp(−S) is approximately the fraction of the absorption due to ZPL when the region being considered lies on the low energy side of the absorption origin band (as is the case here, see Figure 1 of Part IV). Since exp(−0.7) = 0.5, the fractional OD changes given in Table I should be multiplied by a factor of 2. Thus, for example, the change is −0.9 for t_B = 12 min and T_B = 2.2 and 15 K. According to ref. (41) the expected ρ-value is −0.1, which is close to the values observed. However, the ρ-values observed for t_B = 2 and 4 min are low compared to the predicted values. For example, for t_B = 2 min and T_B = 2.2 and 15 K, the predicted ρ-value is −0.3. Although the discrepancy between this number and 0.2 (cf. Table I) may be due, in part, to experimental uncertainty, the fact that the kinetics of NPHB are dispersive is also a factor for consideration (the calculations of ref. (41) do not take into account dispersive kinetics which will cause a lowering of the predicted ρ-values especially for burns that are not close to saturated).

The polarized hole spectra of Figure 6 were obtained with a burn fluence that is over a factor of ten lower than the lowest value used for Table I. The ρ-value of the pseudo-PSBH (0.1 actual fractional OD change for parallel polarization) is 0.40 which can be compared with the theoretical prediction of 0.45 [41]. The ρ-value for the ZPH is low (0.26) due, to a considerable extent, to the fact that the ZPLs contributing to the center of the ZPH have been completely burned. A further complication for the utilization of the pseudo-PSBH is that for the harder burns one expects contributions originating from the 2- and higher-phonon absorption transitions to the intensity of the

peak of the pseudo-PSBH at $\omega_B - 25$ cm^{-1} (position of the maximum of the PSBH from one-phonon transitions). An accurate calculation of the maximum ρ-value of the pseudo-PSBH for a given burn fluence is quite complicated and very lengthy when the hole growth kinetics are dispersive [41] and interferences to the hole structure from anti-holes exist. For this reason we have not attempted such. Here we are primarily interested in the marked polarization change for the anti-hole which accompanies an increase in the burn temperature.

Nevertheless, the observation that for $T_B = 2.2$ K the ρ-values for the anti-hole of the origin hole (centered at $\omega_B - 25$ cm^{-1}) are higher than those of the pseudo-PSBH deserves some comment. As mentioned earlier, the ρ-values for the anti-hole were measured at the apparent maximum of the anti-hole (solid arrows in Figures 4 and 5). A possible explanation emerges when one considers the possibility that the shape of the anti-hole profile may change with increasing burn fluence, although the results for CV/PVOH provide no support for this suggestion because of the severe interference from the 540/580 cm^{-1} vibronic holes to the origin anti-hole (it is likely that this anti-hole may tail out to ~ $\omega_B + 1000$ cm^{-1}, vide infra). It is conceivable that the anti-hole sites which absorb at and to lower energy of the apparent maximum of the anti-hole may correspond to those pre-burn sites that are easier to burn. That is, measurement of ρ at the apparent anti-hole maximum might correspond to a shorter burn time measurement than indicated by the depth of the pseudo-PSBH. Along this line, the harder to burn sites would yield anti-hole sites that tend to absorb in the high energy tail of the

anti-hole. To test this hypothesis one requires a probe molecule whose S_1 state is characterized by weak vibronic activity. The chlorophylls would appear to be ideal since their most intense vibronic mode (~750 cm^{-1}) has an S-value of only 0.05 [32]. Experiments on the chlorophylls are planned.

We consider next the pronounced change in the polarization characteristics of anti-hole as the burn temperature is increased from 2.2 to 15 K (some reduction in the ρ-value is already evident at 8.0 K, data not shown), Figures. 4, 5, 7 8. We note first that the origin anti-hole at 15 K is blue-shifted relative to the anti-hole at 2.2 K. This results in the observation of the real-PSBH at ω_B + 25 cm^{-1} at 15 K, Figs. 7 and 8. The apparent maxima of the origin anti-holes lie at ω_B + 210 and ω_B + 230 cm^{-1} for 2.2 and 15 K, respectively. According to the calculations of ref. (33), which take into account the interference from the real-PSBH, the true maximum of the anti-hole at 2.2 K would occur at ≈ ω_B + 10 cm^{-1}. The true maximum at 15 K would be at ≈ ω_B + 50 cm^{-1}, which is blue shifted by 40 cm^{-1} relative to its value at 2.2 K. With the fact that at both 2.2 and 15 K the pseudo-PSBH can be burned essentially to maximum depth (determined by S) in mind, the blue shift of the anti-hole with increasing burn temperature points to the inadequacy of the standard TLS_{ext} model. That is, the distribution of stable anti-hole sites is strongly temperature dependent. The T_B-dependent NPHB and thermal annealing data for tetracene in ethanol/methanol glasses [30] are consistent with this finding.

The interference from the vibronic holes to the origin anti-hole makes it difficult to

estimate by inspection the extent to which the anti-hole tails to higher energy of its apparent maximum, cf. Figures 4, 5, 7, 8. The asterisk at the position of the 540/580 cm^{-1} vibronic hole in Figures 4 and 5 is useful in this regard. It gives an approximate value for the intensity of the origin anti-hole in parallel polarization which would be observed in the absence of the vibronic hole. The calculation assumes that the vibronic hole carries the same polarization ratio ($I_{\parallel}$:$I_{\perp}$) as the pseudo-PSBH (i.e. the Condon approximation is used) and that the anti-hole for perpendicular polarization is close to $\Delta OD = 0$ at the frequency of the asterisk. It seems that the anti-hole could well tail out to $\approx \omega_B + 1000\ cm^{-1}$. From the pseudo-vibronic hole spectrum of CV/PVOH given in ref. (33) one can estimate that Γ_{inh} for the origin absorption band is $\approx 1000\ cm^{-1}$. A value of 1200 cm^{-1} was used for the simulations of the hole profiles presented in ref. (33). Thus, the frequency extent of the anti-hole indicated above is physically reasonable in that it does not exceed Γ_{inh}.

From the spectra shown and the data in Table I it is clear that the origin anti-hole is significantly less well polarized at 15 K than 2.2 K. The high ρ-values for the anti-hole at 2.2 K indicate that CV does not undergo a substantial rotation during the configurational relaxation that leads to burning. This is not the case at 15 K although we are reticent to give an angle for the rotation given the difficulties associated with the interpretation of the ρ-value for the anti-hole (in addition, there may be a distribution of values for this angle). Nevertheless, a rotation of a few tens of degrees is indicated. The observation that a small amount of thermal energy (15 K = 10 cm^{-1}) has a

profound effect on the photo-induced NPHB mechanism is interesting. In ref. (33) it is shown that the change in anti-hole shape produced by burning and reading at 8 K cannot be achieved by burning at a very low temperature and warming to 8 K. That is, the change is the result of thermally assisted photo-induced relaxation processes.

B. Mechanism of non-photochemical hole burning

The observations that essentially 100% of the ZPL can be burned at very low and higher temperatures, the anti-hole is predominantly blue-shifted and dependent on T_B and the inner shell relaxation coordinate (q_{ext}), which is associated with NPHB, depends on the burn temperature point to the inadequacy of the standard TLS_{ext} model, see Introduction. As discussed in the Introduction, the recent NPHB mechanism of Shu and Small [33] is based on an outside-in hierarchy of configurational relaxation events which culminate in an increase in the free volume of the probe in its inner shell (i.e. a weakening of the overall probe-host interaction which, for a $\pi\pi^*$ state, would lead to a blue-shifted anti-hole). Their model retains the notion that there is a more or less well-defined q_{ext} at any T_B and that the relaxation along q_{ext} occurs in the electronically excited state, i.e. TLS^{β}_{ext} (Figure 1). An important precedent for such an excited state relaxation process, which involves H-bond rearrangement, is provided by the mixed crystal system thioindigo in benzoic acid [42]. Although deuteration experiments on CV/PVOH were not performed, such experiments for resorufin [13] and oxazine 720 [4]

show that q_{ext} involves a substantial amplitude of motion for the hydroxyl proton of the host at $T \approx 1.6$ K. Given the similarity in structure of CV and oxazine 720 one expects this to also be the case for CV.

The observation that at higher burn temperatures NPHB involves a significant rotation of CV provides some support for the mechanism of Shu and Small. Interestingly though, the hole burning quantum efficiency (distribution thereof) does not exhibit a significant dependance on T_B, an observation which was made [4] for oxazine 720 in PVOH for $1.6\ K \leq T_B \leq 7.0\ K$ (range studied). In Figure 9 hole growth data points are shown for several burn temperatures. For these experiments the growth of the pseudo-PSBH was monitored. The advantage of this is that the one-phonon profile is broad (~40 cm^{-1}) and, thus, the absorption cross-section may be safely assumed to be independent of temperature between 2.2 and 15 K (the mean phonon frequency is 25 cm^{-1}). The dashed curve is a theoretical fit based on a model of dispersive kinetics which will be discussed shortly. The lack of dependence on T_B of the quantum efficiency is especially interesting since significant rotation of CV accompanies hole burning at 15 K but apparently not at 2.2 K. One possible explanation for this is that the rate determining step is the same at both temperatures, i.e., for example, H-bond breaking due to tunnelling. At the higher burn temperatures the additional thermal energy could conceivably trigger a rotation of CV which is relatively fast.

The "outside-in" model of NPHB originated, in part, from the observation that 100% of the ZPL can be burned in the low temperature limit. With the critical

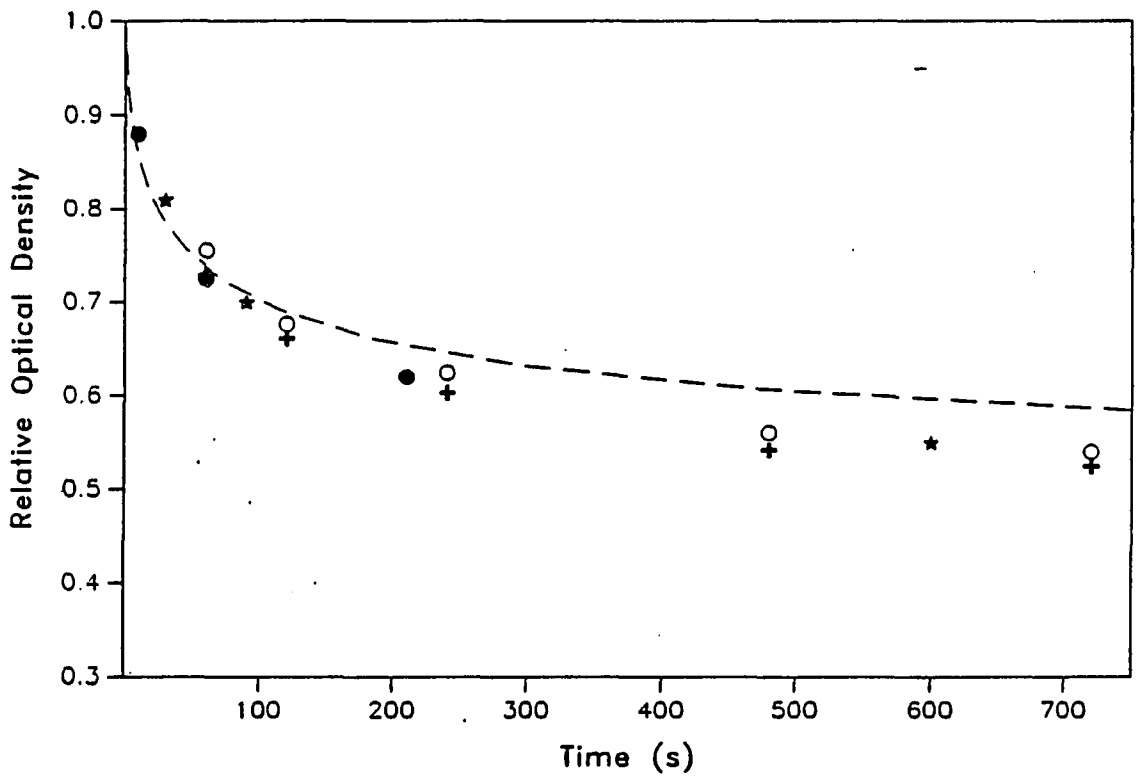

Figure 9. Temperature dependent hole growth curves for the pseudo-PSBH. I_B = 30 mW/cm^2. Dots, stars, crosses and circles represent the data for burn temperatures of 1.6, 2.2, 8.0 and 15 K, respectively. The dashed curve is the simulation based on dispersive kinetics theory, cf. text

relaxation occurring in TLS^{β}_{ext} and initiating from total zero-point level, it is clear that the phonon-assisted tunnelling must involve phonon emission (creation) in the low T limit, i.e. the picture in Figure 1. This energy level-excitation picture is one that, in general, would have to have evolved due to fast configurational relaxation processes in the outer shell. Given the excess free volume of a glass and that the excess free volume may be intimately connected with the bistable configurations (TLS_{int}) [33], Shu and Small suggested that electronic excitation of the probe may lead to a reduction in the excess free volume of the outer shell (energy lowering) which would "draw out" the inner shell and, therefore, increase the free volume of the probe so as to yield a blue-shifted anti-hole, Figure 1.

We discuss next an alternative mechanism for NPHB. Bogner [36] proposed (within the framework of the standard TLS_{ext} model) that the relaxation along q_{ext}, which leads to hole burning, occurs in TLS^{α}_{ext} (α = ground electronic state) by barrier hopping induced by a nonequilibrium distribution of phonons localized at the probe. These phonons are presumed to be produced by electronic relaxation of the S_1 state to intramolecular vibrational sublevels of the ground state which, in turn, undergo relaxation to yield phonons that couple to the TLS_{ext} modes. No consideration was given to TLS^{β}_{ext} and its role in determination of the shifting of the anti-hole. In principle, this model could explain the results presented here and in ref. (36) provided the standard TLS_{ext} model is abandoned and a hierarchy of constrained relaxation events invoked. However, we are not aware of a precedent for the suggestion that

intramolecular vibrational relaxation leads to the creation of localized or pseudo-localized modes which induce inter-site conversion. We are aware of only one experiment that speaks to this question. Mixed crystal absorption and fluorescence studies of tetracene in p-terphenyl have shown that intramolecular vibrational relaxation of tetracene in its S_1 state does not create the localized and pseudo-localized phonons that characterize the phonon sideband (PSB) in absorption [43]. Rather, direct relaxation into delocalized phonons appears to be the dominant process. This system is novel in that optical excitation of the PSB leads to site interconversion in the S_1 state. A possibility which was not considered by Bogner [36] is that the phonons created in fluorescence by virtue of the PSB which accompanies the ZPL might also function in his mechanism. To explore this we have compared the quantum efficiency of ZPH burning with that of the pseudo-PSBH. The dispersive kinetics of ZPH growth for CV/PVOH are analyzed in paper II using the distribution function for the tunnel parameter λ of Jankowiak and Small [44]. The mean tunnel parameter λ_0 and σ_2 (which characterizes the width of the distribution) are 9.85 and 1.3. The Huang-Rhys factor S = 0.7. The dashed curve in Figure 9 is the fit to the T_B-independent hole growth data of the pseudo-PSBH obtained with the same λ_0 σ_2 and S values. The only difference in the calculation is the reduction of the induced absorption rate for the one-phonon profile by the ratio of the homogeneous linewidth of the ZPL (0.015 cm^{-1}, see paper II) to the width of the one-phonon profile (40 cm^{-1}). We note that for S = 0.7 the integrated intensities of the ZPL and one-phonon profile are nearly equal (0.5 and 0.35).

In Figure 9 the fit to the data at early times is quite good. The poorer fit at longer times can be qualitatively understood in terms of the neglect of the contribution to the peak of the pseudo-PSBH at $\omega_B - 25$ cm^{-1} from the 2- and higher-phonon transitions. Although the calculation is not exact, it is sufficiently accurate to establish that the quantum efficiency (distribution thereof) for burning of the pseudo-PSBH is essentially the same as that of the ZPH. Thus, the phonons initially excited via the PSB in the S_1 state do not play a significant role in hole burning. A hole burning experiment was also performed on the photostable molecule 3,5-di-tertbutyl-1,2-benzoquinone in EtOH/glycerol whose S_1 state is $n\pi^*$ with an absorption origin band at 535 nm. Although the photophysics of this molecule have not been determined, its S_1 state can be expected to decay to the triplet manifold in a few picoseconds with an intersystem-crossing yield of ≈ 1 and the T_1 state to decay radiationlessly to the ground state. Although the system features H-bonding, which augers well for a large value of the average NPHB rate constant $\langle k_{NPHB} \rangle$, hole burning at low temperature would be expected to require a high burn fluence, relative to laser dyes, since its room temperature absorption cross-section is a factor of about 10^3 lower than that of laser dyes and the S_1 state lifetime shorter by about the same factor. Thus, its induced absorption rate should be about a factor of 10^6 lower than that of CV. For the model of Bogner, this might be partially compensated for by the fact that the decay of the S_1 state is predominantly radiationless. However, hole burning (ZPH or pseudo-PSBH) was not observed for $I_B = 200$ mW/cmw^End $t_B = 40$ min (the ZPH for CV/PVOH is readily

observed for a fluence which is a factor of ~10^6 lower, see paper II). This negative result only shows that thermal energy equal to the S_1-S_0 energy gap does not lead to particularly facile hole burning for the system studied.

Our failure to observe NPHB for the $^1n\pi^*$ state of 3,5-di-tertbutyl-1,2-benzo-quinone and other molecules [45] is disappointing in that, according to the model of Shu and Small, the anti-hole would be expected to be predominantly red-shifted ($^1n\pi^*$ states typically undergo a blue gas to polar solvent shift [46]). Further attempts to observe NPHB for an $n\pi^*$ state are planned.

CONCLUSIONS

Cresyl violet in a polyvinyl alcohol film provides another example of a NPHB system that exhibits a broad, tailing and blue-shifted anti-hole for a S_1 ($\pi\pi^*$) state as well as complete burning of zero-phonon lines (ZPL) at very low temperatures. Hitherto, polarized hole spectra as a function of burn temperature (T_B) had not been reported for any system. Such spectra for CV/PVOH show that while no substantial rotation of CV accompanies hole burning at the lowest temperature utilized, a significant rotation is involved ($\approx 40°$) for $T_B = 15$ K. Furthermore, the anti-hole is observed to shift further to the blue as T_B is increased from 2.2 K (in ref. (33) it is proven that this change in the anti-hole cannot be produced by burning at $T_B = 2.2$ K and reading at the higher burn temperature). Thus, bulk thermal energy available even at low temperatures has a profound effect on the photo-induced relaxation pathway(s) that leads to persistent hole formation. Taken as a whole, the results show that the early mechanistic models for NPHB based on the standard TLS_{ext} model (cf. Introduction) are inadequate.

Other relevant observations are that for $1.6 \text{ K} \leq T_B \leq 15$ K (range studied) the quantum efficiencies (distributions thereof) of NPHB for the ZPH and pseudo-phonon sideband hole (pseudo-PSBH) are very similar, the quantum efficiency is, at most weakly dependent on T_B and essentially 100% of the ZPL can be burned. The first observation indicates that phonons created via the phonon sideband do not play a key

role in hole burning.

We conclude that the hierarchy of configurational relaxation processes, which lead to persistent hole formation, is triggered by electronic excitation. Although experiments with $T_B < 1.6$ K have not been performed, the available results strongly indicate that NPHB should be operative in the $T_B \rightarrow 0$ K limit. At sufficiently low temperatures, relaxations must involve phonon assisted tunnelling with phonon emission when the tunnelling configurations are not degenerate within $\approx kT$. The data for CV/PVOH reveal that at higher burn temperatures hole burning is a thermally assisted photo-induced process which results in a significant rotation of CV. This rotation is most likely a barrier hopping process which follows a rate limiting step associated with H-bond breaking (tunnelling). The "outside-in" dynamical model of Shu and Small is consistent with the present and earlier results. It suggests that the TLS_{ext} picture of Fig. 1 showing tunnelling along q_{ext} in TLS^{β}_{ext} is one that has evolved as a result of relatively fast relaxation processes in the outer-shell region. The blue-shifted anti-hole is explained in terms of an increase in the free volume of the probe. The ~100% burning of the zero-phonon lines in the low temperature limit can be understood in terms of suitably evolved TLS^{β}_{ext} for which relaxation occurs between quasi-degenerate configurations or from a higher to lower energy configuration. For the former situation, the blue-shifted anti-hole provides a measure of the distribution of <u>minimum</u> barrier heights associated with reverse relaxation in TLS^{α}_{ext}, Figure 1. The CV/PVOH results reveal that at higher temperatures one must go beyond the notion of a single, more or

less well-defined q_{ext} and allow for parallel pathways and/or consecutive relaxation steps of the probe-inner shell. In Part IV the question of whether or not the post-burn configurations retain at least partial memory of their pre-burn configurations is addressed through laser (light)-induced hole filling experiments. In paper II the spontaneous hole filling characteristics of CV/PVOH are discussed.

The problem of understanding NPHB is both intriguing and difficult given that the hierarchy of relaxation events may begin in only a few picoseconds (corresponding, perhaps, to the tunnelling events in the outer-shell that cause pure dephasing at lower temperatures [1,11,13]) and extend into the μs-regime. The experimental results provide a stringent test for dynamical models which must also account for the observation that the post-burn configurations are not populated during formation of the glass with the probe in its ground state. This absence of population also points to the importance of configurational relaxation in the excited electronic state for NPHB.

ACKNOWLEDGEMENTS

This research was supported by the Division of Materials Research of the National Science Foundation under Grant No. DMR-8920515. Useful discussions with J. Hayes and R. Jankowiak are acknowledged.

REFERENCES

[1] J. M. Hayes, R. Jankowiak and G. J. Small, in: Topics in Current Physics, Persistant Spectral Hole Burning: Science and Applications, ed. W. E. Moerner, (Springer, Berlin, 1988) p. 153.

[2] S. G. Johnson, I. J. Lee and G. J. Small, in: Chlorophylls, H. Scheer, ed. (CRC, Boston, 1991), p. 739.

[3] N. R. S. Reddy, P. Lyle and G. J. Small, to be published.

[4] M. J. Kenney, R. Jankowiak and G. J. Small, Chem. Phys. 146 (1990) 47.

[5] R. Jankowiak, R. Richert and H. Bässler, J.Chem. Phys. 89 (1985) 4569.

[6] A. Elschner and H. Bässler, Chem. Phys. 112 (1987) 285.

[7] R. Jankowiak, L. Shu, M. J. Kenney and G. J. Small, J. Lum. 36 (1987) 293.

[8] A. Elschner and H. Bässler, Chem. Phys. 123 (1988) 305.

[9] W. Köhler, J. Meiler and J. Friedrich. Phys. Rev. B35 (1987) 4031.

[10] W. Köhler, J. Friedrich, Phys. Rev. Lett. 59 (1987) 2199.

[11] R. Jankowiak and G. J. Small, Science, 237 (1987) 618.

[12] L. R. Narasimhan, K. A. Littau, Dee William Pack, Y. S. Bai, A. Elschner and M. D. Fayer, Chem. Rev. 90 (1990) 439.

[13] M. Berg, C. A. Walsh, L. R. Narasimhan, K. A. Littau and M. D. Fayer, J. Chem. Phys. 88 (1988) 1564.

[14] S. Völker, in Relaxation Processes in Molecular Excited States, ed. J. Fünfschilling (Kluwer Academic Publishers, 1989).

[15] B. L. Fearey, R. P. Stout, J. M. Hayes and G. J. Small, J. Chem. Phys. 78 (1983) 7013.

[16] P. W. Anderson, B. I. Halperin and C. M. Varma, Phil. Mag. 25 (1972) 1.

[17] W. A. Phillips, J. Low Temp. Phys. 7 (1972) 351.

[18] S. Hunklinger and A. K. Raychandhuri, in: Progress in Low Temperature Physics, ed. D. F. Brewer (North-Holland/Elsevier, Amsterdam, 1986) Vol. 9, p. 265.

[19] P. M. Selzer, D. L. Huber, D. S. Hamilton, Y. M. Yen and M. T. Weber, Phys. Rev. Lett. 36 (1976) 813.

[20] S. K. Lyo and R. Orbach, Phys. Rev. B22 (1980) 4223 .

[21] S. K. Lyo, in: Electronic Excitations and Interactions Processes in Organic Molecular Aggregates, eds. P. Reinecker, H. Haken and H. C. Wolf, Springer S. Solid-State Sci., Vol. 49 (Springer, New York, 1983), p. 215.

[22] D. Haarer, in: Topics in Current Physics, Persistent Spectral Hole Burning: Science and Application, ed. W. E. Moerner (Springer, Berlin, 1988) p. 97.

[23] R. M. Macfarlane and R. M. Shelby, in: Topics in Current Physics. Persistent Spectral Hole Burning: Science and Application, ed. W. E. Moerner (Springer, Berlin, 1988) p. 127.

[24] S. Völker, J. Luminescence 36 (1987) 251.

[25] R. Jankowiak, R. Richert and H. Bässler, J. Phys. Chem. 89 (1985) 4569.

[26] A. Elschner, R. Richert and H. Bässler, Chem. Phys. Lett. 127 (1986) 105.

[27] A. Elschner and H. Bässler, Chem. Phys. 123 (1988) 305.

[28] G. J. Small, in: Spectroscopy and Excitation Dynamics of Condensed Molecular Systems, eds. V. M. Ayranovich and R. M. Hochstrasser (North-Holland, Amsterdam, 1983) p. 555.

[29] J. M. Hayes and G. J. Small, Chem. Phys. 27 (1978) 151 ; Chem. Phys. Lett. 54 (1978) 435.

[30] J. M. Hayes, R. P. Stout and G. J. Small, J. Chem. Phys. 74 (1981) 4266.

[31] When the Huang-Rhys factor is taken into consideration.

[32] J. K. Gillie, G. J. Small and J. H. Golbeck, J. Phys. Chem. 93 (1989) 1620.

[33] L. Shu and G.J. Small, Chem. Phys. 141 (1990) 447.

[34] R. Jankowiak and Bässler, J. Mol. Electron. 1 (1985) 73.

[35] A. F. Childs and A. H. Francis, J. Phys. Chem. 89 (1985) 466.

[36] U. Bogner and R. Schwarz, Phys. Rev. B24 (1981) 2846.

[37] F. Kokai, H. Tanaka, J. I. Brauman and M. D. Fayer, Chem. Phys. Lett. 143 (1988) 1.

[38] Because of the breadth of pseudo-PSBH, its maximum is at $\omega_B - (25 \pm 5)$ cm^{-1}.

[39] B. L. Fearey, T. P. Carter and G. J. Small, J. Phys. Chem. 87 (1983) 3590.

[40] The pseudo-vibronic satellite hole is due to sites that absorb ω_B via their vibronic transition which builds on and to higher energy of their origin ZPL.

[41] W. Köhler and J. Friedrich, Chem. Phys. Lett. 134 (1987) 200.

[42] J. M. Clemens, R. M. Hochstrasser and H. P. Tromssdorff, J. Chem. Phys. 80 (1984) 1744.

[43] G. J. Small, J. Chem. Phys. 58 (1973) 2015.

[44] R. Jankowiak and G. J. Small, Chem. Phys. Lett. 128 (1986) 377; J. Phys. Chem. 90 (1986) 5612.

[45] We have also investigated NPHB for the $S_1(n\pi^*)$ state of benzocinnoline in 2-methyltetrahydrofuran and ether/isopropanol, benzophenone in 2-methyltetrahydrofuran, phenazine in 2-methyltetrahydrofuran, pyridazine in ether/isopropanol, EtOH/glycerol and 2-methyltetrahydrofuran. No hole was observed for any of these systems.

[46] H. McConnell, J. Chem. Phys. 20 (1952) 700.

PART III. DISPERSIVE KINETICS OF NONPHOTOCHEMICAL HOLE BURNING AND SPONTANEOUS HOLE FILLING: CRESYL VIOLET IN POLYVINYL ALCOHOL FILMS

DISPERSIVE KINETICS OF NONPHOTOCHEMICAL HOLE BURNING AND SPONTANEOUS HOLE FILLING: CRESYL VIOLET IN POLYVINYL FILMS

Luchuan Shu and Gerald J. Small

Submitted to the Journal of Optical Society of America
November, 1991

ABSTRACT

The dispersive kinetics of non-photochemical burning and spontaneous filling of the zero-phonon hole of cresyl violet in polyvinyl alcohol at 1.6 K are analyzed in terms of the standard external two-level system (TLS_{ext}) model for probe-glass systems and a distribution function for the tunnel frequency derived from a normal distribution function for the tunnel parameter λ. Average values for the relaxation rates for burning and filling are determined. It is shown that the dominant mechanism for filling is not global spectral diffusion but rather anti-hole reversion. A high degree of positive correlation between the rates of burning and filling associated with TLS_{ext} is found. A new methodology that allows for a more physically reasonable interpretation of spontaneous hole filling kinetics is described. It is based on the hypothesis that only a fraction of burned sites upon reversion in the ground state yield sites with resonance frequencies that lie within the hole profile.

INTRODUCTION

In the preceding paper (referred to hereafter as I) the mechanistic and dynamical aspects of persistent non-photochemical hole burning (NPHB) were discussed in light of the burn temperature dependence of polarized hole spectra of cresyl violet in polyvinyl alcohol films (CV/PVOH). Here we are concerned with the dispersive kinetics associated with the growth of zero-phonon hole (ZPH) and the kinetics associated with its spontaneous filling following termination of the burn with the sample maintained at burn temperature, T_B, and in the dark (spontaneous hole filling, SPHF).

The kinetics of NPHB have been studied in several systems including tetracene in amorphous 2,3-dimethylanthracene and 9,10-diphenylanthracene [1] and in EtOH/MeOH [2] and methyl-tetrahydrofuran glasses [3,4], rhodamine 640 in PVOH [5] and oxazine 720 in PVOH films and glycerol glass [6]. That the kinetics can be highly dispersive for probe molecules in amorphous solids has been demonstrated. The standard external two-level system (TLS_{ext}) model, see I, has generally been used for theoretical simulations [1,6-11] which employ a distribution of relaxation rates, R, for hole burning (or spontaneous hole filling) at low temperatures. Here the distribution of tunnelling frequencies $W = \omega_0 \exp(-\lambda)$ is an important factor [12], where ω_0 is the harmonic frequency of the TLS_{ext} and λ is the tunnel parameter. The tunnel state splitting of the TLS is given by $[W^2 + \Delta^2]^{1/2}$, where Δ is the asymmetry parameter. From the distribution functions for $W(\lambda)$ and Δ one can obtain the distribution function

f(R). For example, Haarer and coworkers [7,8] in their studies of the kinetics associated with hole growth and SPHF have utilized the expression of Jäckle [10] for f(R) which stems from the phenomenological TLS distribution function $P(\Delta,\lambda)$ of Anderson et al. [12] and Phillips [13]. This distribution function is simply a constant for λ and Δ lying within certain intervals and zero otherwise. Jäckle's expression was used to show that the hole growth and filling rates have a logarithmic dependence on time. Other distribution functions for TLS which have been used are reviewed in ref. 9.

Jankowiak et al. [14] have derived analytic forms for the TLS distribution and density of state (DOS) functions under two reasonable assumptions: that a Gaussian distribution function (GDF) for Δ and λ is physically reasonable and that the stochastic variables Δ and λ are independent. Their distribution functions for W and Δ for the DOS functions have been successfully applied to the problems of optical dephasing [15], thermal conductivity [16], specific heat [17], and the dispersive kinetics of hole growth and spontaneous hole filling [6,11]. Utilization of the non-phenomenological distribution functions allows one to avoid questionable assumptions that need to be made in statistical averaging of physical observables when phenomenological functions with no physical basis are employed. Jankowiak and Small [18] have provided arguments that justify the above two assumptions. Kenney et al. [6] have reported the results of an extensive study of the dispersive hole growth kinetics of oxazine 720 in glycerol glass and polyvinyl alcohol (PVOH) hosts as well as their deuterated analogues. The data were produced with burn intensities in the nW to μW range and

fluences which vary over five decades. These data were theoretically analyzed by utilizing the distribution function for W proposed by Jankowiak et al. [1,4,16,18]. For the first time, the linear electron-phonon coupling, which limits the saturated depth of the zero-phonon hole, was taken into account [6] in the analysis. Good agreement between the observed and simulated dispersive growth curves was obtained.

SPHF kinetics have been extensively studied for quinizarin in alcoholic glasses (photochemical hole burning) by Haarer and coworkers [7,8] and several nonphotochemical hole burning systems by Fearey and Small [5]. For quinizarin in alcoholic glasses, the hole area decays logarithmically as a function of observation time and hole width broadening was observed. Fearey and Small have measured SPHF of the systems rhodamine 640, Nd^{3+} and Pr^{3+} in polyvinyl films [5]. Kenney et al. [6,19] have also studied SPHF of oxazine 720 in glycerol glasses and polyvinyl alcohol polymer films. Their results show that the dispersive decay can be well described using the aforementioned distribution function for W. No hole broadening was observed for these nonphotochemical hole burning systems at a read resolution of ~0.1 cm^{-1}. Fearey and Small have developed a model which predicts that [5] hole filling without broadening may occur under certain circumstances.

Although SPHF can be satisfactorily understood in terms of the standard TLS model and dispersive kinetics, the mechanism of SPHF is not well understood. Because of the lack of information on the microscopic structures of TLS, no microscopic description of the tunnelling modes has been given thus far. Studies of the effect of

host deuteration on NPHB for resorufin in ethanol [20] and oxazine 720 in glycerol and PVOH [6] indicate that the TLS_{ext} coordinate, q_{ext}, is localized in the vicinity of the probe with significant amplitude of motion for the hydroxyl proton of the host. It has not been determined whether SPHF is mainly the result of reversion of the TLS^{α}_{ext} (α = ground state of the probe molecule) involved in the burn or global spectral diffusion. Polarized data for 1,4-dihydoroxyanthraquinone and tetracene in an EtOH/MeOH glass [2] indicate that no reorientation of the probe molecule occurs during the SPHF process at 4.2 K. Our temperature-dependent polarized hole burning data for CV/PVOH (see I) have also shown that no significant rotation of CV molecules accompanies NPHB at 2.2 K but that a significant rotation does occur at 15 K. The laser induced hole filling data for CV/PVOH at 1.6 K (see paper III) demonstrate that the post-burn configurations retain at least partial memory of their pre-burn configurations. An understanding of the extent of correlation between the efficacies of NPHB and SPHF is important for an improved understanding of the dynamics of NPHB and SPHF and the nature of TLS_{ext}.

In this paper we present the results of our studies of the dispersive kinetics of hole growth and SPHF for CV/PVOH films at 1.6 K. The data are theoretically analyzed using the approach of Kenney et al. [6] and the tunnelling parameters for both hole growth and SPHF are obtained. An apparent dependence of the SPHF rate on the depth of the zero-phonon hole [4] is explained. The degree of positive correlation between the rates of NPHB and SPHF for TLS_{ext} sites is determined. The results

strongly indicate that SPHF results mainly from back-relaxation of the TLS_{ext} involved in the burn and that global spectral diffusion is of minor importance.

The experimental systems and procedures used in this work are the same as those employed by Kenney et al. [6]. The reader is referred to this reference for detailed discussions. However, the laser used for the present work was a Spectra-Physics 117A frequency and power stabilized He-Ne laser with a linewidth of 6 MHz. The samples were prepared in the same manner as that described in Part II.

DISPERSIVE KINETICS

In this section we briefly review the theoretical expressions of Kenney et al. [6] for the dispersive kinetics of NPHB and SPHF. The rate expressions are based on the TLS distribution functions of Jankowiak et al. [14,11,9,19] which are discussed in the Introduction. Under the assumption that NPHB and SPHF at low temperatures are due to phonon-assisted tunnelling of TLS_{ext}, the relaxation rate is proportional to the square of the tunnelling frequency $W = \omega_0 \exp(-\lambda)$, where λ is the tunnel parameter. For NPHB involving downward phonon-assisted tunnelling in the excited electronic state (β) of the probe, the relaxation rate is expressed as

$$R = \Omega_0 e^{-2\lambda}, \tag{1}$$

where Ω_0 depends on the TLS_{ext} deformation potential and asymmetry parameter Δ [6]. Thus, Ω_0 and Δ are associated with TLS^{β}_{ext} of Figure 1 of Part II. When $\Delta >> kT$, R is temperature independent for sufficiently small variations in temperature. This inequality appears justified in view of recent experimental results [6 and refs. therein, paper I]. It has been argued that the distribution of R-values stems primarily from the distribution of λ-values, which has been taken as normal (a Gaussian centered at λ_0 with variance σ_2). A Gaussian is valid for $\lambda_0/\sigma_2 >> 1$. The fractional hole (ZPH) depth is 1 - D(t),

$$D(t) = \int_0^{\Omega_0} dR\, f(R) \exp(-P\sigma\phi(R)t), \tag{2}$$

where f(R) is the normalized distribution function for R [6], P is the photon flux, σ is the peak absorption cross-section of the ZPL (zero-phonon line) and $\phi(R) = R/(R+k)$ is the quantum yield for NPHB. The rate constant k is the inverse of the excited state (β) lifetime of the probe. Defining $x = (\lambda - \lambda_0)/\sigma_2$ it can be shown that [6]

$$D(t) = (2\pi)^{-1/2} \int_{-\infty}^{+\infty} dx \exp(-x^2/2) \exp(-\Sigma_0 \xi(x) t), \tag{3}$$

where $\Sigma_0 = P\sigma\Omega_0/k$ and $\xi(x) = \exp[-2(\lambda_0 + \sigma_2 x)]$. It is assumed that $\phi(R) \approx R/k$ and that $\lambda_0^2/2\sigma_2^2 >> 1$ (which allows one to extend the lower limit of the integral to $-\infty$). The results for CV/PVOH will be seen to satisfy these conditions. Kenney et al. [6] have considered the contribution from the utilization of linearly polarized light for burning and reading for an isotropic sample to dispersive kinetics. Their results show that this contribution is minor for the first ~50% of the burn for typical σ_2-values (including the σ_2-value given later for CV/PVOH). It is the first ~50% of the burn that is most important for the determination of λ_0 and σ_2 [6].

The expressions for the degree (fractional) of SPHF at time t following termination of the burn is $1 - D(t)$ with

$$D(t) = (2\pi)^{-1/2} \int_{-\infty}^{+\infty} dx \exp(-x^2/2) \exp(-\Omega_0 \xi(x) t), \tag{4}$$

where λ_0 and σ_2 are understood to be associated with TLS^{α}_{ext} (α = ground state of the probe). This expression is considerably more problematic than Eq. 3 for NPHB. Firstly, the temperature does not appear in Eq. 4 although it has been known for some considerable time that the SPHF rate is strongly dependent on T [4,21]. This is consistent with the interpretation given in paper I for NPHB which leads to SPHF in the ground state being thermally assisted. Thus, it is to be understood that the λ_0- and σ_2-values depend on T. To determine the "true" λ_0- and σ_2-values it would be necessary to study SPHF as a function of T. Secondly, to probe the entire distribution of TLS^{α}_{ext} it is necessary to burn a ZPH close to saturation for, as will be discussed later, there is a strong correlation between the efficacies of sites for hole burning and filling.

Finally, it will be assumed in what follows that the values of Ω_0 for TLS^{β}_{ext} and TLS^{α}_{ext} are the same, i.e. it is, for example, diminuation of the TLS_{ext} barrier height V in state β that is responsible for $k_{NPHB} >> k_{SPHF}$. It has been argued that $\Omega_0 \sim 10^{12}$ s^{-1} is a physically reasonable value [22]. For consistency we use this value for the simulations.

RESULTS

The dashed curves in Figure 1 are the ZPH growth curves for CV/PVOH (1.6 K) for burn intensities (top to bottom) of 3.0, 15, 30 and 200 $\mu W/cm^2$. The relative hole depth is ΔOD divided by the pre-burn OD, e.g. 0.6 corresponds to a 40% OD change. The symbols represent the theoretical simulations obtained with Eq. 3. As pointed out by Kenney et al. [6], knowledge of the Huang-Rhys factor S is essential for such simulations since the fraction of the absorption at ω_B (located on the low energy side of the origin absorption band) is ~exp(-S) [23]. From an analysis of the real-phonon sideband hole (see paper I) we determined that S = 0.5-1.0. The bottom growth curve of Figure 1 indicates that the ZPH saturates at a relative OD of ~0.5, which corresponds to an S-value of 0.7. Thus, for the simulations an S-value of 0.7 was used along with a value for σ of 2.0×10^{-11} cm^2 at 1.6 K [24]. The theoretical fits in Figure 1 were obtained with λ_0- and σ_2-values of 9.9 and 1.3. Thus $\lambda_0^2/2\sigma_2^2 >> 1$, justifying the utilization of Eq. 3. For comparison, the λ_0- and σ_2-values for oxazine 720/PVOH at 1.6 K are 7.6 and 1.0 [6]. Discussion of the average NPHB quantum yield is postponed until section IV (see Discussions section).

We turn next to results from SPHF studies conducted at 1.6 K (T_B = 1.6 K). The unsaturated ZPHs used corresponded to fractional ΔOD changes of 0.25-0.35 (generated with burn intensities of 3-13 $\mu W/cm^2$). Monitoring of SPHF was initiated 60 s after termination of the burn and extended to 1500 s. Typical results are shown in

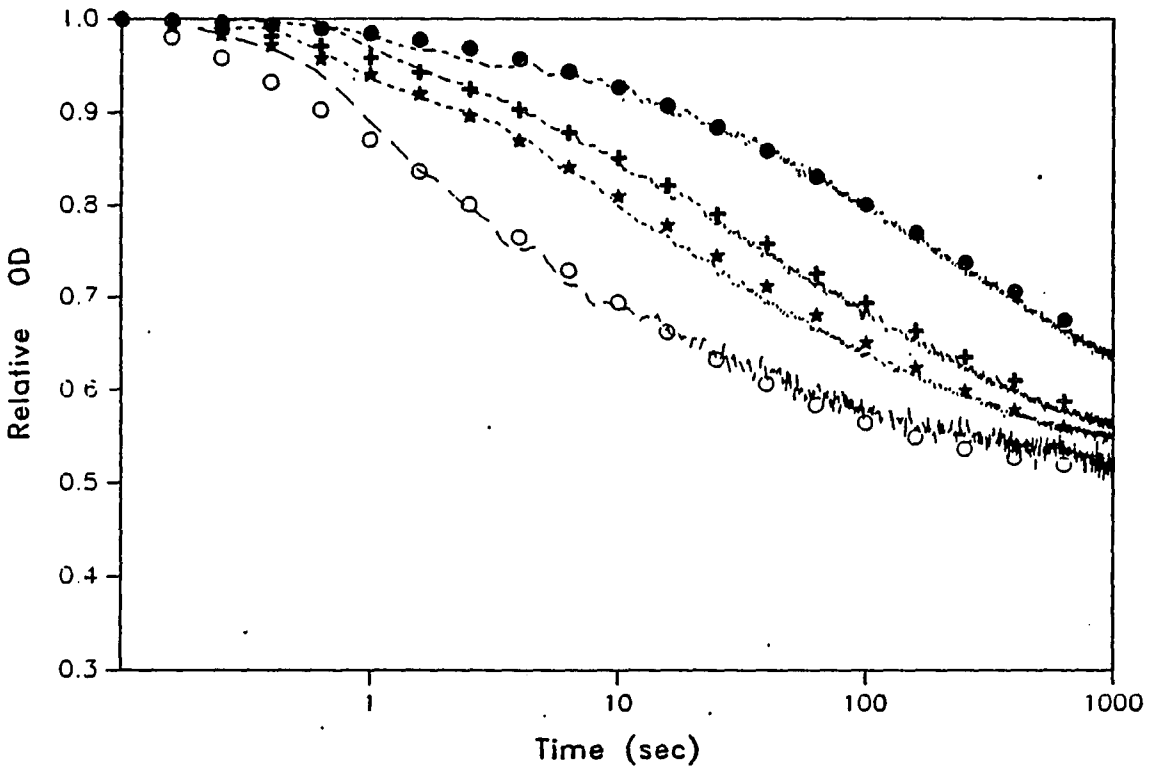

Figure 1. Hole growth curves of cresyl violet in PVOH at 1.6 K for different burn intensities, I_B = 3, 15, 30 and 200 $\mu W/cm^2$ (from top to bottom). The dots, crosses, stars and circles represent theoretical fits. For all simulations, a single set of parameters, $\lambda_0 = 9.85$, $\sigma_0 = 1.3$, $\Omega_0 = 10^{12}$ s^{-1}, $\sigma_0 = 20 \times 10^{-12}$ cm^2 and S = 0.7, were used. The OD of sample is ~0.35 (at 632.8 nm, He-Ne line)

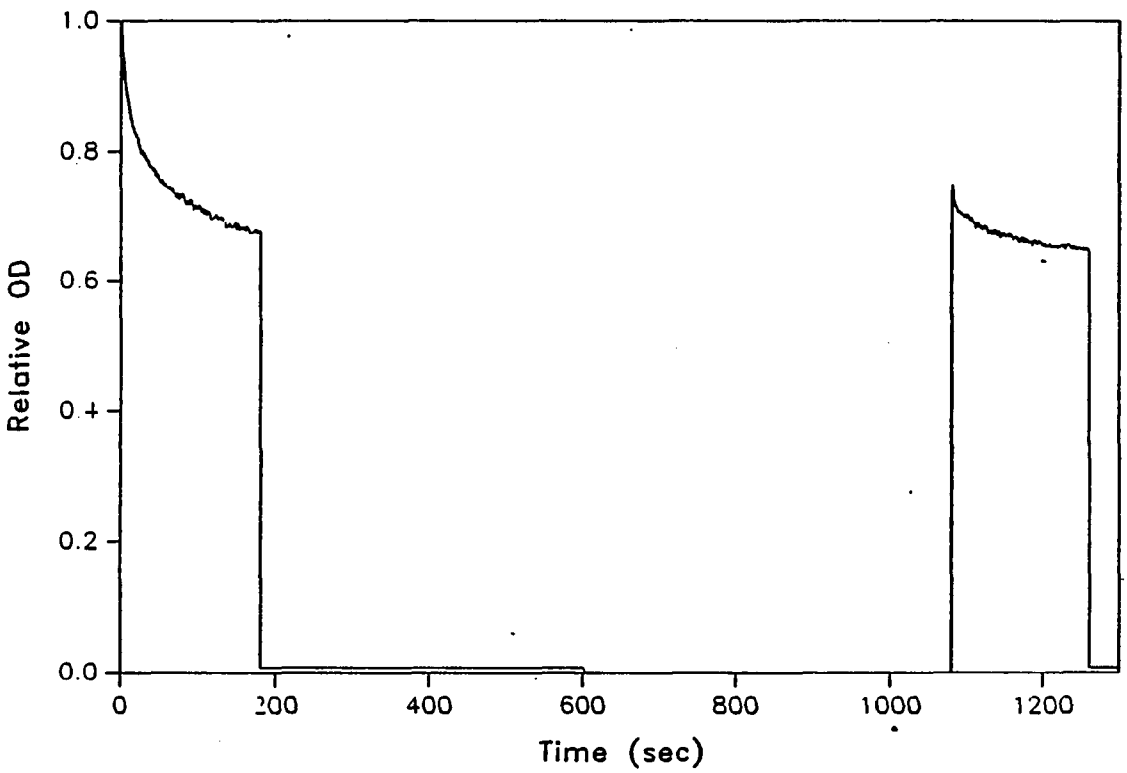

Figure 2. Hole growth and spontaneous hole filling for cresyl violet in PVOH at 1.6 K. See text for explanation and discussion

Figure 2. Following a burn for 180 s (I_B = 13 μW/cm^2), the laser light was blocked for 15 min after which it was unblocked for reinitiation of burning. The extent of SPHF of the ZPH is 20%. Comparison of the hole growth curve near the end of the first burn with the growth curve during the initial stage of the second burn reveals that the growth rate for reburning is significantly greater. Defining t_{B_1} and t_{B_2} as the burn times for the first and second burns, the results show that OD (t_{B_1} = 60 s) = OD (t_{B_2} = 0 s, initiation). For better comparison, the data are replotted in Figure 3 of which the solid circles are points from the first burn. The crosses are data points from the second burn with the left-most cross the data point for t_{B_2} = 0 s. For the same initial OD at t = 60 s, the hole burning rate for the second burn is markedly greater for the first ~100 s but at longer times the two rates become comparable. Evidently, the distributions of TLS_{ext} for the first and second burns are distinct. Another set of experiments (I_B = 13 μW/cm^2) were performed in which t_{B_1} = 4 min, the SPHF duration was 15 min, and the secondary burn fluence was such as to produce the OD prior to SPHF. The cycle was repeated four times with identical results. These results and those of Figs. 2 and 3 indicate that there is a significant degree of positive correlation between the site relaxation distribution functions for NPHB and SPHF.

Figure 4 shows SPHF curves for initial hole depths corresponding to fractional ΔOD values of 0.25 (solid circles) and 0.34 (crosses). Relative hole filling is defined as the value of ΔOD for hole filling divided by the intensity of the hole prior to SPHF. Elschner and Bässler [4] presented their SPHF data for tetracene in a methyl-

tetrahydrofuran glass in this manner and also observed that shallower holes appear to have a faster rate of filling.

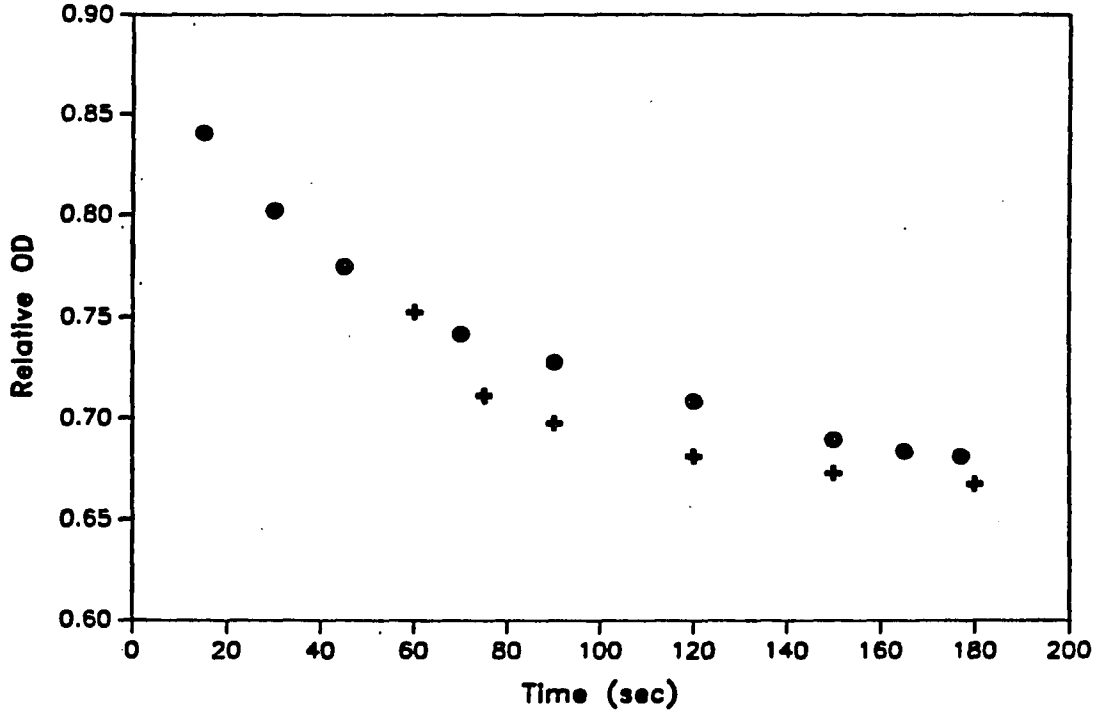

Figure 3. Comparison of the hole growth curves for the first and second burns (solid circles and crosses, respectively). The data are obtained from Figure 2, see text

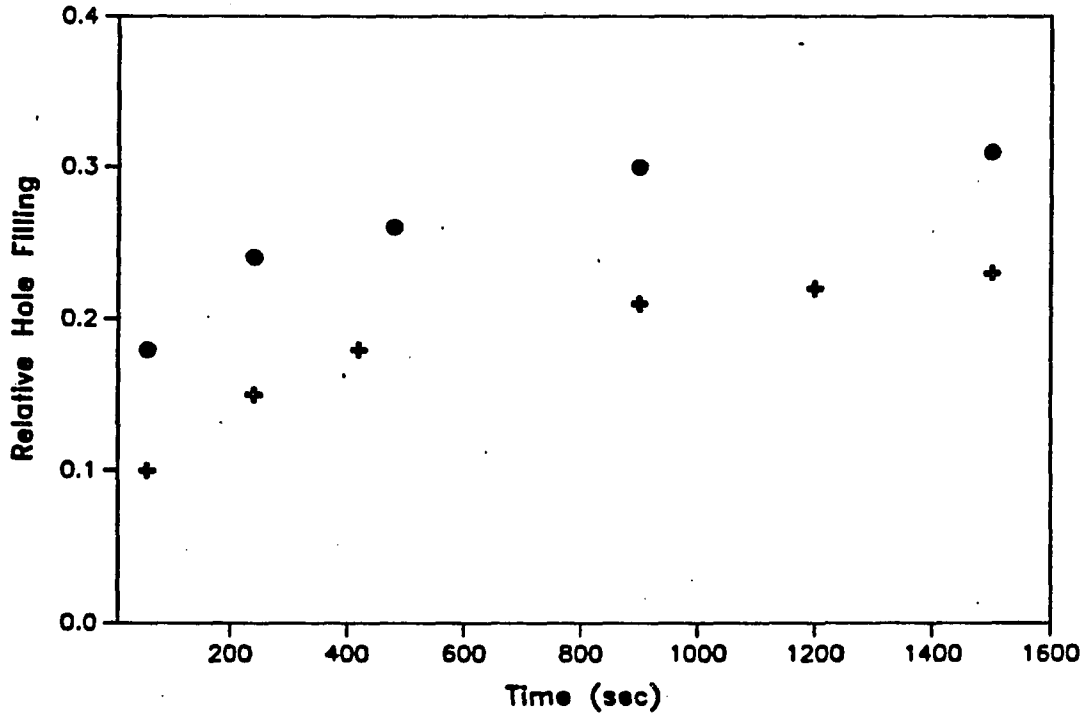

Figure 4. Relative spontaneous hole filling data for cresyl violet in PVOH for two zero-phonon holes of different depths. Solid circles and crosses are data (ΔOD of filling divided by the OD of the initial ZPH) for ZPH of an initial fractional hole depth of 0.25 and 0.36, respectively (I_B = 3 μW/cm^2, t_B = 3 min; I_B = 13 μW/cm^2, t_B = 3 min)

DISCUSSIONS

As stated in ref. 6, oxazine 720 in PVOH is the most efficient NPHB system studied thus far with $\lambda_0 = 7.6$, $\sigma_2 = 1.0$ and $k = 3.8 \times 10^8\ s^{-1}$. The average value of the relaxation rate associated with NPHB is $\langle R \rangle = \Omega_0 \exp(-2\lambda_0) \exp(2\sigma_2^2)$ [18]. The average quantum yield for NPHB is $\langle \phi \rangle_{NPHB} = \langle R \rangle / k$, which for oxazine 720/PVOH yields a value of 5.0×10^{-3}. The λ_0, σ_2 and k values for CV/PVOH lead to $\langle R \rangle = 7.4 \times 10^4\ s^{-1}$ and $\langle \phi \rangle_{NPHB} = 4.6 \times 10^{-4}$. Though quite efficient, CV/PVOH is less so than oxazine 720/PVOH. Since for both systems the host is the same but the $\langle R \rangle$ values differ, it is clear that the probe molecule is an integral part of the TLS_{ext} responsible for hole burning.

Turning to SPHF, the data as plotted in Figure 4 indicate that the filling rate depends on the initial ZPH depth. In this figure the relative hole filling is the value of ΔOD for hole filling divided by the initial value of ΔOD for the ZPH. Theoretical fits to the two would yield different values for (λ_0, σ_2), which is clearly unsatisfactory. When the data are plotted as the absolute amount of filling, ΔOD, divided by the ΔOD value for complete burning of the ZPL at ω_B, one obtains the results shown in Figure 5. The data points for the two ZPH of fractional hole depth 0.25 and 0.35 lie on a common curve (the left-most data points correspond to t = 60 s). For calculation of the absolute hole filling the linear electron-phonon coupling has to be taken into account in order to determine ΔOD for a *complete* burn of the ZPL. Since $S \approx 0.7$, and the

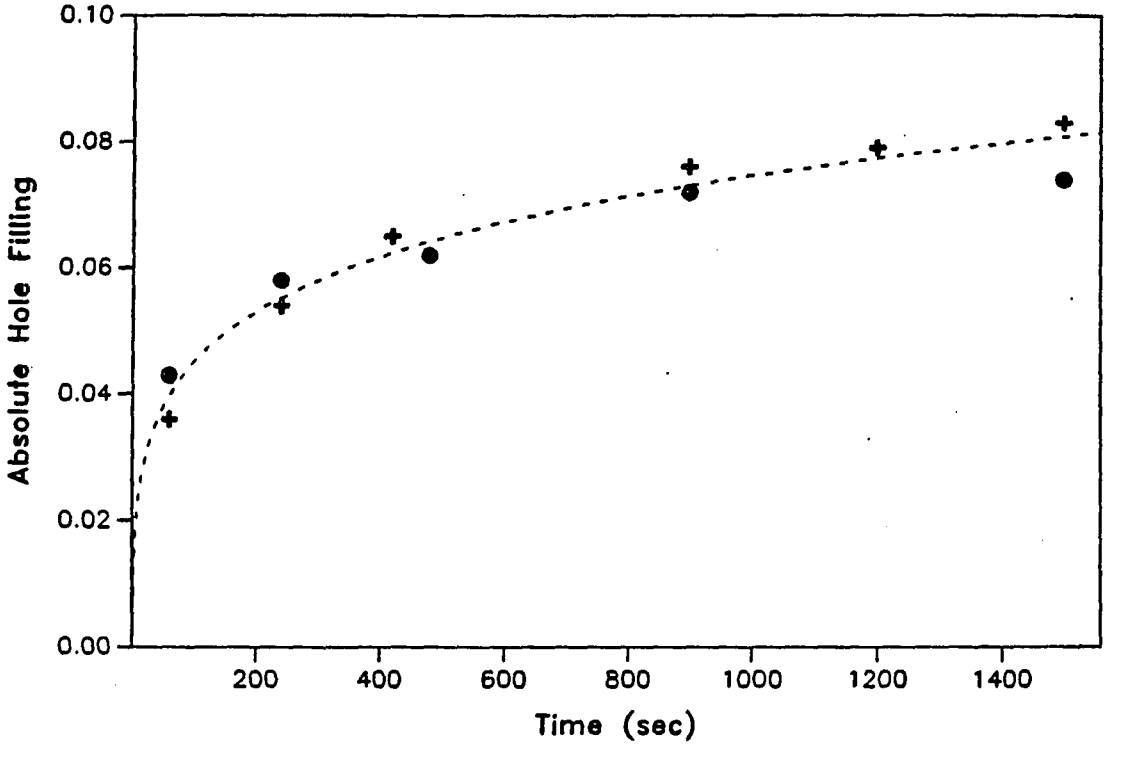

Figure 5. Absolute spontaneous hole filling corresponding to Figure 4. Absolute filling is ΔOD of filling divided by ΔOD of the hole corresponding to complete burning of the zero-phonon lines, see text. The solid circles and crosses are for the same two initial ZPH of Figure 4

fraction of the OD at ω_B due to ZPL is $\approx \exp(-S)$, it follows that the aforementioned ZPH of fractional hole depths 0.25 and 0.35 correspond to burning of ~50 and 70% of the ZPL. Although not saturated, these burns are deep. That the percentage burnings are considerably greater than the maximum percentage filling monitored in our experiments (~20%) is important to the understanding of the results of Figure 5. To see this we recall that our results of the type shown in Figure 2 establish that there is a positive correlation between the ease with which a site burns and fills. That is, the greater hole burning rate for the second burn relative to the first, Figure 3, is due to reburning of sites which have undergone "reversion" to ω_B following their initial burning, see below for further discussion. With this in mind, a plausible explanation for the fact that the two data sets of Figure 5 fall on a common curve is that the subsets of the sites that provide filling for both burns are essentially the same. The data in Figure 5 can be well fit by 1 – D(t), Eq. 4. The fit obtained is not shown because the λ_0- and σ_2-values of 20.9 and 3.8 from the fit pose a dilemma. With these parameter values <R>, see above, has a value of 2×10^6 s^{-1} which is over an order of magnitude larger than the value of <R> for NPHB. The large value of <R> stems mainly from the large σ_2-value that is required to account for the fact that SPHF occurs to a significant extent in the first 60 s and is very slowly increasing for longer times. In fact the value of $P\sigma\langle\phi\rangle_{NPHB} \sim 0.03$ s^{-1} for a burn intensity of 3 $\mu W/cm^2$; an average rate for hole production that is about 8 orders of magnitude smaller than that calculated above for SPHF. Furthermore, the value of 3.8 is considerably larger than $\sigma_2 = 1.3$ for NPHB.

This is difficult to understand within the framework of the standard TLS_{ext} model for NPHB. We conclude that the above approach for kinetic analysis of SPHF, which assumes that all burned TLS_{ext} sites are capable of undergoing reversion in a manner that leads to hole filling is not valid. The mechanism for NPHB presented in Part II suggests that reversion of a TLS^{α}_{ext} need not necessarily lead to a site that absorbs at the pre-burn frequency (ω_B). With this in mind we have fit the data of Figure 5 using the same 1 – D(t) expression as before but with $\sigma_2 = 1.3$ for SPHF, i.e. the value for NPHB. The calculation leads to $\lambda_0 = 16.6$ and the result that only 20% of the burned sites revert to sites whose frequencies lie within the hole. The approach is not inconsistent with the mechanism for laser-induced hole filling proposed in paper III. The average relaxation rate <R> for sites that contribute to SPHF is now 0.1 s^{-1}.

Unfortunately, SPHF studies for shallow ZPH were not performed. According to the above interpretation, the SPHF data would not fall on the curve of Figure 5 since one would be probing only a small subset of the TLS^{α}_{ext} characterized by the most efficient burning and filling. The determination of the absolute filling curves for a wide range of initial hole depths in combination with the known distribution of rates for NPHB would allow the degree of correlation between the hole burning and filling efficiencies to be investigated in considerable detail.

It is important to realize that while the distribution of quantum yields for hole burning of CV/PVOH is at best weakly dependent on T_B [paper I, see also ref. 6], the SPHF rate is strongly dependent on temperature. Since the temperature dependence is

not included in Eq. 4, the values of λ_0 and σ_2 determined above should be viewed as "effective" values for T = 1.6 K. It will be important in future studies of SPHF to study its dependence on T for a series of T_B-values. Data from such experiments conducted over a range of temperatures for which the TLS_{ext} coordinate, q_{ext}, does not change should lead to the true values of λ_0 and σ_2.

The data presented here and by Elschner and Bässler [4] show that SPHF is not significantly contributed to by global spectral diffusion for if this were the case the driving force for filling would be the magnitude of ΔOD for the ZPH divided by the pre-burn OD at ω_B [25].

We return now to the question of the extent to which data of the type shown in Figure 2 indicate positive correlation between the hole burning and filling (reversion) efficiency of a site. In Figure 6 the solid circles are hole growth data points for the *first* burn (from Figure 2). The right-most solid circle is the value of ΔOD relative to the pre-burn value. The left-most cross is the data point for the second burn at which the relative OD is the same as that at the end of the first burn. Importantly, the solid circle- and cross-data points fall on the same curve. Thus, the crosses represent the contribution to burning from virgin sites, i.e. sites not involved in the first burn up to t = 180 s. We define for $t < t_1$ (t_1 is the time required to reburn all molecules which have undergone SPHF and from our data t_1 = 60 s) $\Delta OD_1(t)$ as the OD change of the first burn for burn time t, $\Delta OD_2(t)$ as the OD change of the second burn for burn time t and $r = \Delta OD_1(t)/\Delta OD_2(t)$. The data show that r is a constant, ~3.6, independent of t for

$t < t_1$. This and the results of Figure 6 establish that the aforementioned positive correlation is high and that an anti-hole site has at least partial memory of its pre-burn configuration [see paper III which provides support for this conclusion based on laser-induced hole filling]. In other words, the notion of a reasonably well defined TLS_{ext} coordinate at a given temperature is supported by the results.

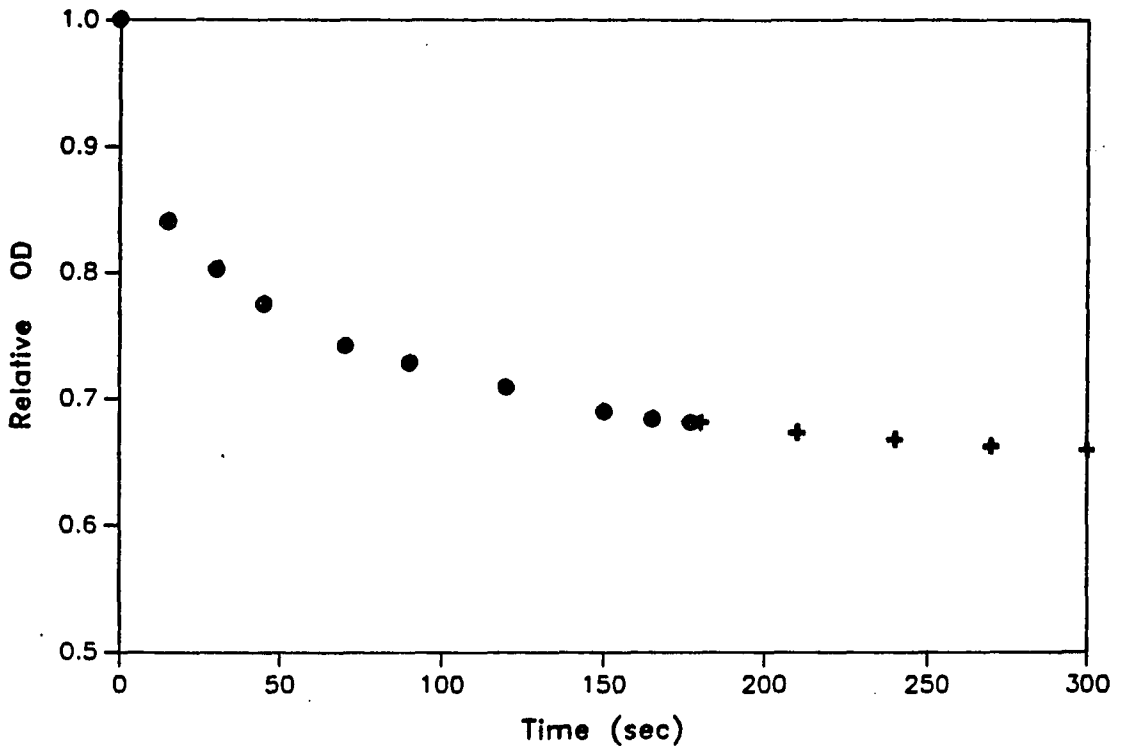

Figure 6. Comparison of hole growth curves for initial burn and reburn (solid circles, crosses). Data are obtained from Figure 2, see text

ACKNOWLEDGEMENTS

This research was supported by the Division of Materials Research of the National Science Foundation under Grant No. DMR-8920515. We would like to thank J. Hayes and R. Jankowiak for useful discussions.

REFERENCES

[1] R. Jankowiak, R. Rechert and H. Bässler, J. Phys. Chem. 89 (1985) 4569.

[2] W. Köhler, W. Breinl, J. Friedrich, J. Chem. Phy. 82 (1985) 2935.

[3] R. Jankowiak and H. Bässler, J. Mol. Electron. 1 (1985) 73.

[4] A. Elschner and H. Bässler, Chem. Phys. 123 (1988) 305.

[5] B. L. Fearey and G. J. Small, Chem. Phys. 101 (1986) 269.

[6] M. J. Kenney, R. Jankowiak and G. J. Small, Chem. Phys. 146 (1990) 47.

[7] D. Haarer in Topics in: Current Physics, Persistent Spectral Hole Burning: Science and Application, ed. W. E. Moerner (Springer, Berlin, 1988) p. 97.

[8] W. Breinl, J. Friedrich and D. Haarer, Chem. Phys. Lett. 106 (1984) 487.

[9] J. M. Hayes, R. Jankowiak and G. J. Small, in: Topics in Current Physics, Persistent Spectral Hole Burning and Applications, ed. W. E. Moerner (Springer, Berlin, 1988), p. 153.

[10] J. Jäckle, Z. Phys. 257 (1972) 212.

[11] R. Jankowiak, L. Shu, M. J. Kenney and G. J. Small, J. Lumin. 36 (1987) 293.

[12] P. W. Anderson, B. I. Halperin and C. M. Varma, Phil. Mag. 25 (1972) 1.

[13] W. A. Phillips, J. Low Temp. Phys. 7 (1972) 351.

[14] R. Jankowiak, G. J. Small and K. B. Athreya, J. Phys. Chem. 90 (1986) 3896.

[15] R. Jankowiak, G. J. Small and B. Ries, Chem. Phys. 118 (1987) 223.

[16] R. Jankowiak and G. J. Small, Phys. Rev. B 37 (1988) 8407.

[17] R. Jankowiak, J. M. Hayes and G. J. Small, Phys. Rev. B 38 (1988) 2084.

[18] R. Jankowiak and G. J. Small, Science 237 (1987) 618.

[19] M. J. Kenney, Ph.D. dissertation, Iowa State University, 1991.

[20] F. Kokai, H. Tanaka, J. I. Brauman and M. D. Fayer, Chem. Phys. Lett. 143 (1988) 1.

[21] J. M. Hayes, R. P. Stout and G. J. Small, J. Chem. Phys. 74 (1981) 4266.

[22] P. Reichert and R. Schilling, Phys. Rev. B32 (1985) 5731.

[23] J. M. Hayes, J. K. Gillie, D. Tang and G. J. Small, Biochem. et Biophys. Acta 932 (1988) 287.

[24] The value of σ was obtained by two approaches described in ref. 6. In the first approach, the standard quantum mechanical expression for σ was utilized and the transition dipole length of cresyl violet was calculated from the measured fluorescence decay constant, 1.8×10^8 s^{-1}. The second approach scales the measured room temperature value for σ of the origin band by the ratio of 1.6 K to room temperature homogeneous linewidths. In both approaches, the Franck-Condon factors (associated with origin band and matrix phonons) and orientation averaging have been taken into account.

[25] J. Friedrich, D. Haarer and R. Silbey, Chem. Phys. Lett. 95 (1983) 11.

[26] L. Shu and G. J. Small, Chem. Phys. 141 (1990) 447.

[27] J. M. Hayes and G. J. Small, Chem. Phys. 27 (1978) 151; Chem. Phys. Lett. 54 (1978) 435.

PART IV. LASER-INDUCED HOLE FILLING: CRESYL VIOLET IN POLYVINYL ALCOHOL FILMS

LASER-INDUCED HOLE FILLING: CRESYL VIOLET IN POLYVINYL ALCOHOL FILMS

Luchuan Shu and Gerald J. Small

Submitted to the Journal of Optical Society of America
November, 1991

ABSTRACT

Laser-induced hole filling (LIHF) results are reported for the case where the primary burn frequency, ω_B, and secondary (filling) frequency, ω_S, lie in the origin absorption band of cresyl violet. Both two-laser and one-laser (with a Fourier transform spectrometer) experiments were performed. The latter allow for monitoring of the entire hole spectrum which consists of the zero-phonon hole at ω_B, its companion phonon sideband holes and the blue-shifted anti-hole. From the dependence of the filling efficiency on $\omega_B - \omega_S$ it is concluded that the dominant mechanism involves electronic excitation of the anti-hole sites via their broad phonon sideband. It is shown that the anti-hole sites retain at least partial memory of their pre-burn configurations.

INTRODUCTION

In the two preceding papers (referred to hereafter as I and II) the mechanisms and kinetics for non-photochemical hole burning (NPHB) and spontaneous hole filling (SPHF) were discussed in terms of data for cresyl violet (CV) in polyvinyl alcohol (PVOH) films as well as other systems. As had been found for oxazine 720 in PVOH and glycerol glasses [1], the dispersive kinetics of NPHB and SPHF for CV in PVOH can be accounted for in terms of the standard TLS-model. In this model the "bistable" configurations of the glass-impurity system are approximated by a static distribution of asymmetric intermolecular double well potentials (TLS). Data which indicate that extrinsic TLS (TLS_{ext}) are responsible for NPHB and SPHF were presented and discussed. On the other hand, pure dephasing of the probe molecule's optical transition at sufficiently low temperatures appears to be the result of diagonal modulation due to tunneling of intrinsic TLS (TLS_{int}) [2-6]. Especially for $^1\pi\pi^*$ states of dye molecules imbedded in hydrogen-bonding hosts, it is clear that the TLS_{ext} coordinate(s) is quite highly localized in the near vicinity of the impurity while the TLS_{int} coordinate(s) is more spatially extended [7-9].

However, despite the apparent success of the standard TLS_{ext}-model and recently developed distribution functions in accounting for the aforementioned dispersive kinetics, the spectral and other results presented in Part II establish that this model is inadequate. These results are the "universal" blue-shift of the anti-hole for $S_1(\pi\pi^*)$

states, the burning of essentially 100% of the zero-phonon lines (ZPL) coincident with the burn frequency in the low T limit, the depolarization of the anti-hole for CV/PVOH as the burn temperature is increased from 1.6 to 15 K and previously reported temperature-dependent results (discussed in I). The results point to a model for NPHB based on a hierarchy of glass-impurity configurational relaxation processes which, although initiated by electronic excitation of the impurity (probe) molecule, are dependent on the temperature at which the hole is burned (T_B).

The first two of the above observations led Shu and Small to extend [10] the simple model of Hayes and Small [11] which is based on a static distribution of TLS_{ext} with phonon-assisted tunneling or barrier hopping occurring in TLS^{β}_{ext} (β denoting the excited electronic state), see Figure 1 of Part II. While retaining the notion of a more or less well-defined q_{ext} coordinate (for a given burn temperature), Shu and Small proposed that tunneling in TLS^{β}_{ext} occurs by phonon *emission* or between quasi-degenerate configurations following relatively rapid temporal evolution of TLS^{β}_{ext} (probe-inner shell structure) produced by configurational relaxation processes of the glass in the outer shell. It was suggested that this outside-in sequence of events could lead to an increase in the free volume of the probe triggered by a reduction in the excess free volume of the glass in the outer shell. The increase in free volume would explain the blue-shifted anti-hole while an evolution of TLS^{β}_{ext} that leads to tunneling by phonon emission would account for 100% burning of ZPLs at very low temperatures [10]. The observation that the mechanism for hole burning of CV in PVOH at higher

temperatures (~15 K) involves substantial rotation of CV (Part II), while at low temperatures it does not, provides some support for the model of Shu and Small.

In this paper we are interested in the phenomenon of laser (light)-induced hole filling (LIHF) for which absorption of secondary irradiation (ω_S) by the sample produces erasure of the hole by some mechanism that does not involve bulk heating (i.e. thermal annealing [12]). Two types of LIHF have been reported: that for which ω_S is located in the same electronic absorption band utilized for hole burning [11,13]; and that for which ω_S is not absorbed by the impurity and lies in the infra-red (i.e. can be absorbed by vibrational states of the host [14,15]). Hereafter we refer to the two types as $LIHF_e$ and $LIHF_v$, respectively. It was our interest in $LIHF_e$ that led to the present work. In addition, it was hoped that the $LIHF_e$ experiments would shed light on the question of whether or not the concept of a more or less well-defined TLS_{ext} with an associated distribution of asymmetry and barrier heights could be retained in the development of more complex models for NPHB.

Hitherto, the most detailed study of $LIHF_e$ is that of Fearey et al. [13]. Pertinent are their 1.7 K data for the origin band of the $S_1(\pi\pi^*)\leftarrow S_0$ transition of rhodamine 640 (R640) in PVOH obtained for a range of ω_S-values to lower and higher energy of the primary burn frequency ω_B, $|\omega_S-\omega_B| \lesssim 400$ cm^{-1}. The extent of filling of the zero-phonon hole (ZPH) at ω_B for $\omega_S > \omega_B$ was found to be about 2.5 times greater than that for $\omega_S < \omega_B$. Furthermore, the extent of filling for $\omega_S > \omega_B$ was essentially independent of ω_S, i.e. did not reflect the variation in optical density across the absorption band.

The same observation was made for $\omega_S < \omega_B$ (located near the absorption maximum at ~580 nm). For the ω_S-fluences used, the %-filling was no greater than 20. Similar behavior was observed for the $^1D_2 \leftarrow {}^3H_4$ transition of Pr^{3+} in PVOH [13]. It was proven that the above step-function behavior at $\omega_S \sim \omega_B$ is not due to electronic energy transfer between R640 molecules. It was remarked that the above LIHF characteristics could be due to the existence of two mechanisms, only one of which is operative for $\omega_S < \omega_B$; however, the data available at that time prevented a plausible model from being proposed. A single mechanism for filling was considered; one that involves global spectral diffusion of zero-phonon lines (ZPL) produced primarily by ω_S-excitation of sites not involved in the primary burn. However, this mechanism could not explain, in any obvious way, the independence of the filling efficiency for $\omega_S > \omega_B$ ($\omega_S < \omega_B$). The present work demonstrates that this mechanism is not the dominant one for $LIHF_e$.

We present new LIHF data for CV/PVOH, whose characteristics mimic those of R640/PVOH, as well as some pertinent results for chlorophyll *a* in the core antenna complex of photosystem I. These results, when viewed in the light of detailed spectral data on the phonon sideband hole structure (linear electron-phonon coupling) which accompanies the ZPH and the anti-hole as well as the recent reports on $LIHF_v$, lead to a model that can account for the principal features of LIHF. The data also show that the anti-hole sites retain at least a partial memory of their pre-burn (primary) configurations in the sense that they undergo a red-shift upon electronic excitation.

EXPERIMENTAL

Two types of laser-induced hole filling (LIHF) experiments were performed. For continuous monitoring of the filling of the ZPH of CV in PVOH at ω_B a two laser setup was employed. The primary burn laser was a frequency stabilized He-Ne laser with a linewidth of 6 MHz (Spectra-Physics model 117A). A Coherent 699-21 ring dye laser (pumped by a 6 W Ar-ion laser) with a linewidth of < 30 MHz was used as the secondary irradiation (filling) source. The primary burn intensity and burn time were I_B = 13 $\mu W/cm^2$ and t_B = 3 min. Part of the He-Ne burn beam (ω_B = 15802 cm^{-1}) was split off and directed to the reference arm of a double beam system which was used for an accurate determination of the fractional OD change at ω_B as the primary burn proceeded (the pre-burn OD of the sampw at ω_B was 0.35, determined using the Fourier transform spectrometer described below). Complete details of the double beam system are given elsewhere [1,16]. For the above primary burn fluence the fractional OD change due to ZPH formation was 0.35 (measured at the end of the burn). Following termination of the burn, the He-Ne laser was attenuated with an OD=3 neutral density filter. The intensity of the attenuated He-Ne laser (probe) transmitted through the sample was used to monitor LIHF. It was determined that the attenuated beam did not produce a measurable ZPH in 1000 s, the time duration of the LIHF experiment. In order to significantly reduce the contribution from spontaneous hole filling, see paper II, probing was initiated 60 s following termination of the primary burn. This initiation time is t=0

in Figsures 2, 5 and 7. Secondary irradiation was delayed 60 s relative to the probe. The secondary irradiation time was 940 s. (Spontaneous hole filling was also monitored for this time period in a separate experiment (cf. curve a in Figure 7)). Great care was taken to ensure that the probe and secondary irradiation beams were optimally overlapped. The two beams were arranged to be counter-propagating in order to reduce the amount of scattered secondary irradiation from reaching the detector (photomultiplier tube, PMT-C 31034). An iris was placed in front of the detector to reduce this scattered light to a negligible level.

The second type of LIHF experiment allowed for monitoring of the entire hole profile (ZPH and associated phonon-sideband holes and anti-hole). Hole spectra were read with a Bruker IFS 120 HR Fourier-transform (FT) spectrometer operated at a resolution of 1 cm^{-1}. Spectra over the desired region were obtained in 120 s (40 scan average) in order to reduce white light (of the FT spectrometer, ~2.5 mW/cm^2 at the sample) filling of the primary hole burned spectrum while maintaining an acceptable signal/noise ratio. The FT spectrometer scan was initiated 20 s after termination of both the primary and secondary irradiation (ω_S) burn. During primary burning and secondary irradiation the FT spectrometer's white light was blocked from the sample. The afore-mentioned ring dye laser was used as the primary burn and secondary irradiation source. The primary burn frequencies used for CV/PVOH and chlorophyll *a* of the photosystem I core antenna complex were ω_B = 15873 and 14917 cm^{-1}, respectively. The ODs of the samples used were $\leq$ 0.3 at the burn frequency. The primary burn and secondary

irradiation burn intensities and times are given in the figure captions. For CV/PVOH the primary burn fluences used in the FT spectrometer LIHF experiments are much higher than those used in the two-laser experiments, vide supra, because of the necessity to produce pronounced phonon sideband hole and anti-hole structure. Two-laser LIHF experiments were not performed on chlorophyll *a*.

As noted, filling from the white light of the FT spectrometer complicates the second type of LIHF experiment. To determine the extent of this filling separate experiments were performed as follows: 20 s after termination of the primary burn (same burn conditions as used for the LIHF experiment) the hole spectrum was recorded and then the white light blocked for a period of time equal to the secondary irradiation time used for LIHF. The hole spectrum was then read and compared with the spectrum obtained following LIHF. For the CV/PVOH experiments the white light filling was 20-25%. For chlorophyll *a* of the core complex the filling was 10%.

The photosystem I particles from spinach were a gift from Dr. John Golbeck and enriched to a 45:1 ratio of antenna chlorophyll *a* to the chlorophyll *a* of the special pair of the reaction center according to the procedure of Mullet et al. [17]. The particles were dissolved in a buffered glycerol/water mixture containing 0.1% Triton X-100 detergent as described in ref. (20). Other experimental details can be found in ref. (10) and Part II.

RESULTS

The lower energy portion of the 1.6 K absorption spectrum of CV in PVOH is shown in Figure 1. The value of ω_B chosen (15873 cm^{-1}, solid arrow), which is midway up the low energy tail, ensures that absorption is not dominated by phonon sideband (PSB) transitions. The ω_S-values utilized are indicated by the dashed arrows and range from ω_B – 200 to ω_B + 250 cm^{-1}. For the sample whose spectrum is given in Figure 1, the optical density ranges from 0.08 at $\omega_S = \omega_B - 200$ to 0.39 at $\omega_S = \omega_B +$ 250 cm^{-1}. (This sample was used for the experiments that employed the FT spectrometer.) From the real-vibronic hole structure (Part II) it has been determined that the most intense intramolecular vibronic bands correspond to the 540 and 580 cm^{-1} modes, each carrying a Franck-Condon factor of only 0.1. Thus, for the ω_B- and ω_S-values used, the absorption is dominated by the inhomogeneous distribution of origin ZPL and their accompanying low frequency PSB.

As discussed in the experimental section, two types of LIHF experiments were performed: one that employed two lasers and a double beam set up for continuous monitoring of the filling of ZPH at ω_B = 15802 cm^{-1} (He-Ne laser); and the other that involved recording of the entire hole spectrum with an FT spectrometer following termination of the burn at ω_B and again after termination of secondary irradiation (ring dye laser) at ω_S. The former setup has the advantage of better time resolution but the latter provides important information on the interferences to the filling of the ZPH at ω_B

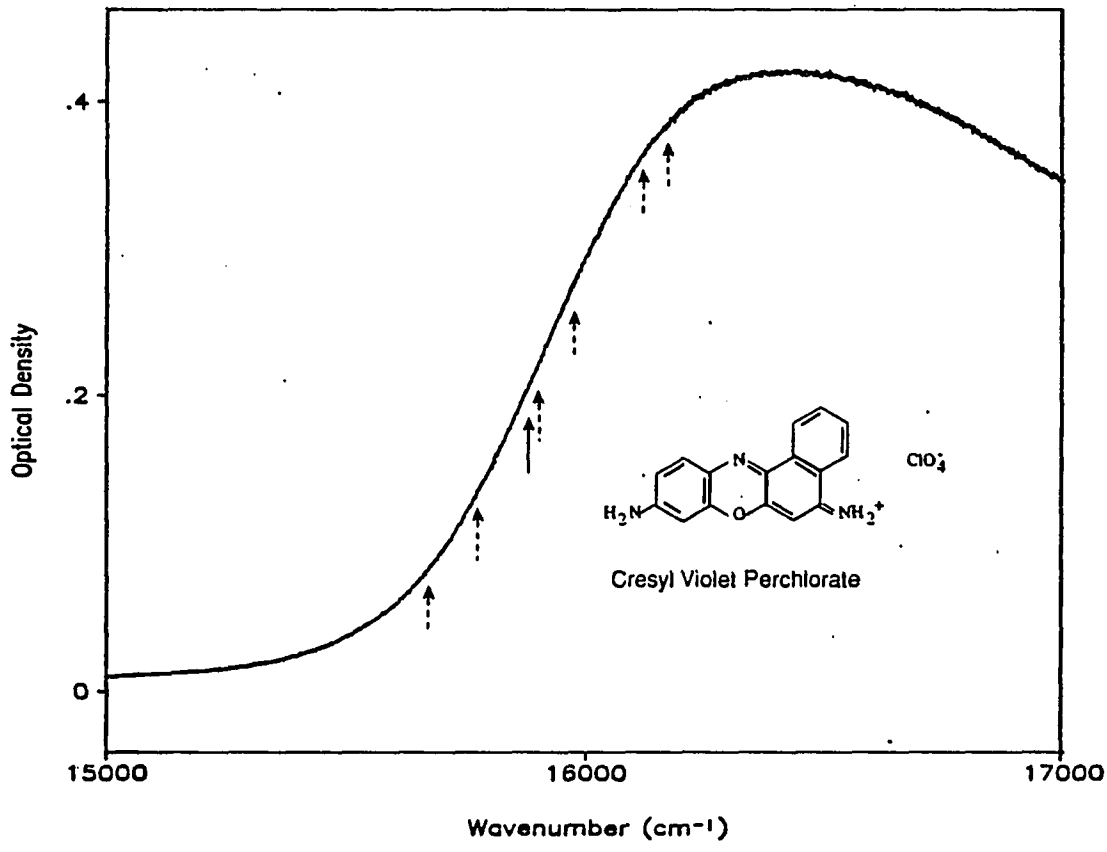

Figure 1. Absorption spectrum of CV in PVOH at 1.6 K. The solid arrow represents the primary burning frequency at ω_B = 15873 cm^{-1}. The dashed arrows represent the secondary burning frequencies at ω_S = ω_B + 20 cm^{-1}, ω_B + 100 cm^{-1}, ω_B + 200 cm^{-1}, ω_B+250 cm^{-1}, ω_B − 100 cm^{-1} and ω_B − 200 cm^{-1}. OD ~ 0.18 at 15873 cm^{-1}. OD ranges from 0.08 at ω_S = ω_B − 200 cm^{-1} to 0.39 at ω_S = ω_B + 250 cm^{-1}

from the phonon sideband hole (PSBH) and anti-hole produced by ω_S-irradiation. Hereafter, we refer to the two experiments as double- and single-beam.

Double-beam ZPH filling curves are shown in Figure 2 for $\omega_S = \omega_B + 100$ cm^{-1} and four different secondary irradiation intensities, I_S = 125, 250, 500 μW and 10 mW/cm^2 (a-d, respectively). For clarity, the noise (see error bar in Fig.) has been removed from the actual experimental curves. As discussed in section II, monitoring of the probe (attenuated He-Ne laser) at the primary ZPH was initiated 60 s after termination of the burn in order to largely eliminate the contribution to filling from SPHF (see paper II). Obviously anomalous is curve d for the highest value of I_S, 10 mW/cm^2. For t_S (secondary irradiation time) > 600 s, the optical density at ω_B is actually lower than its value at the initiation of monitoring. The reason for this is apparent from Fig. 3 which shows the hole burned spectrum generated with ω_B prior to secondary irradiation (curve a) and after secondary irradiation at $\omega_S = \omega_B + 100$ cm^{-1} (curve b) with I_S = 10 mW/cm^2 for 900 s (t_S). Obviously, the pseudo-PSHB [19] (solid arrow) associated with the ZPH at ω_S interferes severely with the remnant of the ZPH at ω_B. For such a large fluence of secondary irradiation, the ZPH is nearly completely erased. Figure 3 underscores the care that must be taken in the interpretation of double-beam filling curves. We see later that curve c of Figure 2 suffers from a small amount of pseudo-PSBH interference for t_S > ~400 s. However, curves a and b corresponding to the two lowest values of I_S are largely unaffected.

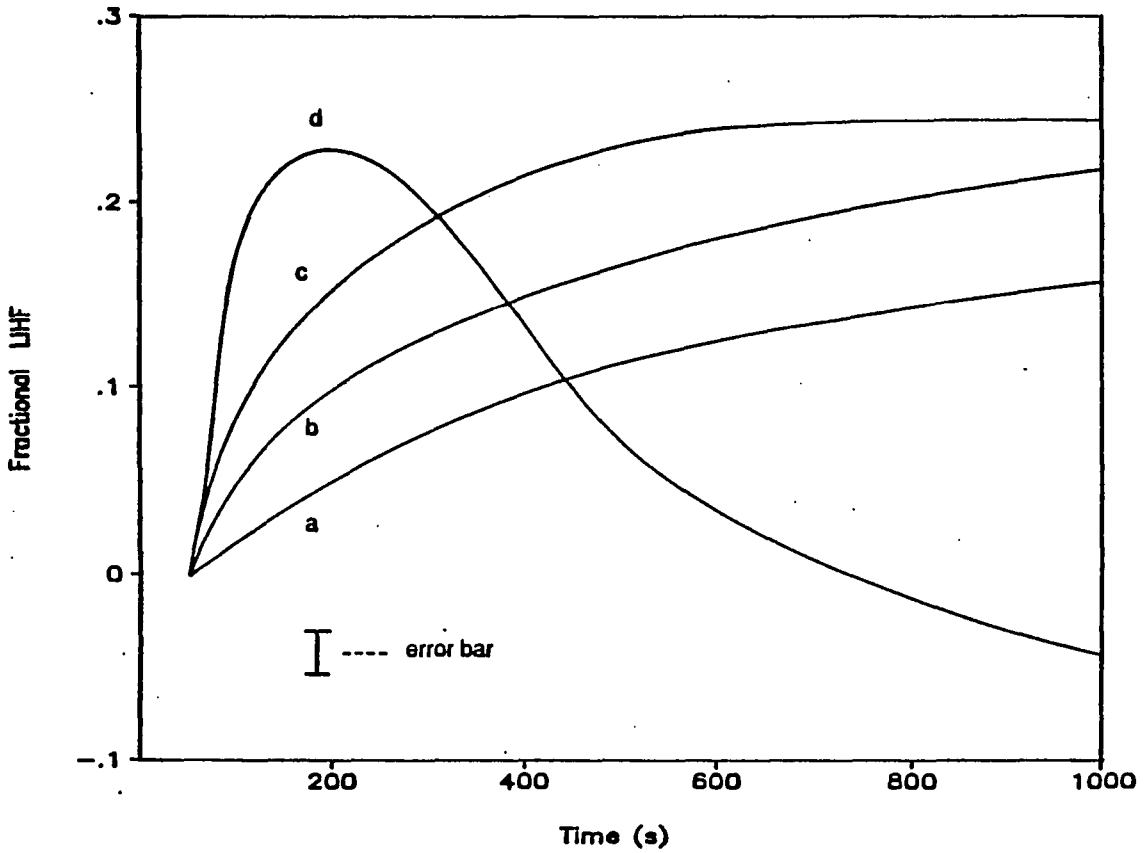

Figure 2. Fractional LIHF curves (double-beam) for four different secondary irradiation intensities. Curve a, b, c and d corresponds to I_S = 125, 250, 500 μW and 10 mW/cm^2, respectively; ω_B = 15802 cm^{-1} (H_e-N_e laser line); $\omega_S = \omega_B + 100$ cm^{-1}. Primary hole depth ~ 35%. For the purpose of clarity the noise (see error bar in Fig.) of original data has been removed. The anomalous behavior of curve d is due to interference from the pseudo-PSBH of the secondary burn with I_S = 10 mW/cm^2 (see text)

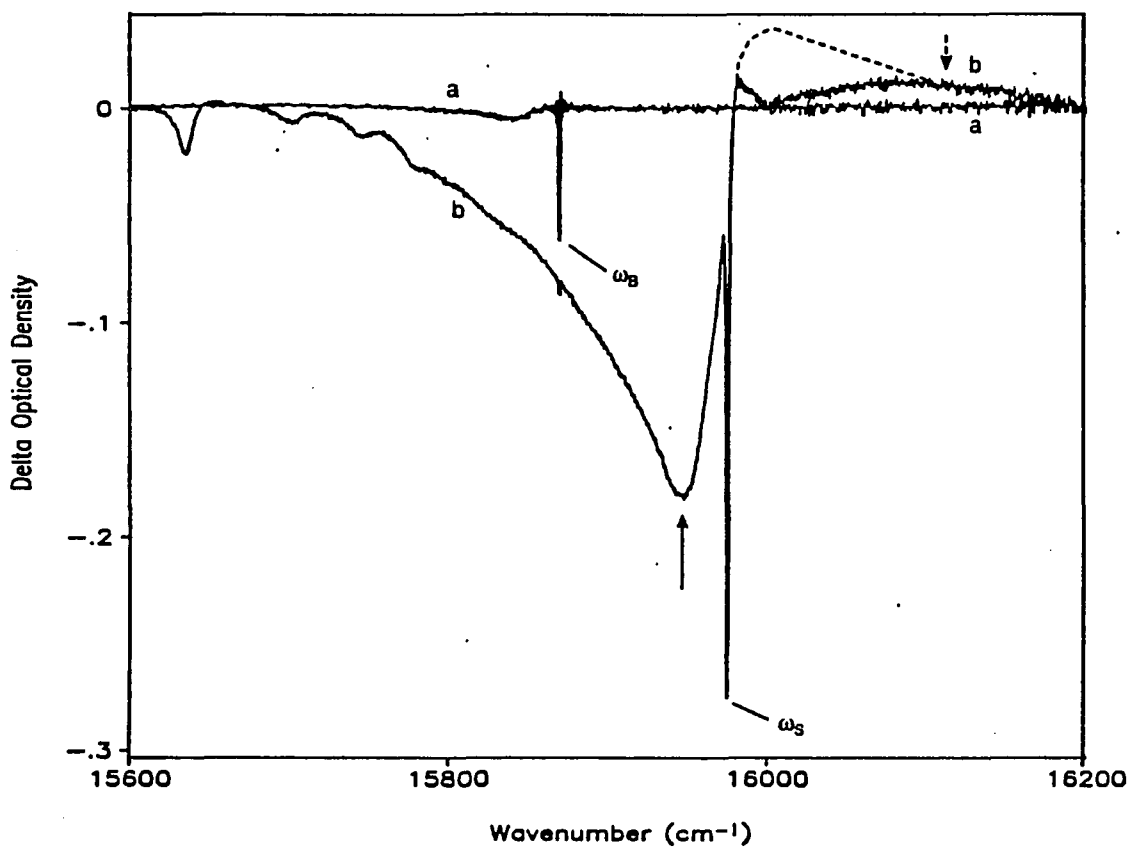

Figure 3. Single-beam (FT) LIHF spectra. Spectra a and b represent hole spectra of primary burn (I_B = 500 μW/cm^2, t_B = 2 min.) and secondary burn (I_S = 10 mW/cm^2, t_S = 15 min.), respectively. ω_B = 15873 cm^{-1}, $\omega_S = \omega_B$ + 100 cm^{-1}. Spectrum b shows that the primary hole is almost completely filled after the secondary irradiation. The interference from pseudo-PSBH of secondary burn is clearly demonstrated. The dashed curve in spectrum b is an approximate indication of the anti-hole without the interference. Spectrum b also shows that the anti-hole of secondary burn undergoes blue shift

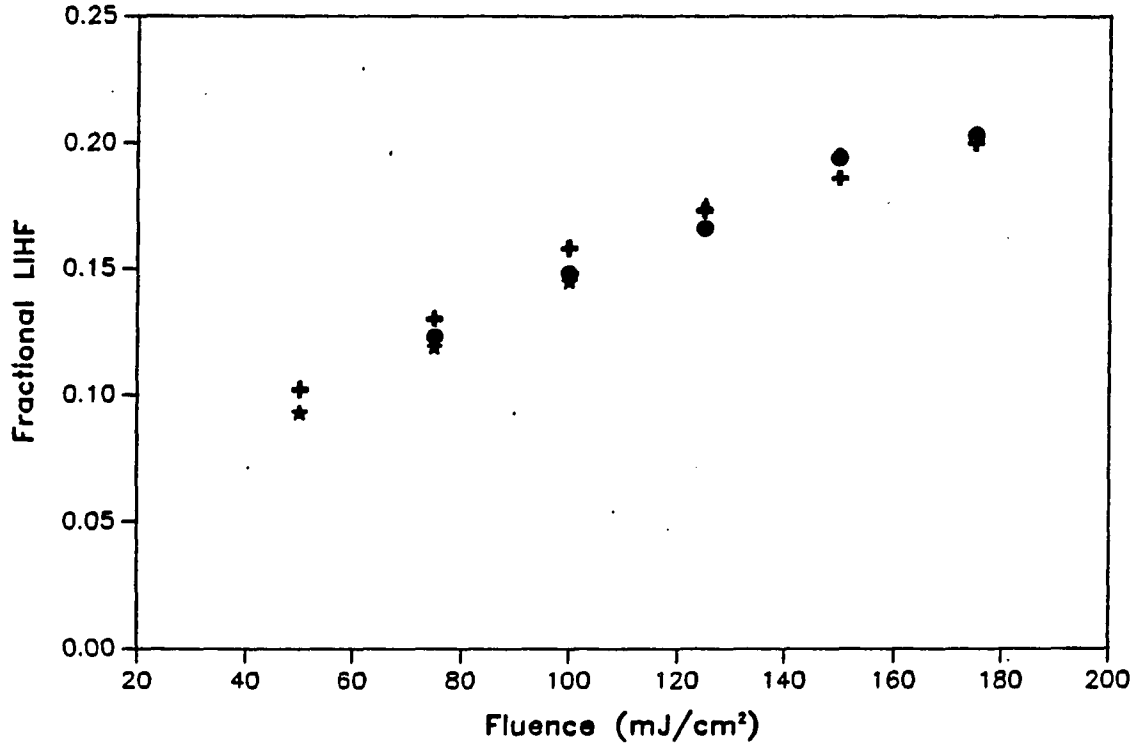

Figure 4. Fluence-dependence data of LIHF. The data are obtained from the curves a, b and c in Figure 2

It was suggested in ref. (13) that LIHF might exhibit a nonlinear dependence on I_S. However Figure 4, for which curves a-c of Figure 2 were utilized, shows that the fractional amount of ZPH filling for a given value of the ω_S-fluence scales with the fluence (for fluence values < 200 mJ/cm^2 the correction to the I_S = 500 μW/cm^2 data points due to the pseudo-PSBH hole produced by ω_S is insignificant).

We present next four figures that pertain to the question of the dependence of the filling efficiency on the value of ω_S. Figure 5 shows filling curves obtained with I_S = 500 μW/cm^2 for $\omega_S = \omega_B$ + 50, 100, 200 and 250 cm^{-1} (curves a-d). Curves b-d are not significantly affected by pseudo-PSBH hole interference from hole burning at ω_S. An approximate correction to curve a, determined with the aid of the FT hole spectra of Figure 6, is indicated by the upward vertical arrow. Thus, the hole filling efficiency for $\omega_S > \omega_B$ is only weakly dependent on the value of ω_S. For the sample used, the optical densities at $\omega_S = \omega_B$ + 50 and ω_B + 250 cm^{-1} were 0.24 and 0.37, respectively. From the discussion given in the Introduction, it is evident that the above characteristics for CV/PVOH are similar to those observed for R640/PVOH.

That the hole filling efficiency is essentially independent of the ω_S-value for $\omega_S > \omega_B$ is further demonstrated by the single-beam results of Figure 6 obtained with I_S = 2 mW/cm^2 and t_S = 300 s for $\omega_S = \omega_B$ + 20, 100 and 250 cm^{-1}. The apparent percentage hole fillings for the three ω_S-values are 50, 47, and 46%, the same within experimental uncertainty. However this percentage, when corrected for white light filling from the FT spectrometer (see section II for discussion), is reduced to 25-30.

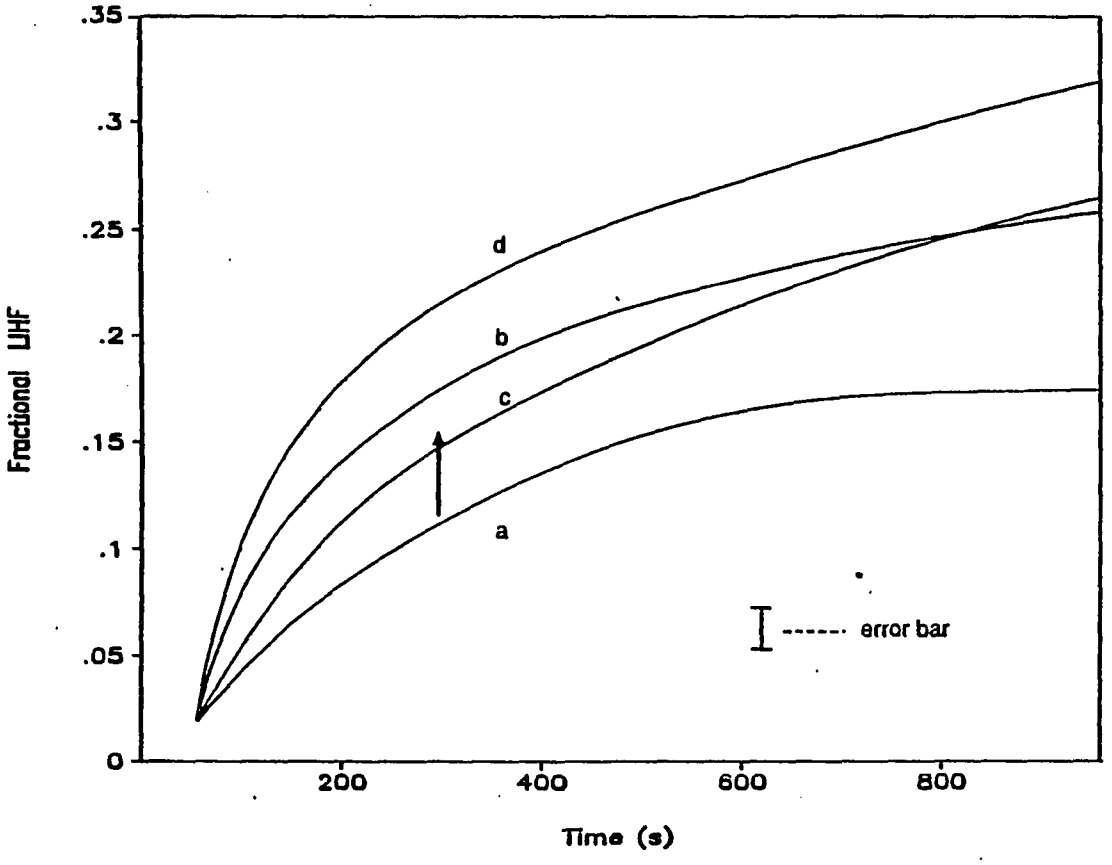

Figure 5. LIHF curves (double-beam) for different secondary burn frequencies $\omega_S = \omega_B + 50$, 100, 200 and 250 cm^{-1} (a, b, c and d). The noise was removed from the original data for the purpose of clarity. Arrow indicates the data point at 300 s for curve (a) after the correction of interference from pseudo-PSBH of secondary burn. For primary hole, $I_B = 13$ $\mu w/cm^2$, $t_B = 3$ min. Hole depth is - 35%, $\omega_B = 15802$ cm^{-1}. For all curves, $I_S = 500$ $\mu W/cm^2$. Fresh samples were used for each ω_S

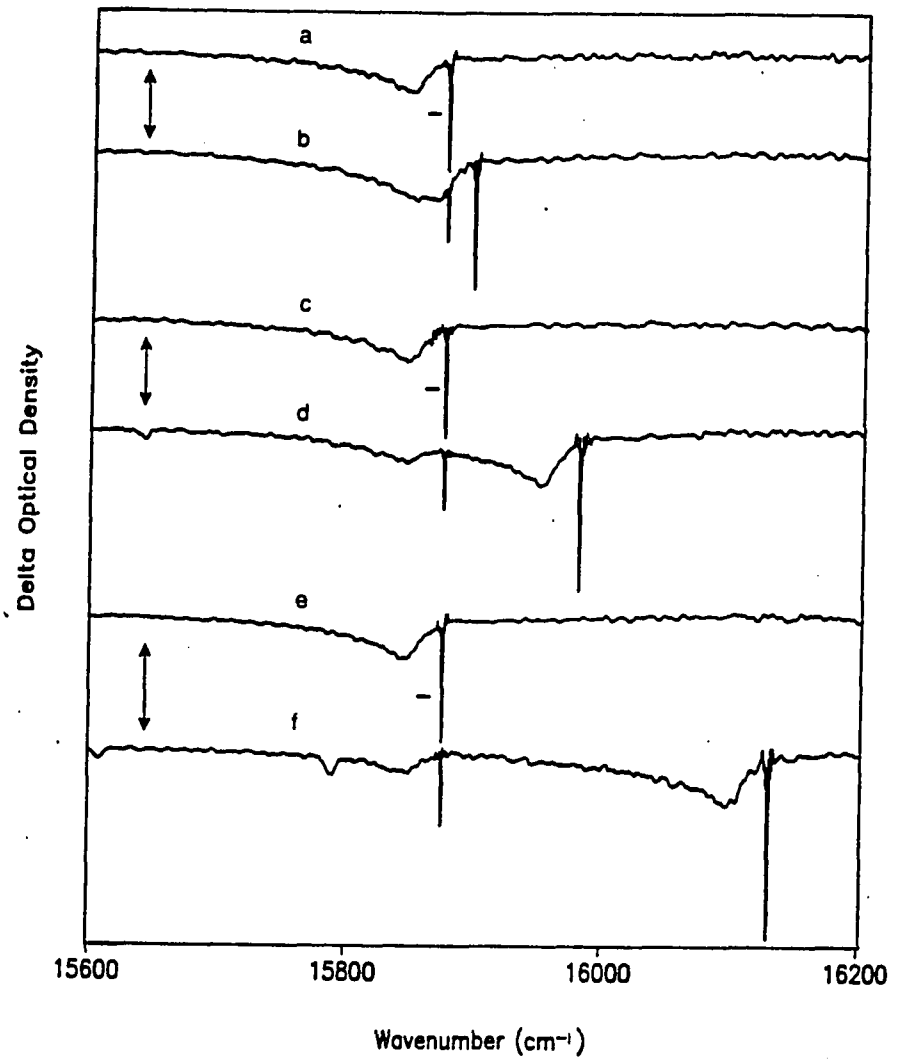

Figure 6. LIHF spectra (single-beam) for different secondary burn frequencies, $\omega_S = \omega_B + 20$, 100 and $\omega_B + 250$ cm^{-1} (a-b, c-d and e-f, respectively). Spectra a, c and e are the hole spectra for primary burn. $I_B = 2$ mW/cm^2, $t_B = 300$ sec, $\omega_B = 15873$ cm^{-1}. Spectra b, d and f are the hole spectra after the secondary irradiations with $I_S = 2$ mW/cm^2 and $t_S = 300$ sec. The horizonal bars indicate the hole depth after secondary irradiations so that the hole fillings can be clearly revealed. The fractional hole fillings are ~ 50, 47 and 45% (b, d and f, respectively), which include about 20% white light hole fillings

From Figure 6 it is apparent that filling of the ZPH at ω_B is accompanied by filling of its pseudo-PSBH.

We consider next hole filling results obtained for $\omega_S < \omega_B$. Double-beam filling curves were obtained with $I_S = 500\ \mu W/cm^2$ for $\omega_S = \omega_B - 50$, -100 and $-200\ cm^{-1}$. The curves for the first and last values are given in Figure 7 as b and c, respectively (the curve for $\omega_S = \omega_B - 100\ cm^{-1}$ lies between these two). For comparison, the LIHF curve (d) for $\omega_S = \omega_B + 100\ cm^{-1}$ and the spontaneous hole filling curve (a) are also given. It is apparent that LIHF for $\omega_S > \omega_B$ is significantly more efficient than for $\omega_S < \omega_B$. For $\omega_S < \omega_B$ the LIHF curves lie only slightly higher than the spontaneous hole filling curve. Furthermore, the results show that the filling for $\omega_S < \omega_B$ is, at most, weakly dependent on ω_B (over an OD range of 0.08 to 0.17).

The single-beam spectra of Figure 8, obtained with $I_S = 500\ \mu W/cm^2$ and $t_S = 360$ s for $\omega_S = \omega_B + 100$, -100 and $-200\ cm^{-1}$, also illustrate that filling for $\omega_S > \omega_B$ is more facile than for $\omega_S < \omega_B$. The fractional values for LIHF are given in the figure caption.

Finally, in Figure 9 is shown the hole spectrum obtained with $I_B = 2\ mW/cm^2$ and $t_B = 5$ min. (dashed line) and the spectrum recorded following secondary irradiation at $\omega_S = \omega_B + 250\ cm^{-1}$ with $I_S = 2\ mW/cm^2$ and $t_S = 5$ min. (solid line). The spectra clearly show that the fractional fillings of the pseudo-PSBH hole (solid arrow) and ZPH at ω_B are nearly equal at ~25% after correction for white light filling from the FT spectrometer. The dashed arrow features associated with solid line spectrum are pseudo-

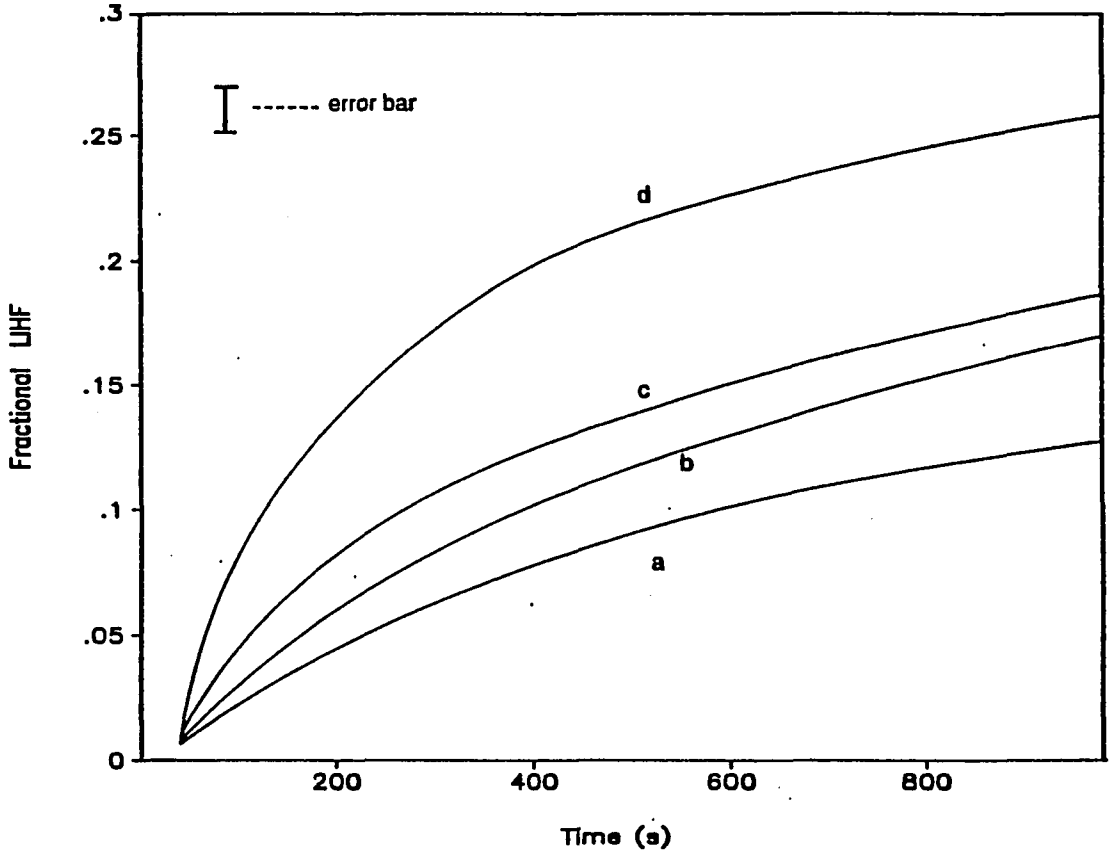

Figure 7. Time-dependence LIHF curves (double-beam) for $\omega_S < \omega_B$ with I_S = 500 $\mu W/cm^2$, $\omega_S = \omega_B - 50$ and $- 200$ cm^{-1} (b and c, respectively). For the comparison of LIHF effect for $\omega_S < \omega_B$ with $\omega_S > \omega_B$, curve d ($\omega_S = \omega_B + 100$ cm^{-1}, I_S = 500 $\mu W/cm^2$) is also shown. Curve (a)2 represents spontaneous hole filling data. For all curves, I_B = 13 $\mu W/cm^2$, t_B = 180 seconds. For the purpose of clarity, the noise was removed from the original spectra

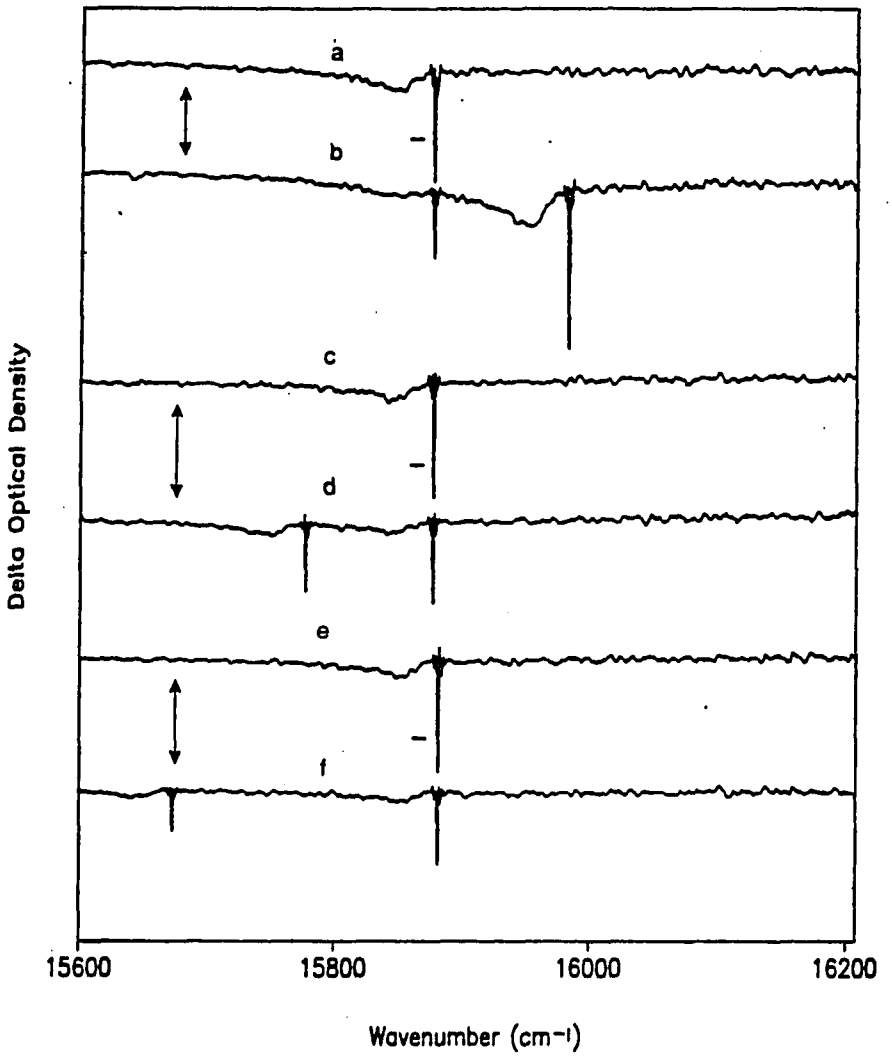

Figure 8. LIHF spectra (single-beam) for different ω_S, $\omega_S = \omega_B + 100, -100,$ and -200 cm^{-1} (a-b, c-d and e-f respectively). Spectra a, c and e are hole spectra for primary burn with $\omega_B = 15873$ cm^{-1}, $I_B = 2$ mW/cm^2 and $t_B = 300$ s. Spectra b, d and f are the LIHF spectra after the secondary irradiation with $I_S = 2$ mW/cm^2 and $t_S = 300$ s. With the correction of white light hole filling, the fractional hole filling is < 8% for $\omega_S < \omega_B$ (for $\omega_S > \omega_B$, fractional hole filling ~ 25 - 30%)

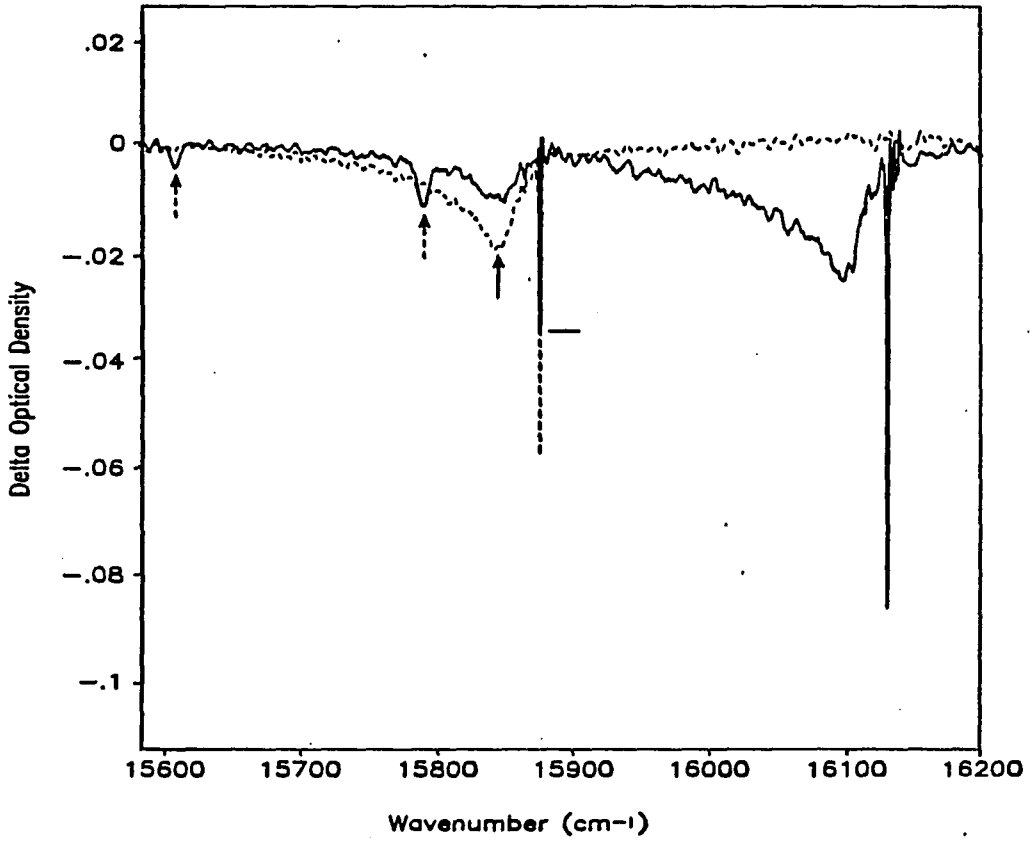

Figure 9. LIHF spectra (single-beam) obtained with 1 cm^{-1} resolution. Primary hole spectrum (dashed line) was obtained with I_B = 2 mW/cm^2, ω_B = 15873 cm^{-1}, t_B = 5 min. and hole depth is ~ 28%. LIHF spectrum (solid line) was obtained after the secondary irradiation with I_S = 2 mW/cm^2 and $\omega_S = \omega_B + 250$ cm^{-1}. The dashed arrows indicate pseudo-vibronic holes which correspond to 520 and 340 cm^{-1} excited state fundamental vibrations. The spectra show that the fractional fillings of the pseudo-PSBH and ZPH at ω_B are nearly equal (25% after correction for white light filling)

vibronic holes corresponding to 520 and 340 cm^{-1} excited state fundamental vibrations.

Lastly, we point out that the extents of LIHF indicated by the FT spectra in Figure 6 for $\omega_S = \omega_B + 20$, +100 and +250 cm^{-1} (I_S = 2 mW/cm^2, t_S = 300 s) are consistent with the double beam filling curves of Figure 5 when the correction for FT white light filling is made. For the conditions used to record the FT spectra following termination

of the secondary irradiation, cf. section II, it was determined that the extent of white light filling is 20-25%, cf. section II. Using this with the total percentages of hole filling given in the caption to Figure 6 yields LIHF percentages of ~25% for each of the three ω_S-values and a secondary irradiation fluence of 600 mJ/cm^2. Noting that the results of Figure 5 were obtained with I_S = 500 $\mu W/cm^2$, the LIHF curves indicate that at 1200 s (600 mJ/cm^2 fluence) the LIHF percentages would be in the range 25-30.

DISCUSSIONS

The four principal observations for CV/PVOH are: (i) fractional filling of the ZPH depends on the secondary irradiation fluence at ω_S (non-linear intensity behavior is not observed); (ii) filling is significantly more efficient for $\omega_S > \omega_B$ than $\omega_S < \omega_B$; (iii) for both $\omega_S >$ and $< \omega_B$ the filling efficiency is independent of ω_S (for the $|\omega_S - \omega_B|$ values employed); and (iv) the ZPH at ω_B and its associated pseudo-PSBH fill in concert. The third observation, which means that the ω_S-dependence of the filling efficiency does not reflect the optical density variation across the absorption band, and the first might appear, at first sight, to present a paradox. It is one that is eliminated by the model presented below.

Unavailable to Fearey et al. [10] was spectral information on the anti-hole associated with NPHB of R640/PVOH. The anti-hole for CV/PVOH has been studied in considerable detail, see ref. (10) and Part II. The spectra given in I show that the anti-hole of the origin ZPH at ω_B and its companion PSBHs extends (tails) roughly 1000 cm^{-1} to the blue of ω_B. However, the presence of moderately intense real vibronic holes (the most intense being 540 and 580 cm^{-1} with Franck-Condon factors of ~0.10) necessitates integration of the hole spectrum out to about 5000 cm^{-1} to the blue of ω_B in order to determine that overall absorption intensity is conserved during NPHB. The extreme breadth of the blue-shifted anti-hole makes it difficult to observe except for "hard" burns which produce an intense pseudo-PSBH, see Part II and spectrum b of

Figure 3 where the anti-hole is indicated by the dashed arrow. It was proven by T-dependent studies that the minimum in the anti-hole profile at ω_S + 25 cm^{-1} is due to the interference between the anti-hole and real-PSBH [10], see also paper I. Based on the results of I, the dashed curve in spectrum b of Figure 3 is an approximate indication of the anti-hole in the absence of the above interference. The anti-hole is predominantly the counterpart of the pseudo-PSBH (in NPHB a sharp anti-hole corresponding to the ZPH is generally not observed due to the immense structural disorder of the amorphous host). It should be emphasized that the blue-shifted anti-hole appears to be a general phenomenon for S_1 ($\pi\pi^*$) states of polyatomic molecules, cf. Part II. Spectrum a of Figure 10 is for the S_1 ($\pi\pi^*$) state of chlorophyll *a* (Chl *a*) in the core antenna complex of photosystem I. As reported on earlier [18], this system provides an excellent example of conservation of absorption intensity between the pseudo-PSBH and anti-hole. To considerable measure this is due to the fact that the vibronic activity for the S_1 state of chlorophyll *a* is very weak [18]. Thus, interferences between the anti-hole and real vibronic holes are not nearly as significant as they are for CV/PVOH.

The fourth observation, vide supra, begged the question of whether or not the anti-hole associated with secondary irradiation of ω_S undergoes a diminuation in intensity that parallels the filling of the ZPH at ω_B and its pseudo-PSBH. The large breadth of the anti-hole for CV/PVOH makes such a determination very difficult. For this reason we turned to Chl *a* of the antenna complex since its anti-hole is considerably

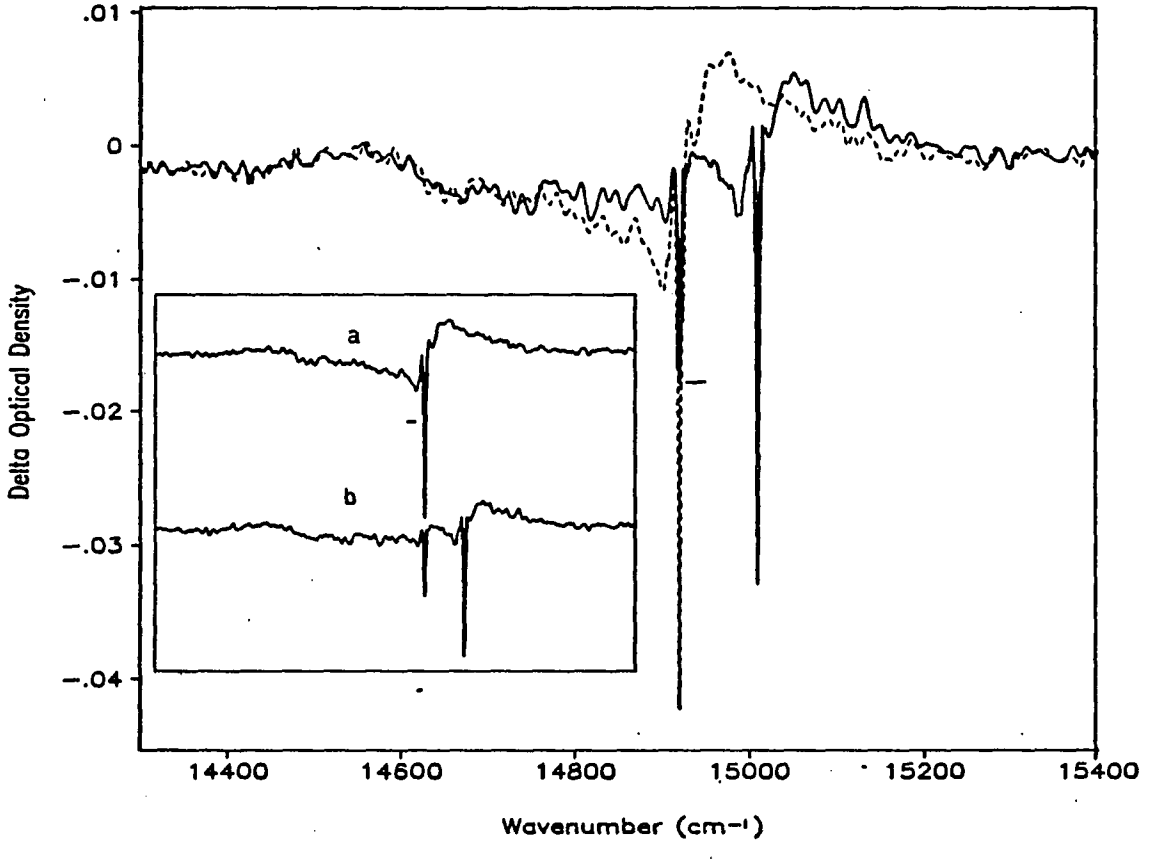

Figure 10. LIHF spectra for Chl a in antenna complex of Photosystem I. Primary hole spectrum (dashed line) was obtained with I_B = 2 W/cm^2, t_B = 20 min. and ω_B = 14917 cm^{-1}. The hole depth is ~ 14%. LIHF spectrum (solid line) was obtained with I_S = 2 W/cm^2, $\omega_S = \omega_B$ + 90 cm^{-1} and t_S = 10 min. The horizontal bar indicates that hole filling is ~ 60% (include 10% white light hole filling). The spectra were displaced in window to show the hole filling for ZPH

more pronounced and narrower. Comparison of spectra a and b in Figure 10 show, as do others obtained for different ω_S-values, that such a diminuation does occur.

This finding, together with the other results, leads to a quite obvious model for the mechanism that is responsible for the *additional* LIHF efficiency observed for $\omega_S > \omega_B$. We define and discuss it with the aid of Figure 11, which shows the ZPH at ω_B and its pseudo-PSBH along with the *blue-shifted* anti-hole. Also shown is the ZPL plus PSB (phonon sideband) for sites whose ZPL is coincident with ω_S along with a representative ZPL + PSB for sites whose ZPL lie to lower energy of ω_S but, nevertheless, can absorb ω_S via their PSB. Note that for a blue-shifted anti-hole, excitation of anti-hole sites is not possible for $\omega_S < \omega_B$. The model proposed for consideration has the hole filling being due to electronic excitation of *anti-hole* sites via (primarily) PSB transitions, i.e. sites not involved in the initial burn at ω_B are of no real consequence. Thus, hole filling is due to light-induced anti-hole reversion. Excitation of anti-hole sites via their phonon wing is a necessary condition because consideration of only anti-hole sites whose ZPL are coincident with ω_S would lead to excitation of only a very small fraction (ca. $\lesssim 10^{-3}$) of the total number of anti-hole sites, i.e. the extent of filling observed could not be explained. On the other hand, the width of the one-phonon profile for CV/PVOH is ~40 cm^{-1} [10] and its Huang-Rhys factor is S ~ 0.7 (paper II). Given that the Poisson distribution $\{\exp(-S)S^r/r!\}$ governs the Franck-Condon factors for the r = 0 (zero-phonon) and r = 1, 2 ... phonon transitions, it is apparent that PSB transitions allows for excitation of a broad distribution of anti-hole

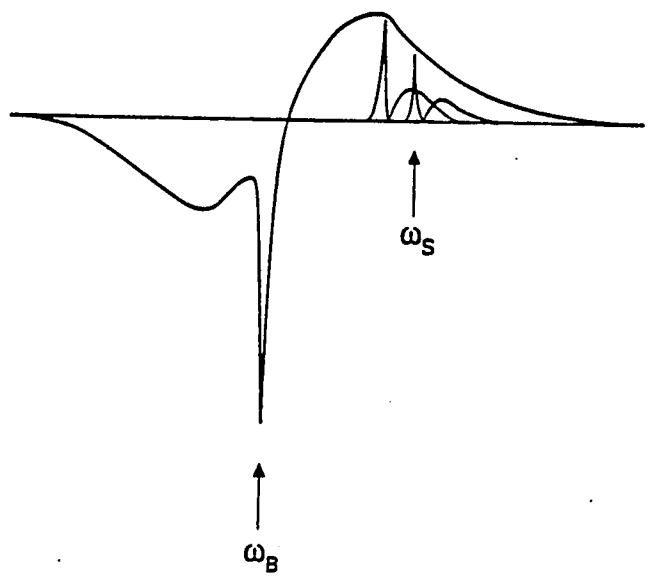

Figure 11. Schematic representation of hole profile and single site absorption profile

sites whose ZPL lie to the red of ω_S. Implicit in the model is that for $\omega_S > \omega_B$ the probability for exciting sites whose ZPL are at $\omega < \omega_S$ is governed by $A(\omega)g(\omega_S-\omega)$, where $A(\omega)$ is the anti-hole profile and $g(\omega_S-\omega)$ is the PSB profile. Given the large width of $A(\omega)$ for CV/PVOH, the absence of a strong dependence of the hole filling efficiency on ω_S ($> \omega_B$) is not surprising. Before considering the above mechanism further we address the question of the mechanism that is responsible for filling for $\omega_S < \omega_B$. Taken as a whole, our results indicate that filling for $\omega_S < \omega_B$ is a factor of about 2-3 times less efficient than for $\omega_S > \omega_B$.

The observation that for $\omega_S < \omega_B$ the filling efficiency for CV/PVOH is, at most, weakly dependent on ω_S (even when located at the edge of the low energy tail of the absorption band) has also been made for R640/PVOH [13] and Chl *a* in the core antenna complex of PSI (results not shown). The CV/PVOH hole spectra of ref. (10) and Part II show no evidence for anti-hole formation to the red of ω_B. Figure 3 and spectra in Part II show very clearly that the anti-hole for CV/PVOH is predominantly blue-shifted. This suggests that filling for $\omega_S < \omega_B$ is not due primarily to optical excitation of anti-hole sites produced by the burn at ω_B. We suggest that the mechanism may involve optical excitation of high energy vibrational overtone and combination bands of the host. Such bands would provide a more or less uniform but weak background absorption in the region of the probe's electronic absorption band, which could explain the independence of the filling efficiency on ω_S. For PVOH, the -OH stretching mode (3600 cm^{-1}) could be an important contributing fundamental.

Recent infra-red light induced filling experiments on metal-free phthalocyanine in polyethylene and polymethyl-methacrylate [14] provide support for this mechanism as do the results for R560/PVOH [13]. In the latter experiments a burn wavelength (λ_B) of 514.5 nm was used for the primary burn of R560. It was found that the filling efficiency for a secondary irradiation wavelength (λ_S) of 617.0 nm, where absorption due to R560 is negligibly small, is comparable to that observed for $\omega_S < \omega_B$ with ω_S located in the R560 absorption band. Furthermore, when CV was added to R560/CV, so as to provide significant electronic absorption at λ_S = 617.0 nm, the filling efficiency of the R560 hole underwent a substantial decrease. This decrease can be rationalized in terms of the reduction of ω_S-intensity for host vibrational excitation due to CV absorption. We note that electronic relaxation (primarily by fluorescence) of the S_1 state of CV populates CV vibrational levels in S_0 but that the vast majority of these levels would not be able to relax to -OH vibrational states of PVOH because of the higher frequency of the -OH stretch mode.

We turn now to further discussion of our mechanism for $LIHF_e$ based on anti-hole reversion triggered by electronic excitation at ω_S of anti-hole sites produced by the primary burn at ω_B. Excitation of these sites via their PSB is a key feature of the mechanism. For S_1 ($\pi\pi^*$) states, which generally appear to yield a blue-shifted anti-hole, a requirement for $LIHF_e$ with ω_S located in the origin absorption band is that $\omega_S > \omega_B$. From the data presented here and elsewhere [11,13] it is apparent that, for appreciable $LIHF_e$ to occur, an ω_S-fluence comparable to the ω_B-fluence used to

generate the primary hole spectrum must be employed. This and the double-beam spectra shown indicate that the mechanisms of NPHB and $LIHF_e$ are intimately connected. In fact, our results show that the kinetics for $LIHF_e$ are dispersive as is the case for NPHB. Figure 12 shows a data set for fractional LIHF that exhibits the logarithmic dependence on time which is a signature of dispersive kinetics [1,20].

As discussed in the Introduction and Part II, there are several types of data that establish that the standard TLS_{ext} model [10,21] for NPHB is inadequate. The model of Shu and Small [10], which is based on an outside-in hierarchy of glass-probe configurational relaxations processes, can qualitatively account for the available observations. Nevertheless, it needs to be more stringently tested by new types of experiments. A similar model, but one based on TLS_{ext} relaxation in the ground electronic state (TLS^{α}_{ext}) induced by non-equilibrium phonons produced by radiative and non-radiative decay of the probe's S_1 state, was also considered in Part II. The observation that excitation at ω_S of anti-hole sites produced by the primary burn causes them to red-shift (to produce hole filling) while excitation of "virgin" sites at ω_S still produces a blue-shifted anti-hole is important because it proves that the probe-glass configurations of the virgin sites at $\omega_S > \omega_B$ are kinetically inaccessible to the sites produced at ω_B. Furthermore, the fact that ω_S-irradiation of anti-hole sites produces hole filling through red-shifting strongly suggests that the notion of a more or less well-defined TLS_{ext} relaxation coordinate(s) for NPHB (at a given burn temperature) can be retained in complex models of NPHB. The red-shifting of the anti-hole sites produced by ω_S-

irradiation shows that these sites retain at least partial memory of their pre-burn configurations. It is unlikely, given the inherent disorder of the glass and complex dynamics that lead to hole formation, that each and every probe would be returned to precisely its pre-burn configuration following its excitation in the post-burn configuration (perfect memory). Nevertheless, the propensity of the entire anti-hole to red-shift (partial memory) provides the means for filling of the primary hole profile (ZPH plus PSBHs).

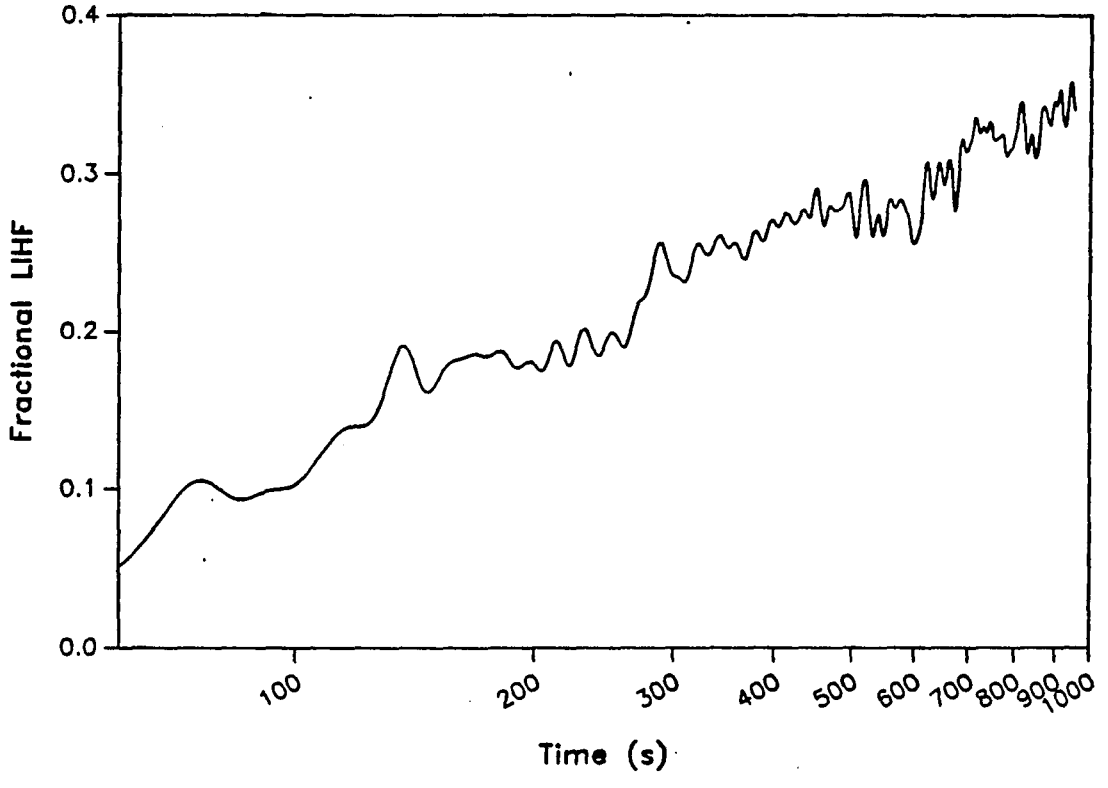

Figure 12. Fractional LIHF spectrum plotted in log (t) scale. The spectrum was obtained with I_S = 500 $\mu W/cm^2$, $\omega_S = \omega_B$ + 250 cm^{-1} and ω_B = 15802 cm^{-1}

CONCLUSIONS

The results of single- and two-laser experiments on cresyl violet in PVOH films establish that the primary mechanism of laser-induced hole filling, for the case where the secondary irradiation frequency (ω_S) is located in the origin absorption band, is electronic excitation of the anti-hole sites produced by the primary burn at ω_B. Because $^1\pi\pi^*$ probe states typically yield a blue-shifted anti-hole, the above mechanism is operative for $\omega_S > \omega_B$. The principal mode of excitation of the anti-hole sites is suggested to involve the broad phonon sideband which builds on the zero-phonon line. For systems like CV/PVOH, which exhibit a very broad anti-hole, it follows that $LIHF_e$ should be weakly dependent on $\omega_S - \omega_B$, as observed. The observation that ω_S-excitation of anti-hole sites results in their being red-shifted (with concomitant filling of the primary hole profile) while ω_S-excitation of virgin sites leads to a blue-shifted anti-hole shows that the anti-hole sites produced by the primary burn retain at least a partial memory of their pre-burn configurations. This suggests that the notion of a more or less well-defined extrinsic (probe-inner shell) relaxation coordinate(s), q_{ext}, at a given burn temperature can be retained in mechanistic models which go beyond the standard TLS_{ext} model.

ACKNOWLEDGEMENTS

This research was supported by the Division of Materials Research of the National Science Foundation under Grant No. DMR-8920515. We would like to thank J. Hayes and R. Jankowiak for useful discussions.

REFERENCES

[1] M. J. Kenney, R. Jankowiak and G. J. Small, Chem. Phys. 146 (1990) 47.

[2] S. K. Lyo, Phys. Rev. Lett. 48 (1982) 688.

[3] S. K. Lyo, in Electronic Excitions and Interaction Processes in Organic Molecular Aggregates, eds. P. Reineker, H. Haken and H. C. Wolf, Springer S. Solid-State Sci. Vol. 49 (Springer, Berlin, 1983).

[4] D. L. Huber, M. M. Broer and B. Golding, Phys. Rev. Lett. 52 (1984) 2281.

[5] R. Jankowiak and G. J. Small, J. Phys. Chem. 90 (1986) 5612.

[6] J. M. Hayes, R. Jankowiak and G. J. Small, in: Topics in Current Physics, Persistent Hole-Burning: Science and Applications, ed. W. E. Moerner (Springer, Berlin, 1988) p. 153.

[7] M. Berg, C. A. Walsh, L. R. Narasimhan, K. A. Littau and M. D. Fayer, J. Chem. Phys. 88 (1988) 1564.

[8] F. Kokai, H. Tanaka, J. I. Brauman and M. D. Fayer, Chem. Phys. Lett. 143 (1988) 1.

[9] B. L. Fearey, R. P. Stout, J. M. Hayes and G. J. Small, J. Chem. Phys. 78 (1983) 7013.

[10] L. Shu and G. J. Small, Chem. Phys. 141 (1990) 447.

[11] J. M. Hayes and G. J. Small, Chem. Phys. 27 (1978) 151; Chem. Phys. Lett. 54 (1978) 435.

[12] 'Dark' thermally induced host-impurity configuration changes which serve to fill the gradient in frequency space produced by the primary burn.

[13] B. L. Fearey, T. P. Carter and G. J. Small, Chem. Phys. 101 (1986) 279.

[14] W. Richter, Th. Sesselmann, D. Haarer, Chem. Phys. Lett. 159 (1989) 235.

[15] A. A. Gorokhvoskii, G. S. Zavt, V. V. Palm, JETP Lett. 48 (1988) 369.

[16] T. P. Carter, Ph.D. Dissertation (Iowa State University, 1986).

[17] J. E. Mullet, J. J. Burke and C. J. Arntzen, Plant Physiol, 65 (1980) 814.

[18] J. K. Gillie, G. J. Small and J. H. Golbeck, J. Phys Chem. 93 (1989) 1620.

[19] The pseudo-PSBH is due to sites that absorb ω_B via phonon side band transitions which build on and to higher energy of their ZPL.

[20] R. Jankowiak, L. Shu, M. J. Kenney and G. J. Small, J. Luminescence 36 (1987) 293.

[21] J. M. Hayes, R. P. Stout and G. J. Small, J. Chem. Phys. 74 (1981) 4266.

GENERAL CONCLUSIONS

Extensive studies of nonphotochemical hole burning (NPHB) on cresyl violet in polyvinyl alcohol films (CV/PVOH) at low temperatures have been performed during the course of this work. The research is directed toward the understanding of the mechanism of NPHB and the relaxation dynamics of amorphous solids at low temperatures, which involves detailed investigations on temperature-dependent NPHB, polarized NPHB, spontaneous hole filling (SPHF) and laser (light) induced hole filling (LIHF).

New temperature-dependent hole burning results together with the blue shifting of anti-hole and burning of 100% zero-phonon lines indicate that the simple model for spectral hole burning based on a static statistical distribution of two-level systems provides an inadequate description. The polarized hole burning results reveal that there is a significant rotation of the probe at higher temperatures and one must go beyond the notation of a single, more or less well-defined q_{ext} and allow for parallel pathways and/or consecutive relaxation steps of the probe-inner shell. A new mechanism, based on an "outside-in" hierarchy of constrained configurational tunneling events, was proposed in which the time evolution of free volumes plays an important role. The model is consistent with the available data and lends itself to testing by further experiments. The conservation of hole and anti-hole area for CV/PVOH was observed for the first time, thus the mechanism of hole burning on CV/PVOH is determined as

nonphotochemical.

The data of NPHB for CV/PVOH at 1.6 K have shown that the kinetics of both hole burning and SPHF can be satisfactorily described by the dispersive kinetics theory. A high degree of positive correlation between the rates of burning and filling associated with TLS_{ext} was found, which indicate that anti-hole site has at least partial memory of its pre-burn configuration. A more physically reasonable interpretation of SPHF kinetics is described by a new methodology in which absolute hole filling (not relative hole filling) is considered. The data of absolute hole filling together with the observation of high degree of positive correlation between the rates of burning and filling indicate that the dominant mechanism for filling is not global spectral diffusion but rather anti-hole reversion.

LIHF is the least studied aspect of NPHB even though it may be the most intriguing one. Two types of LIHF have been reported: that for which ω_S (secondary burn frequency) is located in the same electronic absorption band utilized for hole burning [11,13]; and that for which ω_S is not absorbed by the impurity and lies in the infra-red (i.e. can be absorbed by vibrational states of the host [14,15]). We refer to the two types as $LIHF_e$ and $LIHF_v$, respectively. It is the $LIHF_e$ which was studied in this work. The results of LIHF on cresyl violet in PVOH films established that the primary mechanism of laser-induced hole filling ($LIHF_e$) is electronic excitation of the anti-hole sites produced by the primary burn at ω_B for $\omega_S > \omega_B$, which can account for the principal features of LIHF. The observation that anti-hole sites undergo a red-shift

upon ω_S-excitation (with concomitant filling of the primary hole profile) shows that the anti-hole sites produced by the primary burn retain at least a partial memory of their pre-burn configurations. This suggests that the notion of a more or less well-defined TLS_{ext} coordinate(s) at a given burn temperature can be retained in mechanistic models which go beyond the standard two-level systems model.

GENERAL REFERENCES

[1] W. E. Moerner, In: Topics in Current Physics, Persistent Spectral Hole Burning: Science and Applications, ed. W. E. Moerner (Springer, Berlin, 1988) p. 5.

[2] J. K. Gillie, J. M. Hayes, G. J. Small and J. H. Golbeck, J. Phys. Chem. 91 (1987) 5524.

[3] K. Mauring, I. Renge and R. Avarmaa, FEBS Letters 223 (1987) 165.

[4] I. Renge, K. Mauring and R. Vladkova, R. Biochim. Biophys. Acta 935 (1988) 333.

[5] W. Köhler, J. Friedrich, R. Fischur and H. Scheer, J. Chem. Phys. 89 (1988) 871.

[6] S. G. Johnson and G. J. Small, Chem. Phys. Letter 155 (1989) 371.

[7] J. K. Gillie, G. J. Small and J. H. Golbeck, J. Phys. Chem. 93 (1989) 1620.

[8] R. Jankewiak, D. Tang, G. J. Small and J. Seibert, Phys. Chem. 93 (1989) 1649.

[9] I. Renge, K. Mauring and R. Avarmaa, Biochim. Biophys. Acta 766 (1984) 766.

[10] W. Köhler, J. Friedrich, R. Fischer and H. Scherr, Chem. Phys. Letters 143 (1988) 169.

[11] W. E. Moerner, W. Lenth and G. C. Bjorkland, in: Topics in Current Physics, Persisten Spectral Hole Burning: Science and Applications, ed. W. E. Moerner(Springer, Berlin, 1988) p. 251.

[12] A. C. G. Mitchell and M. W. Zemansky, In: Resonance Radiations and Excited Atoms (Cambridge University Press, Cambridge, 1934).

[13] Ph. Dc Bree and D. A. Wiersma, J. Chem. Phys. 70 (1979) 790.

[14] W. H. Lonisell, In: Quantum Statistical Properties of Radiation, (Wiley, New York, 1973) chap. 6.

[15] C. Cohen-Jannoudji, R. Balian and S. Haroche, In: Frontiers in laser Spectroscopy, ed. S. Liberman (North Holland: Amsterdam, 1977) Vol. 1.

[16] M. Sargent III, M. O. Scully and W. E. Lamb, Jr., In: Laser Physics (Addison-Wesley, Reading, 1974.

[17] K. Blum, In: Physics of Atoms and Molecules, eds. P. G. Bruker and H. Keimpoppen (Plenum Press, New York, 1981)

[18] J. M. Hayes, R. Jankowiak and G. J. Small, In: Topics in Current Physics, Persistent Spectral Hole Burning: Science and Applications, ed. W. E. Moerner (Springer, Berlin, 1988) p. 153.

[19] B. M. Kharlamov, R. I. Personov and L. A. Bykovskaya, Opt. Commun. 12 (1974) 191.

[20] A. A. Gorokhovskii, R. K. Kaarli and L. A. Rebane, JETP Lett. 20 (1974) 216.

[21] G. J. Small, In: Spectroscopy and Excitation Dynamics of Condensed Molecular systems, eds. V. M. Agranovish and R. M. Hochstrasser (North-Holland, Amsterdam, 1983) p. 555.

[22] R. C. Zeller and O. R. Pohl, Phys. Rev. B 4 (1971) 2029.

[23] P. W. Anderson, B. I. Halperin and C. M. Varma, Phil. Mag. 25 (1972) 1.

[24] W. A. Phillips, J. Low Temp. Phys. 7 (1972) 351.

[25] F. H. Stillinger, Science 225 (1984) 983.

[26] T. A. Weber and F. H. Stillinger, Phys. Rev. B 32 (1985) 5402.

[27] F. H. Stillinger and T. A. Weber, Phys. Rev. A 28 (1983) 2408.

[28] J. M. Hayes and G. J. Small, Chem. Phys. 27 (1978) 151.

[29] J. M. Hayes and G. J. Small, Chem. Phys. Lett. 54 (1978) 435.

[30] J. M. Hayes and G. J. Small, J. Lumn. 18/19 (1979) 219.

[31] S. K. Lyo and R. Orbach, Phys. Rev. B 22 (1980) 4223.

[32] J. M. Hayes, R. P. Stout and G. J. Small, J. Chem. Phys. 74 (1981) 4266.

[33] H. Hardle, G. Weiss, S. Hunklinger and F. Z. Baumann, Physik B 65 (1987) 291.

[34] M. J. Kenney, R. Jankowiak and G. J. Small, Chem. Phys. 146 (1990) 47.

[35] J. Friedrich and D. Haarer, In: Opeical Spectroscopy of Glasses, ed. I. Zschokke (Reidel, Dordrecht, 1986) p. 149.

[36] M. Berg, C. A. Walsh, L. R. Narasimhan, K. A. Littau and M. D. Fayer, J. Chem. Phys. 88 (1988) 1564.

[37] S. Völkler, In: Relaxation Processes in Molecular Excited States, ed. J. Fünfschilling (Kluwer, Derenter, 1989) p. 113.

[38] L. Guttman and S. M. Rahman, Phys. Rev. B 33 (1986 5665.

[39] B. L. Fearey, R. P. Stout, J. M. Hayes and G. J. Small, J. Chem. Phys. 78 (1983) 7013.

[40] Part I. This dissertation.

[41] P. Doussineau, G. Frenois, R. G. Leisure, A. Levelut and J. Y. Prieur, J. Physique 41 (1980) 1193.

[42] B. Golding, J. E. Graebner, A. B. Kane and J. L. Black, Phys. Rev. Lett. 41 (1978) 1487.

[43] J. Jäckle, Z. Phys. 257 (1972) 212.

[44] J. Jäckle and K. L. Jüngst, Z. Physik B 30 (1971) 243.

[45] J. L. Black and B. I. Halperin, Phys. Rev. B 16 (1977) 2879

[46] T. L. Smith, P. J. Anthony and A. C. Anderson, Phys. Rev. B 17 (1978) 4997.

[47] J. C. Lasjaunias, A. Ravex, M. Vandorpe and S. Hunklinger, Solid State Commun. 17 (1975) 1045.

[48] P. J. Anthony and A. C. Anderson, Phys. Rev. B 20 (1979) 763.

[49] G. Frossati, J le G. Gilchrist, J. C. Lasjaunias and W. Meyer, J. Phys. C-10 (1977) 515.

[50] M. W. Klein, B. Fisher, A. C. Anderson and P. J. Anthony, Phys. Rev. B 18 (1978) 5887.

[51] R. Jankowiak, G. J. Small and K. B. Athreya, J. Phys. Chem. 90 (1986) 3896.

[52] R. Jankowiak, G. J. Small and B. Ries, Chem. Phys. 118 (1987) 223.

[53] R. Jankowiak and G. J. Small, Phys. Rev. B 37 (1988) 8407.

[54] R. Jankowiak, J. M. Hayes and G. J. Small, Phys. Rev. B 38 (1988) 2084.

[55] R. Jandowiak, L. Shu, M. J. Kenney and G. J. Small, J. Lumin. 36 (1987) 293.

[56] Part III. This dissertation.

[57] R. Jankowiak and G. J. Small, Science. 237 (1987) 618.

[58] V. Bogner and R. Schwarz, Phys. Rev. B 24 (1981) 2846.

[59] B. L. Fearey and G. J. Small, Chem. Phys. 101 (1986) 269.

[60] W. Breinl, J. Friedrich and D. Haarer, Chem. Phys. Lett. 106 (1984) 487.

[61] W. Breinl, J. Friedrich and D. Haarer, J. Chem. Phys. 81 (1984) 3915.

[62] A. Elschner and H. Bässler, Chem. Phys. 123 (1988) 305.

[63] F. Kokai, H. Tanak, J. I. Brauman and M. D. Fayer, Chem. Phys. Lett. 143 (1988) 1.

[64] W. Köhler, W. Breinl and J. Friedrich, J. Chem. Phys. 82 (1985) 2935.

[65] B. L. Fearey, T. P. Carter and G. J. Small, Chem. Phys. 101 (1986) 279.

[66] A. A. Gorokhovskii, G. S. Zavt and V. V. Palm, JETF Lett. 48 (1988) 369.

[67] W. Richter, Th. Sesselmann and D. Haarer, Chem. Phys. Lett. 159 (1989) 235.

[68] T. P. Carter and G. J. Small, Chem. Phys. Lett. 120 (1985) 178.

[69] J. M. Hayes, B. L. Fearey, T. P. Carter and G. J. Small, Int. Rev. Phys. Chem. 5 (1986) 175.

[70] T. P. Carter and G. J. Small, J. Phys. Chem. 90 (1986) 1997-1998.

[71] M. J. Kenney, Iowa State University, unpublished results.

[72] T. P. Carter, B. L. Fearey, J. M. Hayes and G. J. Small, Chem. Phys. Lett. 102 (1983) 272.

[73] Part IV. This dissertation.

[74] B. L. Fearey, T. P. Carter and G. J. Small, J. Phys. Chem. 87 (1983) 3590.

[75] R. Van Den Berg and S. Völker, Chem. Phys. 128 (1988) 257.

[76] KODAK Laser dyes, KODAK publication JJ-169.

[77] T. P. Carter, Ph.D. Dissertation, Iowa State University, Ames, Iowa, 1985.

ACKNOWLEDGEMENTS

This dissertation is dedicated to my parents, Professor Weiguang Shu (1933-1988) and Zhanru Shen. I would have not succeeded without their love, encouragement and support. Especially, I want to thank my mother for her care and hard sacrifice. I may never be able to make it up to her.

I am particularly grateful to my advisor, Professor Gerald J. Small, for his guidance, patience and thoughtful discussions throughout the course of this study. His advice was very important.

I wish to thank Dr. John M. Hayes and Dr. Ryszard Jankowiak for their advice and useful discussions. I also thank Dr. Kevin Gillie and Dr. Michael Kenney who helped me start on the experiments. I am appreciative of Dr. Raja Reddy's help in one of my projects. Also, I would like to thank Mr. Paul Lyle for his proofing of the part of this dissertation.

I also want to express my thanks to my young sister and brother, Lingyan and Jianchuan, who took the responsibility of the elderest son while I studied in U.S.A. My thanks are also due to my grandmother for her love and care.

Lastly and most importantly, I want to thank my wife, Hongyu, who not only provided dinners and typed the part of this dissertation but also provided love and security. She shared my good and bad times and helped me go through some difficult times in my life.

APPENDIX

This section includs three parts: (1) The calculation of σ (absorption cross-section) for cresyl violet in poly vinyl alcohol films; (2) The results of nonphotochemical hole burning on $n\pi^*$ states; (3) Additional figures (figures and figure captions).

CALCULATION OF σ (absorption cross-section) For ZERO-PHONON LINE

Two approaches has been used to calculate σ (absorption cross-section). The first involves the calculation of dipole length from the measured fluorescence decay constant and the standard quantum mechanical expression for σ (standard approach). The second approach scales the measured room temperature value for σ of origin band by the ratio of low temperature (in our case, T = 1.6 K) to room temperature homogeneous linewidths (linewidth scale approach). In both approaches, the Frank-Condon factors associated with origin band and matrix phonons have been taken into account.

Standard Approach

$$k = 16\pi^2(\omega_{ab}^3 e^2 d^2) / (3h^2 c) \qquad (1)$$

where ω_{ab} is the peak absorption frequency and d is dipole length. k is the decay constant with h is Plank constant and c is light velocity.

$$\sigma = (2\pi)^3 \omega_{ab} e^2 d^2 g(\omega) / 3ch \quad (2)$$

where σ is absorption cross-section and $g(\omega)$ is single site line profile. With the

assumption that $g(\omega)$ is Lorentzian, thus that

$$g(\omega) = 2\gamma / \pi[4(\omega_{ab} - \omega)^2 + \gamma^2] \quad (3)$$

where γ is the homogeneous linewidth. At peak of the profile,

$$g(\omega) = 2 / (\pi\gamma) \quad (4)$$

Therefore,

$$\sigma = 4(2\pi)^3\omega_{ab}e^2d^2 / 3h\gamma \quad (5)$$

Where γ is in the unit of s^{-1}.

For cresyl violet, $k = 1.8 \times 10^8\ s^{-1}$, $\gamma \sim 0.015\ cm^{-1} \rightarrow 2.8 \times 10^9\ s^{-1}$ [ ]. From equations (1), (2), (3), (4) and (5), one can get that,

$$\sigma = 4.0 \times 10^{-11}\ cm^2 \quad (6)$$

Considering the Frank-Condon factor F = 0.45 (estimate from absorption spectrum of cresyl violet) and electron-phonon coupling $F_p = 0.5$ (Huang-Rays factor S = 0.7, see Part III).

$$\sigma' = 1 \times 10^{-11}\ cm^2 \qquad (7)$$

Considering the transition dipole is parallel to the laser light and the index of refraction for ethanol n = 1.36,

$$\sigma'' = 3\sigma' / n^2 \sim 14 \times 10^{-12}\ cm^2 \qquad (8)$$

Linewidth Scale Approach

$$\sigma = 2.3 \times 10^3 \varepsilon_0\ cm^2/mole \qquad (9)$$

where ε_0 is room temperature extinction coefficient. For cresyl violet $\varepsilon_0 \sim 4.4 \times 10^4$ and,

$$\sigma = 1.68 \times 10^{-16}\ cm^2 \qquad (10)$$

For room temperature homogeneous linewidth $\Gamma \sim 1000\ cm^{-1}$, (estimate from room temperature absorption profile for cresyl violet in poly vinyl alcohol film) and low temperature homogeneous linewidth $\gamma \sim 0.015\ cm^{-1}$, considering electron-phonon coupling $F_p \sim 0.5$,

$$\sigma' = \Gamma F_p \sigma / \gamma \qquad (11)$$

$$= 5.6 \times 10^{-12}$$

Considering the transition dipole is parallel to the laser light,

$$\sigma'' = 3\sigma' \sim 16 \times 10^{-12} \quad (12)$$

Comparing equation (8) with (12), it is shown that the results from the two approaches is well agree with each other.

THE RESULTS OF NONPHOTOCHEMICAL HOLE BURNING ON $n\pi^*$ STATES

impurity	host	λ_b (nm)	burn intensity (mW/cm^2)	burn time (min)	hole
benzo cinnoline	MTHF [a]	440.0	12	150	no
	EPA [b]	440.0	0.1	150	no
benzophenone	MTHF	360.0	45	45	no
o-benzoquinone [c]	EtOH/Gly [d]	541.5	200	40	no
phenazine	MTHF	435.0	15	150	no
pyridazine	EPA	356.0	18	60	no
	EtOH/Gly	356.0	40	35	no
	MTHF	362.0	15	40	no

a : 2-methyltetrahydrofuran

b : ether / isopropanol 5 : 2

c : 3,5-Di-tert-butyl-1,2-benzoquinone

d : EtOH / glycerin 1:1

ADDITIONAL FIGURES

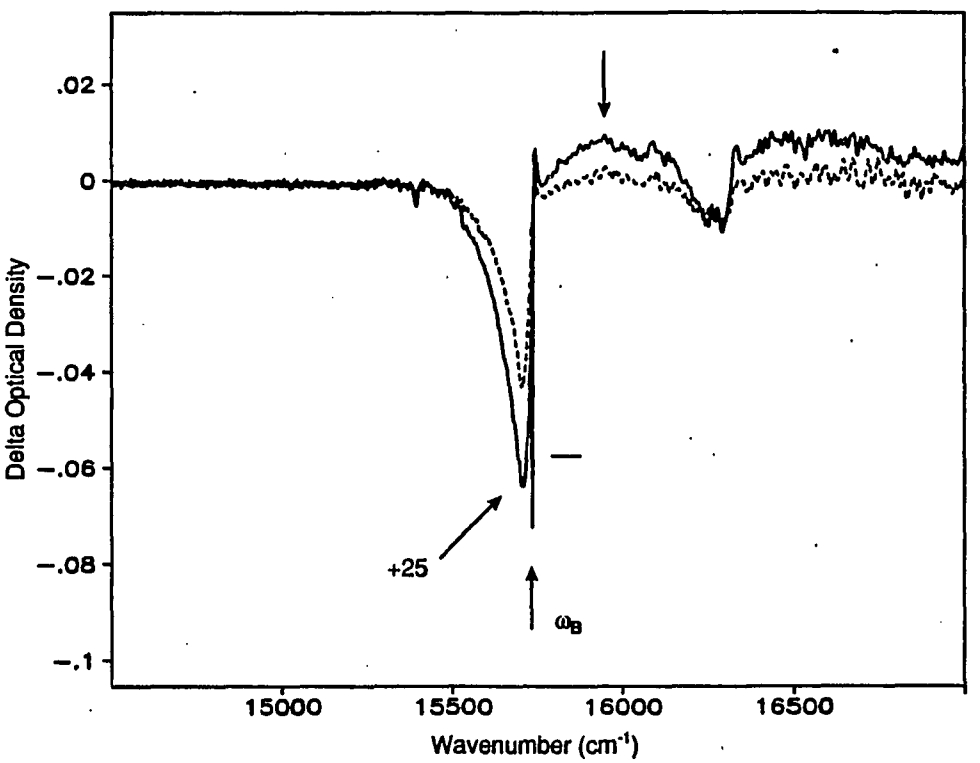

Figure 1. Polarized hole spectra for cresyl violet in PVOH burned and read at 2.2 K. The solid line and dashed line spectra correspond to a read polarization that is parallel and perpendicular to the burn polarization respectively. I_B = 30 mW/cm^2 and t_B = 2 minutes. ω_B = 15735 cm^{-1} (pre-burn OD ~ 0.18). The horizontal bar of the zero-phonon hole indicates ZPH depth for the dashed spectrum

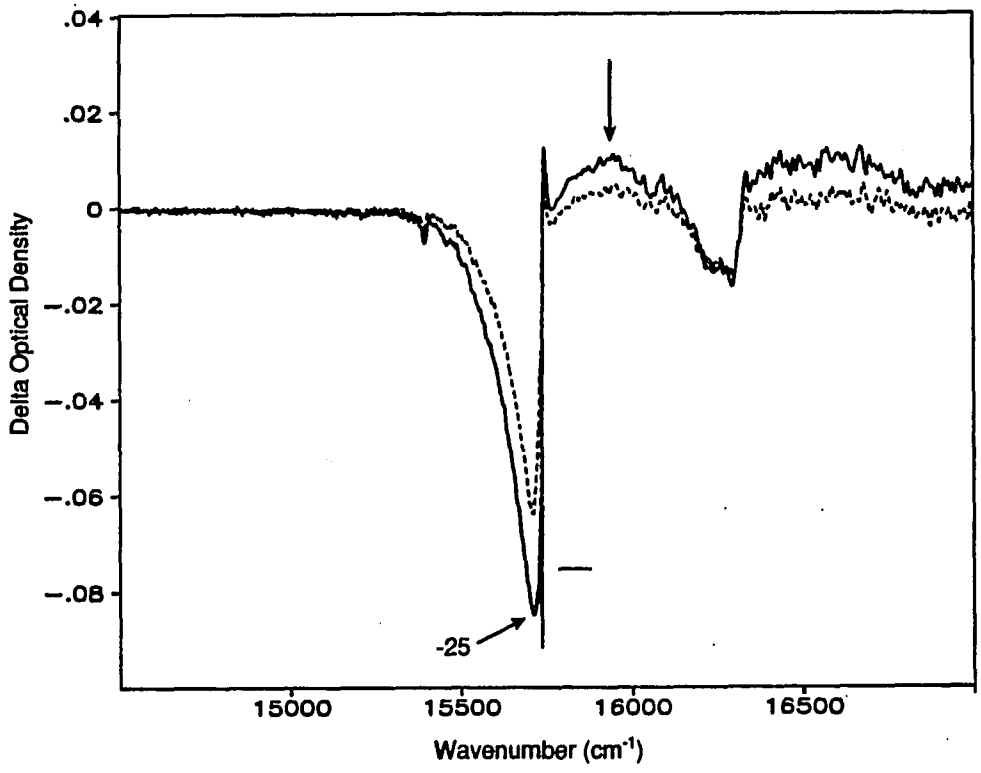

Figure 2. Polarized hole spectra for cresyl violet in PVOH for a burn time of 8 minutes. The other conditions are the same as those for Figure 1

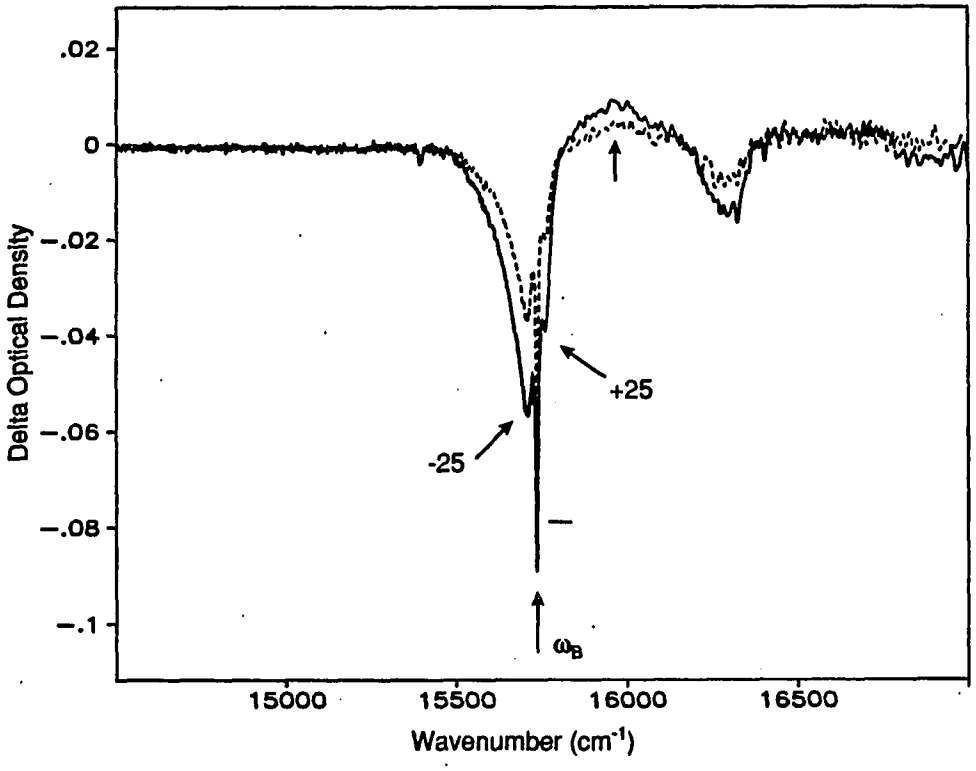

Figure 3. Polarized hole spectra of cresyl violet in PVOH burned and read at 15 K. t_B = 2 minutes with other burn conditions the same as those given in the caption to Figure 1

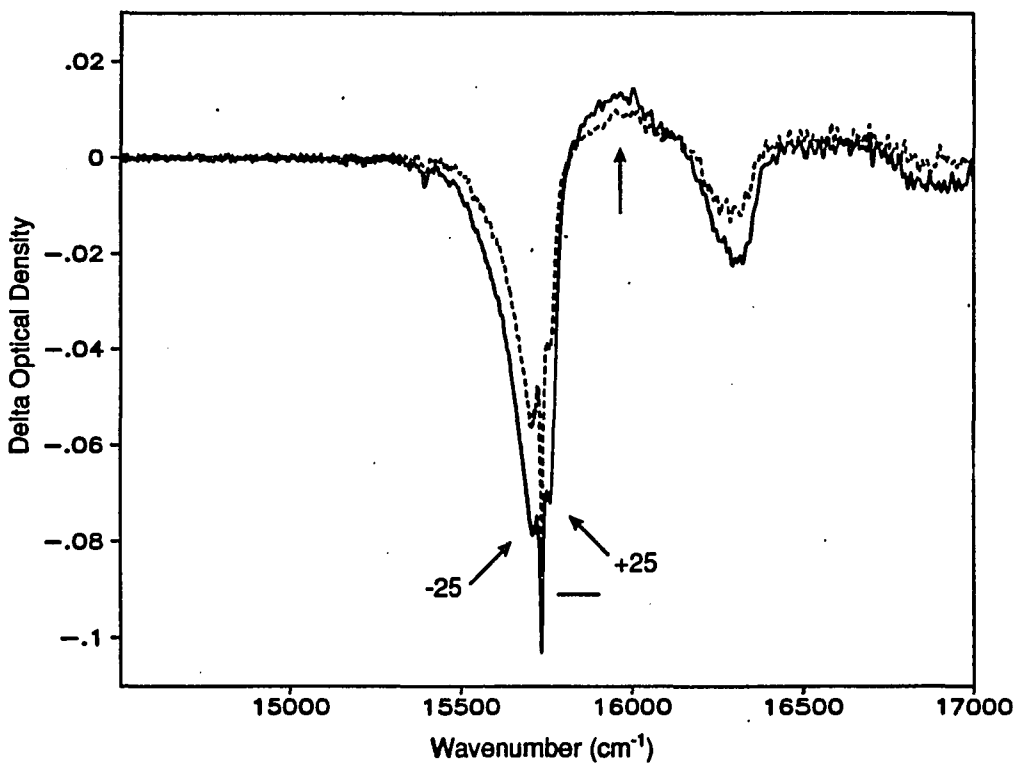

Figure 4. Polarized hole spectra of cresyl violet in PVOH burned and read at 15 K. t_B = 8 minutes with other burn conditions the same as those given in the caption to Figure 1